TAMPEREEN TEKNILLINEN YLIOPISTO
TAMPERE UNIVERSITY OF TECHNOLOGY

LEO LAAKKONEN

PREDICTIVE SUPPLY TEMPERATURE OPTIMIZATION OF DISTRICT HEATING NETWORKS

Master of Science thesis

Examiner: prof. Matti Vilkko
Examiner and topic approved by the Faculty Council of the Faculty of Engineering Sciences
on 17th August 2016

ABSTRACT

LEO LAAKKONEN: Predictive supply temperature optimization of district heating networks
Tampere University of Technology
Master of Science Thesis, 71 pages
November 2016
Master's Degree Programme in Automation Technology
Major: Process automation
Examiner: Professor Matti Vilkko

Keywords: district heating, flexibility, supply temperature, optimization

In combined heat and power (CHP) the waste heat of power production is used for heating the water in district heating (DH) plants. Fluctuating power production in CHP plants may cause unwanted disturbances in district heating networks (DHN), which leads to the situation that the best efficiency in CHP production is not achieved. Although DH -systems are usually automated, the supply temperature is still primarily chosen manually by the operator or it is based on current outdoor temperature. This is because of the uncertain heat demand in near future and uncertain behaviour of delay from heat supplier to consumers, which make the temperature scheduling challenging.

In this work, future heat demand and return water temperature are predicted based on outdoor temperature forecast and process data history using neural network predictors. Consumers in network are presumed to be similar, but their distances from production sites vary thus creating a distribution function of range. Delay is modelled as a distribution function based on the distances between heat consumers and the suppliers, which weights the supply temperatures from last few hours calculating the average supply temperature received by the consumers. The brute force optimizer utilizes these models to optimize the supply temperature by minimizing heat loss and pumping costs. Delays are dependent on mass flows, but they are not set as variables during optimizations due to formulation and performance challenges. Instead, the delays are determined for each optimization cycle based on mass flows of earlier cycle and they are iterated as long as delays are converged. The resulting supply temperature curve is a discrete curve that cuts the heat load peaks by charging and discharging the energy content of the DHN. Optimization keeps the supply water temperature and flow rates in control and stabilizes the network smoothly and efficiently after disturbances.

In this work, the optimization is demonstrated in case study of Kuopio DHN, operated by Kuopion Energia Oy. Models are fitted and calibrated into Kuopio DHN and the optimization is compared to the measured supply temperatures and instructional temperatures by Energiateollisuus ry. Standard deviation of heat load predictor was 6.3 MW, return temperature predictor 0.78 ℃ and for delay distribution model 0.30 ℃. Main actions of optimization were delay prediction, reduction of supply temperature and minimizing pumping during high pumping costs. Optimization gave savings of 1.2 – 1.7 % on heat delivery.

TIIVISTELMÄ

LEO LAAKKONEN: Kaukolämpöverkon menolämpötilan ennustava optimointi
Tampereen teknillinen yliopisto
Diplomityö, 71 sivua
Marraskuu 2016
Automaatiotekniikan diplomi-insinöörin tutkinto-ohjelma
Pääaine: Prosessien Hallinta
Tarkastaja: Professori Matti Vilkko

Avainsanat: Kaukolämpö, joustavuus, menoveden lämpötila, optimointi

Vaihteleva sähköntuotanto sähkön ja lämmön yhteistuotannossa (CHP) voi aiheuttaa haitallista häiriötä kaukolämpöjärjestelmään (DHS), joka heikentää yhteistuotannoin hyötysuhdetta. Vaikka kaukolämpöjärjestelmät ovat usein pitkälle automatisoituja, menoveden lämpötilan säätö tehdään pääasiallisesti manuaalisesti operaattorin toimesta tai suoraan ulkolämpötilan mukaisesti. Tämä johtuu epävarmuudesta lähitulevaisuuden lämmöntarpeen arvioinnissa, sekä tuottajan ja kuluttajan välisestä viiveen käyttäytymisestä, jotka tekevät lämpötilan säädöstä haasteellisen.

Tässä työssä asiakkaan lämpökuorma ja paluuveden lämpötila ennustettaan neuroverkkoennusteella, joka perustuu ulkolämpötilaan ja prosessin historia-arvoihin. Verkon kuluttajien käytös oletetaan yhteneväiseksi, mutta niiden etäisyys tuotantolaitokselle vaihtelee, muodostaen etäisyyteen perustuvan jakaumafunktion. Jakauma laskee asiakkaan saaman menoveden lämpötilan painottamalla edellisten tuntien menolämpötiloja tuottajalla jakaumafunktion mukaisesti. Brute force optimoija hyödyntää edellä mainittuja malleja optimoidakseen menolämpötilan minimoimalla lämpöhäviön ja pumppauksen aiheuttamat kustannukset. Muuttuva viive on optimoinnissa haasteellinen, joten viive ei muutu kesken optimointikierroksen, vaan se lasketaan optimointikierroksen jälkeen ja optimointia iteroidaan, kunnes viiveet asettuvat. Tuloksena saadaan diskreetti menolämpötilakäyrä, joka leikkaa kulutushuippuja lataamalla ja purkamalla kaukolämpöverkon (DHN) varausta. Optimoija pitää menoveden lämpötilan ja virtausnopeuden hallinnassa ja stabiloi järjestelmän pehmeästi ja tehokkaasti häiriöiden jälkeen.

Optimointia havainnollistetaan Kuopion kaukolämpöverkon tapauksella, jota operoi Kuopion Energia Oy. Mallit sovitetaan ja kalibroidaan Kuopion kaukolämpöverkkoon ja optimointia verrataan mitattuun menolämpötilaan, sekä Energiateollisuus ry:n tarjoamaan ohjekäyrään. Lämmöntarve-ennusteen keskihajonta oli 6.3 MW, paluulämpöennusteen 0.78 ℃ ja viivemallin 0.30 ℃. Optimoinnin merkittävimmät toiminnot olivat viiveennakointi, menolämpötilan laskeminen ja korkeiden pumppauskustannusten ennakointi, joilla saavutettiin 1.2 – 1.7 % säästöt lämmönsiirtokustannuksissa.

PREFACE

This work was carried out in the research program Flexible Energy Systems (FLEXe) and supported by Tekes – the Finnish Funding Agency for Innovation. The aim of FLEXe is to create novel technological and business concepts enhancing the radical transition from the current energy systems towards sustainable systems. FLEXe consortium consists of 17 industrial partners and 10 research organisations. The programme is coordinated by CLIC Innovation Ltd. *www.clicinnovation.fi*

This Master's thesis was done in Valmet Automation during 2015-2016. I would like to thank my superior Maria Nurmoranta and supervisor Jyri Kaivosoja in Valmet. Also thanks to the staff of TUT department of Automation science and Engineering, Timo Korpela who have greatly instructed in writing process, also thanks to Matti Vilkko and Yrjö Majanne who have been planning the contents and methods of the project. Special thanks to Kuopion Energia Oy that I could use their district heating network as a case study and they were happy to provide all the possible information to finish the study successfully.

There is also a conference paper (Laakkonen et al. 2016) that has been written concerning the same research to The 15th International Symposium on District Heating and Cooling 2016, Seoul, Republic of Korea (South Korea). The topic of that paper is "Predictive supply temperature optimization of district heating networks using delay distributions". Few minor corrections in equations were found after submission of the conference paper that are corrected into the results of this Master's thesis paper.

Thanks to my family, friends and betrothed who have given me motivation and support during my studies in university and this thesis work.

Tampere, 14.10.2016

Leo Laakkonen

CONTENTS

LIST OF SYMBOLS AND ABBREVIATIONS

ANN	Artificial Neural Network
CHP	Combined Heat and Power
COP	Coefficient of Performance
DH	District Heating
DHN	District Heating Network
DHS	District Heating System
LTD	Least Temperature Difference (*fin. asteisuus*)
ME	Mean Error
SD	Standard Deviation

Δp	Pressure difference
λ	Friction coefficient of pipe
τ	Delay
η	Efficiency
ϕ_{del}	Delivered heat load
ϕ_{prod}	Produced heat load
ϕ_{loss}	Heat loss load
ρ	Density
c_p	Specific heat capacity
d	Diameter of pipe
E_{el}	Electricity price
E_{fuel}	Fuel price
h	Enthalpy
h_c	Heat transfer coefficient
k	Heat conductivity
k	Discrete moment of time
L	Length of pipe
$\dot{m}_c$	Mass flow through consumer
$\dot{m}_{bp}$	Mass flow through connection loops (by-pass)
P	Power
R	Heat resistance
T	Temperature
T_C	Cold water temperature of secondary circuit of heat exchanger
T_H	Hot water temperature of secondary circuit of heat exchanger
$T_{s,s}$	Supply temperature at heat supplier
$T_{s,c}$	Supply temperature at customer
$T_{r,s}$	Return temperature at heat supplier
$T_{r,c}$	Return temperature at customer

Subscripts

e	Electricity
g	Ground
q	Heat
r	Return
s	Supply
w	Water

1. INTRODUCTION

This chapter firstly introduces briefly the principles of district heating systems (DHS) and then concentrates on district heating (DH) control methods and challenges. State-of-the-art covers the most important studies concerning the research question. The last part clarifies the currently applied technology in Finland and briefly explains the methods used in this study.

District heating in Finland is a growing method of heating properties, as district heating networks (DHN) expand and more people move to urban areas that are connected to DHN. Therefore, the DH consumption in Finland has increased by 22 % between 2005 - 2014 (Energiateollisuus 2015). DH is invented to make benefit of the condensation heat of power plant. The heat is extracted from condenser after steam turbine in power plant. Power plant that provides both electricity and heat are called combined heat and power (CHP) plants. In CHP –plants the steam is condensed into DH water through heat exchanger as drawn in Figure 1. In most of the systems, the DH water is pressurized much enough that it to stays constantly liquid. Pressure difference distributes the water from supplier to customers along the pipes. Hot water is pumped into supply pipes providing pressure difference for all of the consumers. Consumers control the flow to their heat exchangers using control valves. Chilled DH water is returned from consumer back to heat provider along the return pipe. These pipes form a district heating network. When the production, consumption and DHN are connected, they form a DHS.

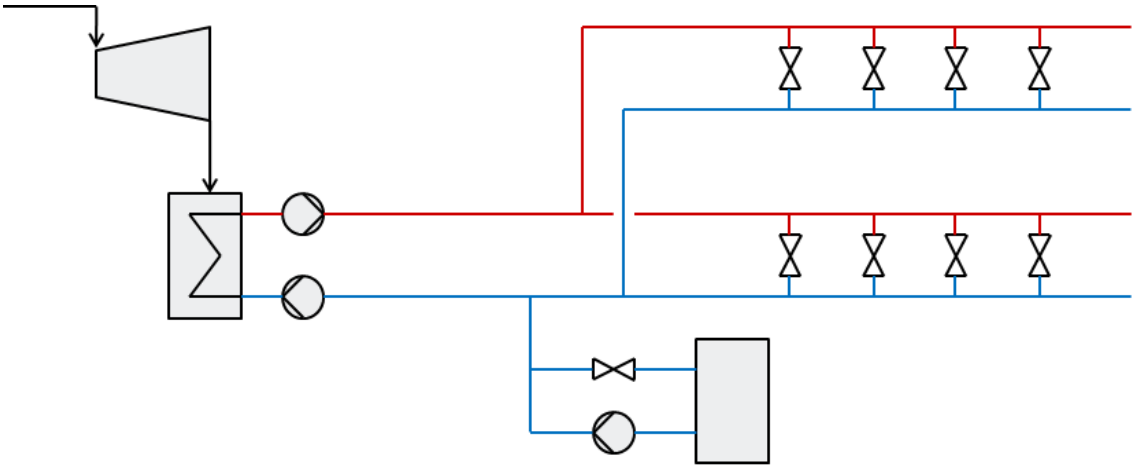

Figure 1. *Sketch of district heating system. Red pipes are supply pipes and blue pipes are return pipe. Vertical valves are customers and the device in the bottom is a pressure level control system.*

DHS has three main controlled variables: medium pressure, pressure difference at customer and supply water temperature. There are certain regulations by consumer substations that limit the temperature and pressure controls. The regulations are mostly based on consumer substation and DHN constraints. Temperature limitations are more specifically regarded in chapter 2.5.1. The main objectives of the controls are: (Koskelainen et al. 2006)

- Medium pressure must be high enough to avoid saturation into steam or cavitation in pumps at any point.
- Pressure difference at customer control valve must be high enough to provide decent flow controllability for customer.
- Supply temperature should be at right level so that pumps can produce necessary mass flow to transport the demanded heat. The lower the supply temperature is the higher the demanded flow rate is, which increases the need for pumping. Also the supply temperature at consumers should not be outside the boundaries.

DHS operators usually are electricity companies, who run CHP plants to produce both heat and power. The different pricing of the heat and electricity raises the interest of producer to schedule the consumption and production peaks differently. As the incomes of the delivered heat are constant, the incomes of sold electricity are dependent on electricity markets. Hereby CHP provider may want to maximize the electricity production when its price is high and minimize when it is not profitable. Electricity price also has an effect on DH distribution as pumping costs are proportional to the electricity price.

As the DH water flows rather slowly along the vast networks, the distribution delays may be from few minutes up to more than ten hours. The delay is a challenge, but properly controlled it can be used as a buffer to store heat. Accumulation of DHN means that current supply temperature of the DH supplier diverge from the average supply temperature of the DHN. Network is charged when current supply temperature is higher than the current average temperature of the supply water in the network and respectively discharged when the current supply temperature is lower than the average temperature. Hereby accumulation is usage of DHN dynamics for short term storage of heat. This kind of accumulation is generally applied to prepare for heat load peaks to avoid start-up of heat-only boilers that use expensive fuels.

Even though the DHSs are usually automated, the supply temperature is still generally manually chosen or it is a function of current outdoor temperature. The challenge is that because of the long delays and complex dynamics the behaviour of the system is rather difficult to predict and it is not possible to control the temperature using basic control methods.

1.1 Aim of this work

Level of automation in DH temperature controls is generally very low. Hereby motivation for this work was to find out the reasons for lack of advanced control methods. Aim of this work is to find out what is the state-of-the-art of the DH temperature controls and create a viable solution. There has been quite a lot research on this subject, but as I am doing the research in Valmet Automation, I should be able to implement the methods in practice. Heat suppliers generally prefer robust and simple methods such that the operations of the system are predictable and understandable. Hereby, modelling and forecasting the system behaviour are the important objectives by themselves.

1.2 Advanced supply water temperature controls

In advanced control methods of DHN the network dynamics and heat consumption prediction have to be modelled, because the system delays are too long for static analysis. Response in supply temperature controls is so long that environmental circumstances may change significantly during transport delay. District heating is a multivariable process with varying time delay. The basis of DH controls is to determine the energy equation (1-1) of the customers, as they set the mass flow of the network according to temperature difference and heat load (Frederiksen & Werner 2013)

$$\phi_{del} = \dot{m} c_p \left(T_{s,c} - T_{r,c}\right), \qquad (1\text{-}1)$$

where ϕ_{del} is consumer heat load and $T_{r,c}$ consumer return temperature that cannot be controlled. As specific heat of water c_p is constant, the mass flow $\dot{m}$ is totally controlled by supply temperature received by customer $T_{s,c}$. The control problem can be divided into three parts, starting from defining the unmeasured and uncontrolled variables.

The first part of the supply water temperature control development is the determination DH consumption and customer return temperature. They are based on human behaviour and environmental disturbances e.g. weather. To be able to utilize these estimations, the variables have to be predicted at least as far in the future as is the transport delay.

Secondly, the dynamics of DHN has to be modelled. There is a delay between heat suppliers and consumers that is dependent on current flow rate and distances based DHN layout. There are different ways to model the transport delay. Simple way is to assume it to be constant or mass flow variant scalar, but as the consumers really form a great mesh, the delay is individual for each of the consumers. With proper modelling the advanced control methods can be used and the dynamics of the network can be utilized to schedule the production.

The third part of the supply water temperature controls is to determine the optimal supply temperature. Supply water temperature is a control variable that has effect on many other

process variables for example mass flow, return temperature, heat loss and pumping energy. The system can be operated with many different temperatures, but the optimal temperature is dependent on many process variables, environmental disturbances and electricity price on the market. High supply temperature lead to high heat loss and high mass flow lead to high pumping requirements. As water mass flow rate increases when supply water temperature decreases, there must always be a minimum when summing pumping and heat loss costs.

1.3 State-of-the-art

A lot of research has been done on controls and optimization of DHS. There are few comprehensive methods, such as model-based supply temperature control approach, production optimization with linear and nonlinear modelling, and optimization based on dynamic simulator.

A study of DHN modelling and supply water temperature optimizing has been released by Benonysson et al. (1995). They have modelled the DHN using node method. Flow rates in pipes are calculated through consumption and temperatures and pumping energy is calculated using flow rates. To determine optimal production, supply temperature was optimized. (Benonysson et al. 1995)

Linn Saarinen has done several researches in DH modelling and controls. The main motivation of Saarinen (2008) was to increase efficiency of electricity production in CHP plant by decreasing supply temperature to the DHS. Dynamic model was used for prediction and simulation so that heat distribution was not compromised. Heat load was modelled with an ARX model and the control was based on a dynamic model. Pressure controls in simulations was omitted, and a quasi-static view of pressure was used. Saarinen states that a simple model is usually enough for control purposes, because exact model would make the control slower without benefits. The biggest difference in the set-up of Saarinen compared to this paper is that here electricity price is not all the time high enough that electricity production would be profitable. (Saarinen 2008)

Saarinen (2010) continues from the earlier research (Saarinen 2008). Weak spots were fixed and the system was tested in real CHP plant. The main objective was still to improve the efficiency of electricity production. No measurement data was available from network, only CHP plant was modelled and measured. Load model was a greybox of a diurnal difference model and a blackbox ARX model. Model-based control worked well so that supply water temperature could be set lower improving efficiency of electricity production. However, the simple model worked only because there were only one heat producer that makes this model inappropriate for larger networks without further simplifications. Also electricity price was assumed to be high enough to produce electricity continuously. (Saarinen 2010)

A report by Saarinen & Boman (2012) considers optimization of large district heating network with several production units. Accurate model was created using TERMIS simulation application, including pipes, pumps, diameters, elevations etc. Load prediction model was implemented to replace outdoor temperature prognosis. TERMIS model was used to simulate the control strategy. Allowing higher 8 bar differential pressure, temperature could be decreased by average 8 °C during January-April, increasing the electricity production by 2.5 %. Load prediction model is based on estimated constant delay between producer and the centre of the DHN. Pressure and flow restrictions have to be determined for each network. The accurate TERMIS model was found to be useful for simulations, but too slow for control purposes because of the complexity. Hereby simple Matlab model for controls had to be created. (Saarinen & Boman 2012)

Falkvall & Nilsson (2013) have researched the supply water temperature effects in DHS. The study was carried out by simulations on accurate DHN model of Lund in southern Sweden. There are two heat pumps in addition to heat and CHP plants in the DHS. The main goal was to study the effects of lowering the supply water temperature and find out how the increased pressure differences would influence. Simulations were implemented with exact model of Netsim simulator, where actual network including pressure modelling could be simulated. Supply temperature was minimized, so that differential pressure could be held high enough. Weakness of Netsim simulator was the restriction to simulate only fixed values for return temperature. As a result, the supply temperature could be lowered by 2 to 6 °C earning annual savings of 3 million SEK (~300 000 €). The main reason for that pointed out to be the increased coefficient of performance (COP) for the heat pumps. The COP enhances significantly when supply temperature reduces, especially because the heat pumps cannot produce higher temperatures than 80 °C. Maximum improvements were gained by feeding supply water at minimum restriction of 70 °C always when it was possible.

Velut et al. (2013) have researched how short-term production planning could be implemented by basic mixed integer linear programming and physics based non-linear models with nonlinear optimization techniques. Compared to earlier studies, the whole heat production was optimized such that supply temperature, heat accumulator and used heat production plants were optimized. Nonlinear model forms an economic dispatch sub-problem (EDP), which apart from production units optimization, can also solve supply temperature, flow rates and by-pass valve usage in CHP plant. Optimization simulations gave good revenues maximizing low cost plant usage and increasing average mass flows of supply water decreasing average supply temperatures. This gave significant improvement in revenues compared to un-optimized measurement data. The transport delay was found difficult to model. There were no network model in optimization and it was agreed to be a future work to design a DHN model. (Velut et al. 2013)

Another approach to DHN modelling is introduced by (Vesterlund & Dahl 2014). In the research, DHN of Kiruna in northern Sweden is modelled by simplified Matlab Simulink

model and ReMIND model. Simulink models the physical characteristics of the DHN and ReMIND forms the model of heat production plant for optimization. The optimization was performed by CPLEX. Simulink model calculates pressure differences that generates the mass flow based on pipe length and diameter. Also heat losses of supply temperature are considered. The modelling method was found to be good in simulating the DHN with loops and finding the bottlenecks in the network. Also optimization could minimize the operating costs. The lack of return temperature simulation weakens the simulation results of (Vesterlund & Dahl 2014). Also Haikarainen et al. (2014) have implemented a Matlab model with CPLEX optimization. The report focuses on production optimization and the model was found to be useful for future development of the network. Supply and return water temperatures were calculated by function of outdoor temperature, which leaves some margin for improvements.

The earlier researches have some good solutions to the similar problems that exist in this study. Most significant deficiency on the earlier studies is the modelling of the DHN. There are simulators with exact modelling of DHN, but in control purposes the delay is usually considered as an estimated scalar. In this work the supply temperature delivery is seen as distribution function that models better the network accumulation and heat transfer. The supply temperature controls is an optimization problem with varying time delays. No successful implementation of varying time delay modelling was found. Hereby primitive brute force method is used to solve the problem in this work.

1.4 Currently applied technology

Nowadays the applied technology in DH supply water temperature is mostly based on static analysis. As the heat demand has an obvious correlation with outdoor temperature, the supply water temperature is often controlled by function of current outdoor temperature. Finnish energy association Energiateollisuus (ET) has provided an instructional control curve based on outdoor temperature that is presented in Figure 2. Many heat suppliers in Finland use an applied curve based on ET curve to control the supply temperature.

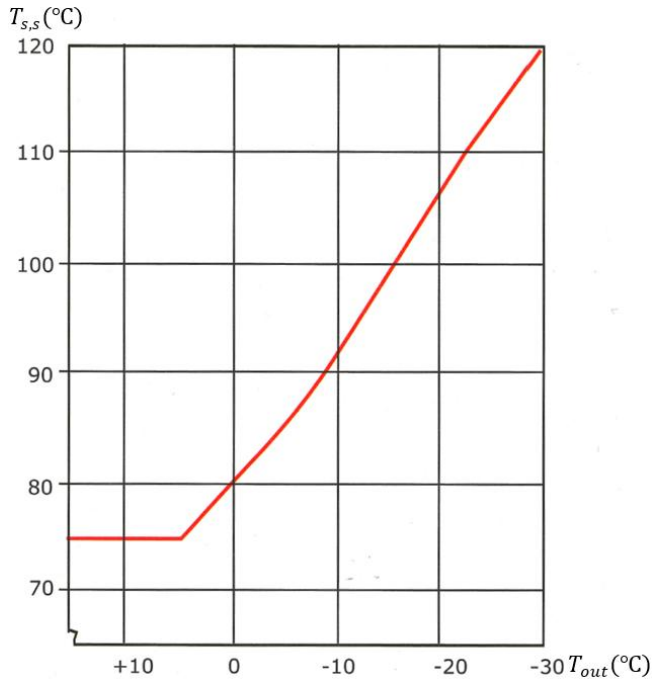

Figure 2. *Instructional control curve of supply temperature by Energiateollisuus ry* (Koskelainen et al. 2006)

Viander (2014) studied the optimal operation of DHS of Kotka in Southern Finland. He found that the supply water temperature was operated using a control curve that is significantly warmer than the ET control curve in warm outdoor temperatures. A new curve was proposed with lower temperatures, but still higher than the ET curve. Operators were also instructed to deviate from the new curve to accumulate the network before expected peak loads. It turned out to be difficult for operators to deviate from the curve, leading to situation that oil-fired heat-only boilers were forced to be switched on. Because the supply water temperature set point was manually set, it was laborious to follow the control curve and simultaneously consider accumulation. Also, operators had to monitor the states of furnace and turbine of the CHP plant, which took the attraction from DHS. To ensure high enough supply temperature and careless operation, supply temperature was set higher than instructed and the set point was rarely updated. (Viander 2014)

The research by Viander (2014) appoints that supply temperature is not that remarkable control variable in Kotka. There are many small DHNs in Finland that have lower level of automation. However, in Kuopio DHS the supply water temperature is operated more cautiously, the yearly average supply temperature being only 2 °C above the instructed ET curve method. Also manual network accumulation is practiced to cut peak loads. According to Energiateollisuus (2015) the heat losses in Finnish DHSs are between 1.0 – 36.2 % if they are calculated at all. Hereby there are big differences in calculation methods and accuracy that appoints the variety of DH control systems is vast and many of them are not correctly measured. There are not many DH applications in Finland that model supply delay and compute the supply water temperature considering delays. Therefore, there is a room for improvements, which are proposed in this work.

1.5 The applied methods

The first part of the comprehensive solution is the modelling of heat load and return temperature. Stochastic models are suitable as the variables that are partly based on human behaviour and partly on heat leakage of buildings. Among the methods, neural network was chosen as the Matlab tool and the results appeared to be good for this use. As the heat load and return temperature modelling is not the main focus of the thesis, it is chosen with no further justification.

The second part is the modelling of the system thermal dynamics. Pressure dynamics are excluded from the model. The model determines the average temperature at average customer according to network specifications, supply temperature at supplier, mass flow etc. Even though Saarinen & Boman (2012) introduced a distributed heat transport delay, similar delay distribution models were not introduced in other studies. This model was developed to model the heat loss and delay dynamics of the DHN.

The third part of the solution is the optimizer itself. When all variables are determined by the models, the optimizer searches the supply temperature that produce the lowest total costs. Primitive brute force search was chosen due to connectivity to the delay distribution model, robustness and independence from any optimization software.

2. DISTRICT HEATING SYSTEM

This chapter introduces the main parts of DHS and the key principles and equations. DHS consist of three parts; suppliers, pipe networks and customers. There are usually plenty of customers and several production units in one DHS. DHN is a network formed by the DH pipes that connect all of the heat consumers and suppliers. Some DHSs have no return pipes being open systems. However, modern DHSs are closed systems, where water circulates through the pipes transferring heat from plant into water and further to the consumers without any mass transfer in heat exchangers. Cooled water flows back to supplier along return pipes.

There are currently four generations of DHS. Main difference between them is the temperature and phase of supply water. The differences are substantial when regarding pressure levels, heat losses and requirements of pipe material. In the 1st generation DHSs, the supply phase of water is steam and they might be open systems with no return pipe. In the 2nd generation system the medium is pressurized water, where most of the time supply temperature is $T_{s,s} > 100$ °C. In 3rd generation system the supply water is pressurized but most of the time $T_{s,s} < 100$ °C to reduce heat losses. The 4th generation is more or less under development, where the maximum supply temperature is $T_{s,s} < 80$ °C. In Finland the DHSs are generally the 3rd generation, where water is pressurized and the supply temperature vary on scale 75 – 120 °C based on heat consumption. (Frederiksen & Werner 2013)

The heat transfer in DHS can be simplified into model presented in Figure 3. The heat producer produces certain temperature $T_{s,s}$ for supply water. The network transports the water to consumer, who receives the cooled water after delay τ_s as a consumer supply temperature $T_{s,c}$. Consumer has a heat consumption load ϕ_{del} and return temperature $T_{r,c}$. The mass flow of the network $\dot{m}$ is dependent on ϕ_{del} and the difference between $T_{s,c}$ and $T_{r,c}$. The return water reaches the producer after delay τ_r at the supplier return temperature $T_{r,s}$. The heat production load ϕ_{prod} is dependent on $\dot{m}$ and the temperature difference between $T_{s,s}$ and $T_{r,s}$.

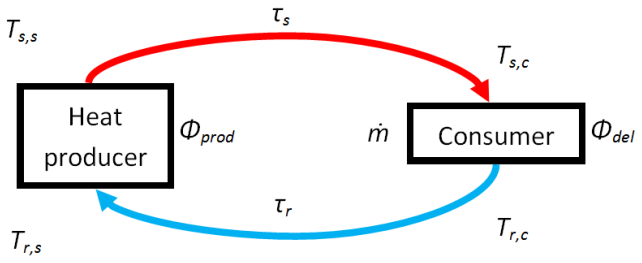

Figure 3. *Simplified model of DHS heat transfer dynamics.*

2.1 Suppliers

Supplier (aka producer) in DHS is a heat source that heats the cold return water and supplies it as hot supply water. Traditionally these are CHP plants and heat stations which heat is based on combustion of fuels. There are also geothermal heat pumps, solar heat, wind heat and electric boilers that may produce the heat. It is presumable that these will displace many oil-, coal- and gas-fired boilers in future.

2.1.1 CHP

Electricity production used to be the main product of CHP –plant, but due to reduced electricity prices in Nord pool spot area, the heat has become more important merchandise for local electricity companies in last 15 years according to Figure 4. The prices are not comparable among themselves as the DH price is the total taxed price for customers but the electricity price does not include taxes nor transfer fees, but the rising trend of DH price is obvious.

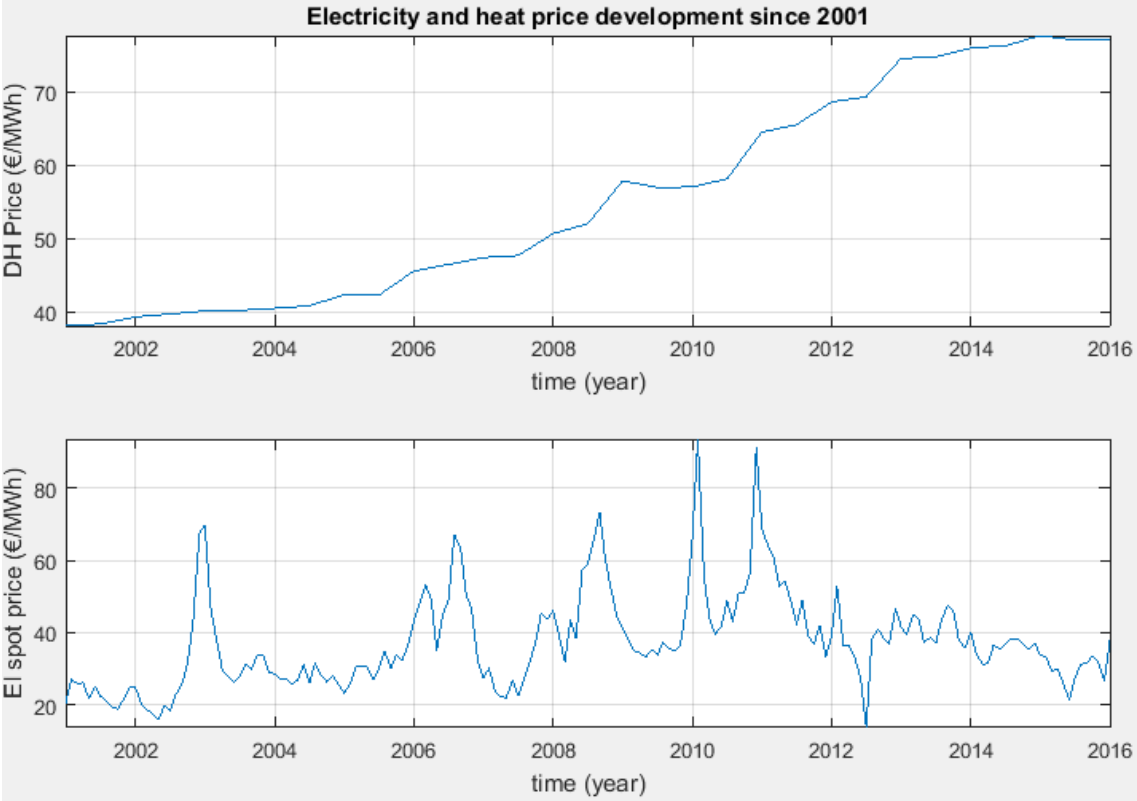

Figure 4. *Electricity and DH price in Finland from 2001. El spot price is the monthly average of Finnish regional electricity price without taxes nor transfer fees and DH Price is the half year average of energy total price for small apartment house in Finland. (Statistics Finland 2016) (Nord Pool Spot 2016)*

Because the electricity price is occasionally lower than the costs of electricity production, CHP-plant operation needs planning according to electricity prices and DH consumption forecasts. Nowadays the strategy is to produce electricity only when it is profitable with full power and simultaneously satisfy DH customers' demand as efficiently as possible. CHP plant may have only back-pressure condenser or additionally condensing end turbine. In condensing end turbine, the DH water is heated with extraction steam and the main condenser is cooled down usually by sea/lake water. Electricity production efficiency is maximized when the steam is directed to main condenser instead of DH heat exchanger. Back-pressure turbine is fully condensed by DH water. Because the mean temperature of DH water is much higher than lake/sea, the maximum electricity production efficiency is lower than in condensing end turbine. The total efficiency of condensing end turbine is worse as part of the heat is conducted into sea/lake, even though the electricity production efficiency is better.

Following equations are an example of a CHP plant with simplified back-pressure turbine and are based on (Frederiksen & Werner 2013). Real turbine would have several steam extractions, but those are simplified in this example. Connection of following variables can be found in Figure 5. Produced electricity and heat forms a power-to-heat ratio

$$\alpha = \frac{P_e}{P_q}, \tag{2-1}$$

where power-to-heat ratio α depends on electricity load P_e and heat load P_q. They are determined by ideal enthalpy differences across the each stage of a back-pressure turbine

$$P_e = \dot{m}_{turb}(h_B - h_C), \tag{2-2}$$

$$P_q = \dot{m}_{cond}(h_C - h_D), \tag{2-3}$$

where enthalpy h_B is for live steam, h_C for saturated steam and h_D for saturated water. Note that the subscripts *B*, *C* and *D* are names of stages based on Figure 5. $\dot{m}_{turb}$ is the mass flow of circulation steam through turbine and $\dot{m}_{cond}$ through condenser. In normal run without turbine by-pass flow $\dot{m}_{cond} = \dot{m}_{turb}$ and they can be marked as $\dot{m}$. Saturation enthalpies h_C and h_D are determined by condensation temperature, which depends several factors. DH supply water temperature sets the condensing temperature T_C. The transferred heat through heat exchanger is determined by (Raiko & Saarenpää 2014)

$$P_q = UA\Delta T_m, \tag{2-4}$$

where *U* is heat transfer coefficient, *A* is the contact area of heat exchanger and ΔT_m is logarithmic mean temperature difference, which is calculated from DH water and condensing temperatures accordingly (Raiko & Saarenpää 2014)

$$\Delta T_m = \frac{T_{s,s} - T_{r,s}}{ln\left(\frac{T_C - T_{r,s}}{T_C - T_{s,s}}\right)}, \tag{2-5}$$

where $T_{s,s}$ is the DH supply temperature and $T_{r,s}$ is the DH return temperature. Combining (2-4) and (2-5), the T_C can be presented as

$$T_C = \frac{T_{r,s} - T_{s,s} e^{\frac{(T_{s,s} - T_{r,s})UA}{P_q}}}{1 - e^{\frac{(T_{s,s} - T_{r,s})UA}{P_q}}}. \qquad (2\text{-}6)$$

However, the minimum condensing temperature $T_{C,min}$ is determined by supply temperature and least temperature difference (*LTD*) (*Fin. asteisuus*), which is limited by structural feature of a heat exchanger (Frederiksen & Werner 2013)

$$T_{C,min} = T_{s,s} + LTD. \qquad (2\text{-}7)$$

LTD is the difference between condensing and supply water temperature. LTD decreases along with mass flow, as there is more time to transfer the heat, even though higher flow rate increase the heat transfer coefficient. LTD in condenser normally varies between 2 … 6℃ (Raiko & Saarenpää 2014). By lowering the condensing temperature T_C, both h_C and h_D decrease according to Figure 5.

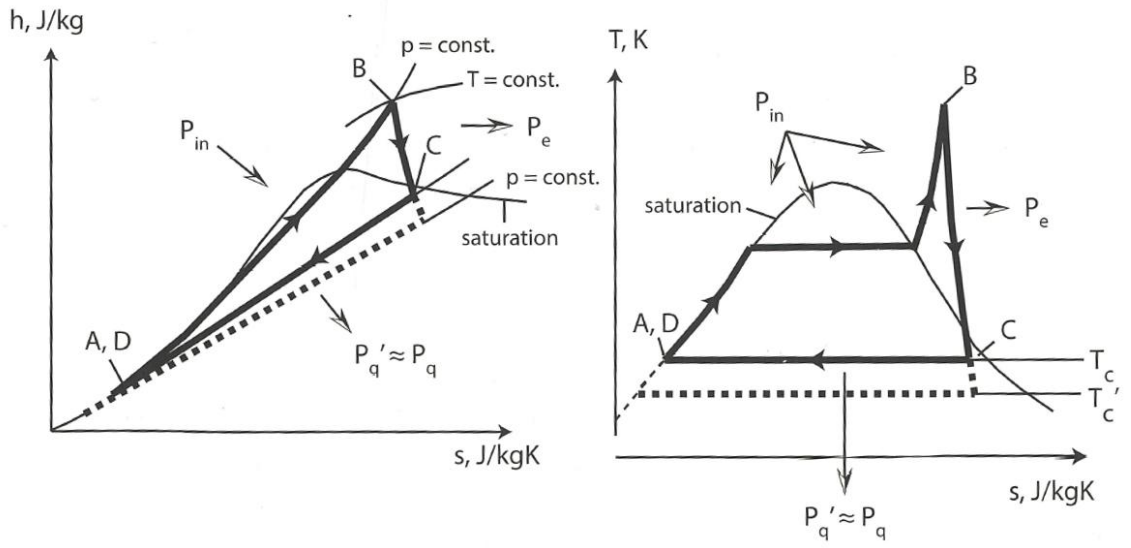

Figure 5. *Mollier hs- and Ts-chart of CHP plant. Dotted line describes the difference of a non-CHP plant (Frederiksen & Werner 2013, p.158).*

According to (2-1), (2-2) and (2-3), the power-to-heat ratio increases as h_C decreases

$$\alpha = \frac{(h_B - h_C)}{(h_C - h_D)}. \qquad (2\text{-}8)$$

In the non-CHP electricity production α defines the total efficiency of the plant, but in CHP, also heat is a valuable product. To respond to the fluctuating heat and electricity demand, a reduction valve can be used for live steam to by-pass the turbine. When reduction valve is used, part of the live steam is directed straight to condenser, reducing power

production and increasing heat production. This decreases the α, but it is used only in case of high demand of heat and low price of electricity.

Heat supplier products heat into network according to

$$\phi_{prod} = \dot{m}\, c_p(T_{s,s} - T_{r,s}), \qquad (2\text{-}9)$$

where produced heat ϕ_{prod} is formed by c_p which is specific heat of water, which is slightly affected by temperature and very slightly by pressure. Fluctuation in DH concept is $c_p = 4.18 \rightarrow 4.24\ \mathrm{kJ/kgK}$, when $(T = 35℃, p = 2bar) \rightarrow (T = 120℃, p = 10bar)$. Temperature difference $T_{s,s} - T_{r,s}$ is the temperature between heated DH water and returning DH water. $\dot{m}$ is the mass flow rate of heated DH water.

On closer review it can be realized that there are not many variables that can be controlled. Return temperature is formed by a sum of heat losses, customer behaviour, outdoor temperature and other disturbances. Mass flow $\dot{m}$ depends on the customer heat consumption with given temperature difference. Hereby the customer supply temperature can be set by supplying the certain supply water temperature for customers.

There might be an urge to increase the heat production as quickly as possible to maximize the condensing load for power production. In short time scale supply water temperature can be increased without decrease in mass flow. This method increases the heat production, which increases the total heat accumulated into the DHN. This might be possible method to implement short time frequency support. Based on Eq. (2-9), the increase in heat production $\Delta\phi$ is achieved by supply temperature difference $\Delta T_{s,s}$ accordingly as $\phi_{prod,0}$ is initial heat production

$$\phi_{prod,0} + \Delta\phi = \dot{m}\, c_p((T_{s,s,0} + \Delta T_{s,s}) - T_{r,s}), \qquad (2\text{-}10)$$

which is reorganized into

$$\phi_{prod,0} + \Delta\phi = \dot{m}\, c_p\left(T_{s,s,0} - T_{r,s}\right) + \dot{m} c_p \Delta T_{s,s}. \qquad (2\text{-}11)$$

By removing the initial heat production, (2-11) is simplified into

$$\Delta\phi = \dot{m} c_p \Delta T_{s,s}. \qquad (2\text{-}12)$$

As a conclusion, with certain change of supply temperature, greater responses on heat production and condensing load can be achieved when mass flow is constantly high.

2.1.2 Heat station

In DHSs, the heat suppliers need to fulfil the customers' needs continuously. As the customer heat load varies significantly, the production has to respond on the demand. The production plants should be planned to produce heat continuously and efficiently and also

to be able to respond to high heat load peaks with heat stations that have low fixed costs. Typically, during high demand of heat, all the demand cannot be produced by CHP plants as their capacity is insufficient, when the heat stations have to be set on. There are also small-to-middle sized bio fuel heat plants and incinerators that are operated continuously. Usage of heat stations depend on local heat and electricity production strategies and prices of the fuels that CHP and heat plants are using.

Principles of heat station are simple compared to CHP, ideally all the produced heat is transferred to DH water according to (2-9).

2.2 DH Customers

All of the DH customers (aka. consumers) have a connection to supply and return pipes of DHN. Each customer has a substation, which consist of heat exchangers and valves. District heating consumer substation usually consist of substation circuits shown in Figure 6 or Figure 7. There are two or more heat exchangers, one for heating system and at least one for domestic water heating. There are control valves after the heat exchangers that control the heat transfer by mass flow.

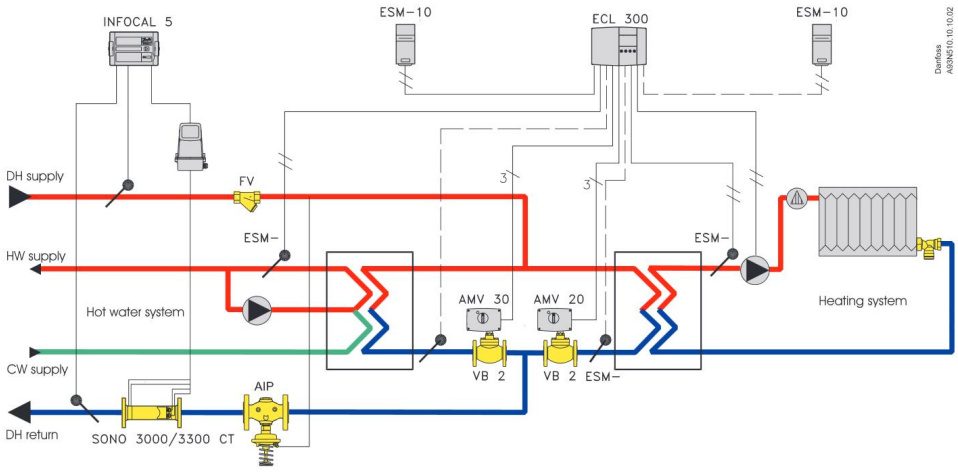

Figure 6. *Parallel system with instantaneous DH domestic water heating system. HW = Hot domestic water, CW = Cold domestic water. (Boysen 2004)*

In Figure 7 the system is similar to Figure 6, but warm $<43\ °C$ return water is used for preheating domestic water.

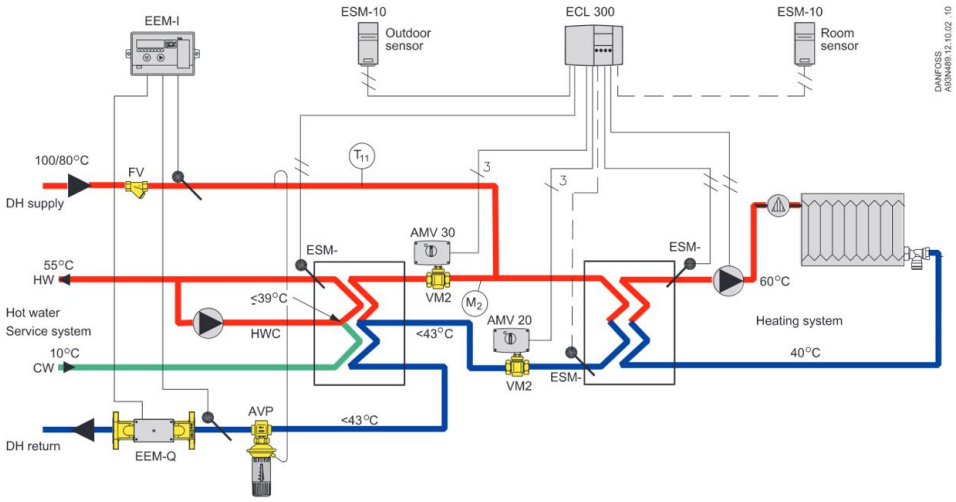

Figure 7. *Two stage system with one DH domestic water heat exchanger. HW = Hot domestic water, CW = Cold domestic water, HWC = Hot water circulation.* (Boysen 2004)

District heating consumer may be a private apartment, a public building or an industrial customer. Their consumption vary a lot during a day and a week. Figure 8 shows the weekly variation patterns of different kind of buildings demonstrating different behaviour and needs for heat usage.

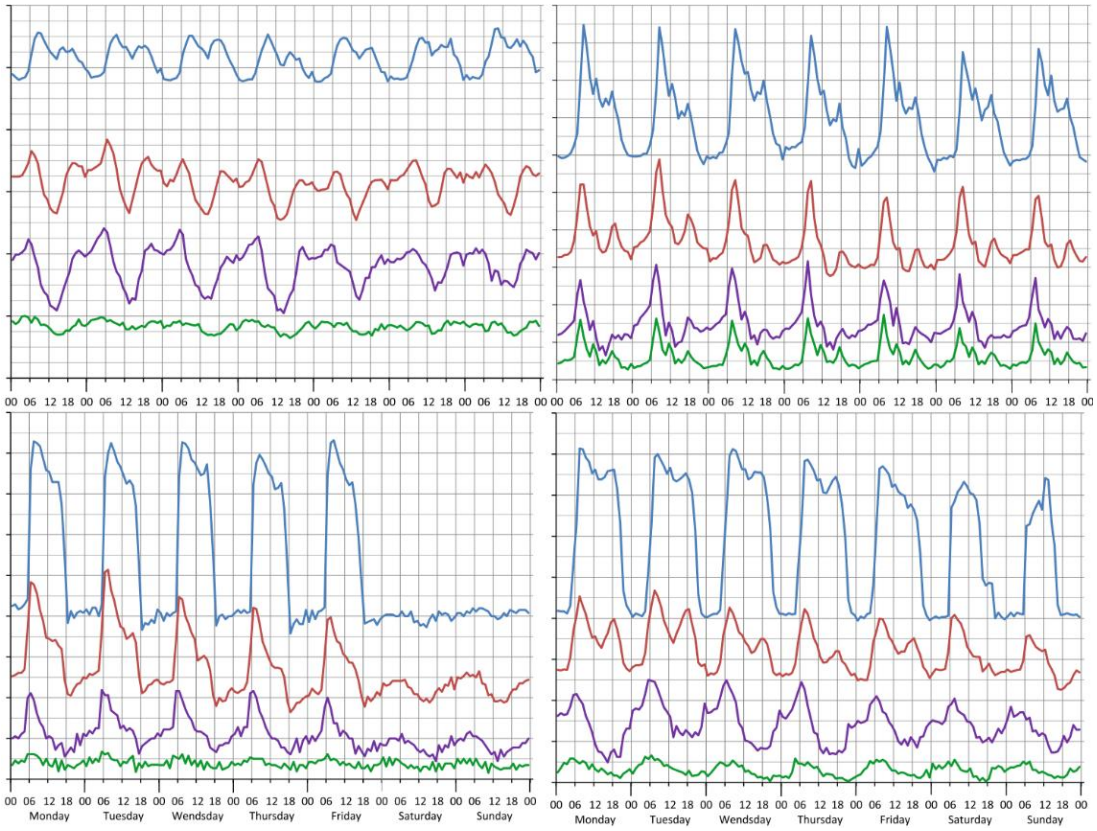

Figure 8. *There are heat loads on vertical axes, green curves are summer loads, violet curves are late spring/early autumn loads, red curves are early spring/late autumn loads and blue curves are winter loads. There are different type of heat consumers, on upper left there is a multi-dwelling apartment house, upper right a public building with night setback, lower left a public building with time clock operation 5 days a week and lower right a commercial building with time clock operation 7 days a week. (Gadd & Werner 2013)*

The heat load seen by the heat supplier is a sum of different kinds of consumers. Even though the consumers' behaviour vary a lot, the differences level off when the consumptions are summed up. For supplier the total heat load variation is more interesting than consumption of individual ones.

Heat load is the quantity of consumption, but quality means how efficiently the customer extracts the heat. The better the heat exchanger and heating system is, the lower the return temperature is. For supplier, low return temperature $T_{r,s}$ is desired, because it reduces flow rate, reduces heat losses, enables lower supply temperature, and also enhances the power-to-heat ratio of CHP plant. Return temperature $T_{r,c}$ depends on the heat exchanger characteristics, which determines the LTD. (Frederiksen & Werner 2013)

$$LTD = T_{r,c} - T_C, \qquad (2\text{-}13)$$

where T_C is the return water temperature of secondary circuit of heat exchanger, which can be seen in example circuit in Figure 9. The $T_{r,c}$ is dependent on LTD and T_C, which can be $T_C \approx 5\,°C$ in domestic water heat exchanger, or $T_C \approx 38\,°C$ in heating system heat

exchanger. As considered in Chapter 2.1.1 the LTD is dependent on flow rate. In Finland there are regulations for heat exchangers, stating that in new building $LTD_{max} = 3\,°C$ (Energiateollisuus 2014).

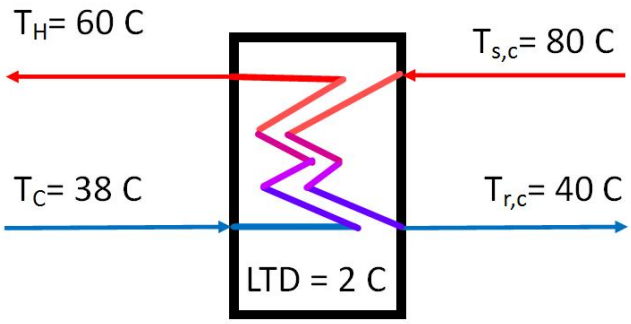

Figure 9. *Simplified heat exchanger. On the right side there is DH circulation and on left side heating system circulation. Values demonstrative.* T_H *can maximally be* $T_{s,c} - LTD$ *and* $T_{r,c} = T_C + LTD$.

Return temperature depends on the system structure. According to Gadd & Werner (2014) the average supply and return temperatures in 142 Swedish DH systems were $86.0\,°C$ and $47.2\,°C$, respectively in 207 Danish DH systems $77.6\,°C$ and $43.1\,°C$. Return temperature was significantly lower in Denmark, mainly because there are no secondary circuits for domestic heating. When the heat exchanger in Figure 9 is left out $T_{r,c} = T_C$ and $T_{s,c} = T_H$. Hereby the supply temperature can be as much lower as the average LTD of heat exchangers in the network. This is the main reason why also the supply temperature in Denmark is lower than in Sweden. Finland was not mentioned in research, but there the substations are similar to Sweden. (Gadd & Werner 2014)

There is a simple parallel heat exchanger system in Figure 10, similar to Figure 6 substation. It demonstrates how the return temperature is formed by mass flows and temperatures after heat exchangers. Hot domestic water circulation (HWC) causes a significant interference in temperature value $T_{r,c,w}$.

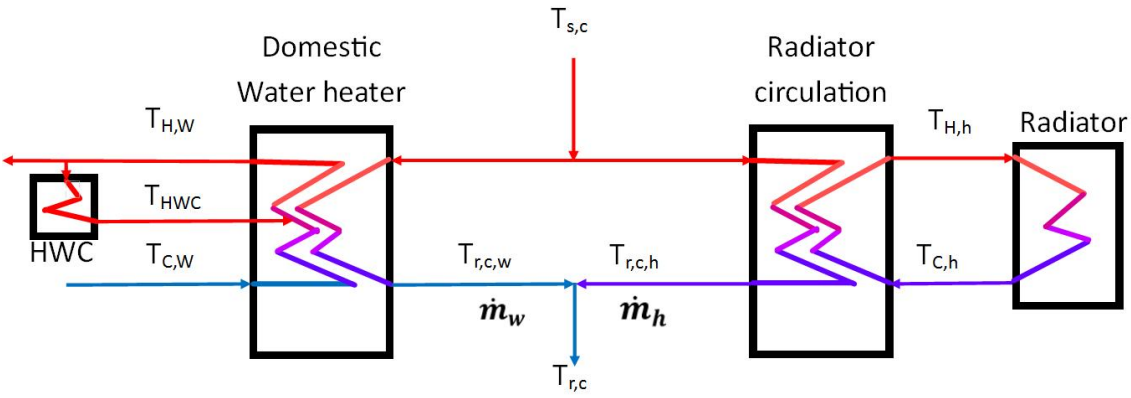

Figure 10. *Simplified figure of heat exchangers in parallel system*

The return temperature of consumer consist of two different temperatures and their mass flows accordingly

$$T_{r,c} = \frac{T_{r,c,w}\dot{m}_w + T_{r,c,h}\dot{m}_h}{\dot{m}_w + \dot{m}_h}, \quad (2\text{-}14)$$

$$\dot{m}_w = \frac{\phi_w}{c_p(T_{s,c} - T_{r,c,w})}, \quad (2\text{-}15)$$

$$\dot{m}_h = \frac{\phi_h}{c_p(T_{s,c} - T_{r,c,h})}. \quad (2\text{-}16)$$

Differences in secondary circuit temperatures $T_{C,W}$ and $T_{C,h}$ cause difference also in $T_{r,c,w}$ and $T_{r,c,h}$.

The domestic water heater is more closely examined in Figure 11 that is similar to more complex system presented in Figure 7. The HWC heats humid rooms by hot domestic water and returns it to domestic water heater at relatively high temperature $T_{HWC} = 54\,°C$, when $T_{H,W} = 58\,°C$. When domestic water is used, the heat exchanger acts efficiently cooling the DH water return temperature near to the cold domestic water temperature. When there is no demand of hot water, but HWC circulates, the return temperature may eventually rise into $T_{r,c,w} = T_{HWC} + LTD$.

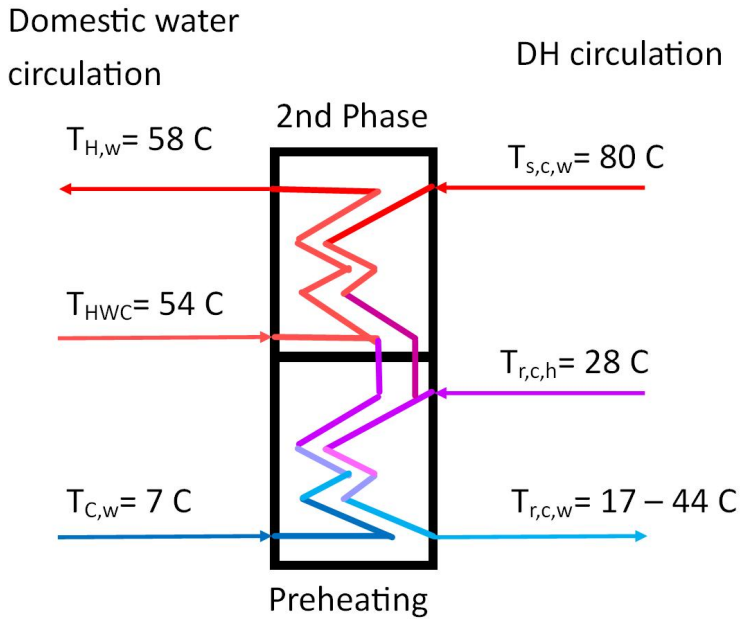

Figure 11. *2-Phase domestic water heat exchanger with hot domestic water circulation and preheating using heating circuit return water. The values in the figure are measured from a case building and are therefore realistic. See Figure 7 for the connections to other devices.*

Figure 12 demonstrates the static response on return temperature and mass flow on function of supply temperature according to (2-14), (2-15) and (2-16). This result show that in theory higher supply temperature would lower the return temperature in parallel heat exchanger system.

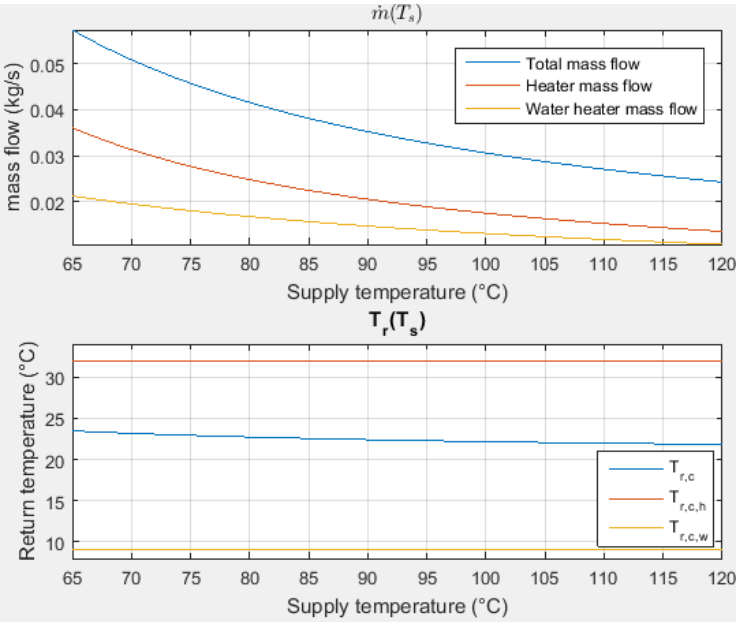

Figure 12. *Supply temperature effect on mass flow and return temperature. Calculations were implemented with demonstrative constant values* $T_{C,h} = 30\ °C$, $T_{C,w} = 7\ °C$, $T_{H,h} = 45\ °C$, $T_{H,h} = 58\ °$, *heat load of both heat exchangers* $P_h = P_w = 5\ kW$ *and* $LTD = 2\ °C$. *h = heating system, w = domestic water heating.*

However, Falkvall & Nilsson (2013) studied that even though return temperature would behave according to Figure 12 as function of supply temperature, there are disturbances and circulation loops that behave oppositely. Those raise the return temperature along with higher supply temperature and their effect in practise is more dominant.

2.3 DH Network and temperature dynamics

The pipeline network connects the heat suppliers and customers, transports the hot water to consumers and cooled water back to supplier. Pipes form a network where the water flows due to pressure difference made by pumps. DHN can be vast and therefore transport delays from heat suppliers to customers vary depending on heat load, supply temperature and the distance from supplier of individual consumer.

A customer heat load can be derived from Eq. (2-9) of produced heat, considering transfer delay dynamics and excluding heat loss, such that sum of produced and consumed heat are equal. In this approach the delay is scalar such that customer supply temperature is only dependent on one supplied temperature (Saarinen 2008)

$$\phi_{del}(t) = \dot{m}(t) c_p \frac{\int_{t-\tau}^{t} T_{s,s}(\delta)d\delta - \int_{t}^{t+\tau} T_{r,s}(\delta)d\delta}{\tau}, \qquad (2\text{-}17)$$

where τ is the transport delay and ϕ_{del} delivered heat load. In this notation the supply water temperature is supplied into the network a time delay τ before consumption and supplier receives the return water temperature after a time delay τ. Note that supply and return delays are same. This is the method to assume heat consumption in case there is no

measurements in the network and the assumption has to be made based on measurements in production plant. However, consumption is measured to charge the customers, but it is not usually possible nowadays to utilize them as online measurements in distributed control systems (DCS). Without customer substation measurements, the current heat load is impossible to determine exactly. It can be calculated afterwards using the measured return temperature at the supplier $T_{r,s}$ to predict earlier return temperatures at customer $T_{r,c}$. Heat demand equation (2-17) can be calculated into form so that uniform delay τ is reviewed as supply τ_s and return τ_r delays.

$$\phi_{del}(t) = \dot{m}(t)c_p\left(T_{s,s}(t-\tau_s) - T_{r,s}(t+\tau_r)\right). \quad (2\text{-}18)$$

To remove the negative delay, (2-18) is delayed by τ_s

$$\phi_{del}(t+\tau_s) = \dot{m}(t+\tau_s)c_p\left(T_{s,s}(t) - T_{r,s}(t+\tau_s+\tau_r)\right), \quad (2\text{-}19)$$

where τ_s is supply heat transfer delay, τ_r return delay, $T_{s,s}$ supply and $T_{r,s}$ return temperature at heat supplier. $\dot{m}$ is the mass flow and ϕ_{del} is delivered heat at customer. Eq. (2-19) can be rearranged to $T_{s,s}(t)$ function

$$T_{s,s}(t) = T_{r,s}(t+\tau_s+\tau_r) + \frac{\phi_{del}(t+\tau_s)}{c_p * \dot{m}(t+\tau_s)}. \quad (2\text{-}20)$$

Equation (2-20) shows that the supply water temperature optimization requires the future predictions of the return water temperature, the mass flow and the heat load. ϕ_{del} is formed by customer behaviour, which can be predicted. $T_{r,s}$ is mostly determined by customer behaviour, therefore it also needs to be predicted. Only two variables, $\dot{m}$ and T_s are detached from customer consumption. They are inversely proportional among themselves and the optimal balance depends on the system characteristics and operation methods. As increased mass flow increases pumping costs and respectively increased supply temperature increases heat losses, there is an optimization problem to determine the right supply temperature.

Delay τ_s in (2-20) is a scalar as there is only one customer and supplier in the model that makes the delay homogenous overall the network. When there are many customers with different delays, the delay is a vector $\boldsymbol{\tau_s}$ that forms a distribution function. The varying delay and determination of optimal rate between temperature and mass flow are challenges for standard control methods.

2.3.1 Pressure dynamics

Water moves in the pipes and forms a mass flow because of the pressure difference between pipe ends. The pressure is formed by a pump at heat production plant and distribution pumps along the pipeline. The flow can be assumed to be always turbulent, as the critical velocity of fully turbulent flow in 100℃ water, in diameter of 30 cm pipe is 0.004

$^{m}/_{s}$. When flow is assumed to be fully turbulent and it flows through the pipes, the pressure drops can be calculated by (Frederiksen & Werner 2013)

$$\Delta p = -\frac{8\lambda L}{d^5\pi^2\rho}\dot{m}^2, \qquad (2\text{-}21)$$

where pressure drop Δp is affected by mass flow $\dot{m}$. Other variables, as Darcy friction factor λ, water density ρ, pipe length L and pipe diameter d can be assumed to be constant. Pipe friction coefficient is calculated through Darcy friction factor. There is an equation by Swamee and Jain, who have solved the friction factor without iteration by equation (Swamee & Jain 1976)

$$\lambda = 0.25\left[log\left(\frac{^{e}/_{d}}{3.7} + \frac{5.74}{Re^{0.9}}\right)\right]^{-2}, \qquad (2\text{-}22)$$

where e is the roughness of surface and Re the Reynolds number of the flow. Reynolds number Re being in denominator, it is significant only at really low flow rate ($v < 0.01\ ^{m}/_{s}$), which is far too low for district heating pipe transfer. Consequently on normal flow rates, the friction factor depends on pipe characteristics and can be generalized to be constant.

Pump stations are controlled to keep the medium pressure and differential pressures at demanded levels. Pressure changes spread in the network at the speed of sound, which in water is 1555 $^{m}/_{s}$ at 80 °C (The Engineering ToolBox 2015). The rapid response simplifies the pressure controls. However, mass flow changes stiffly as there is much inertia in moving water that slowly respond to pressure variations.

Figure 13 demonstrates pressure levels of supply and return pipes. Vertical height of red curve demonstrates the absolute pressure of supply pipe and respectively blue demonstrates the return pipe. It describes how pressure difference decreases towards the end of the DHN and how distribution pumps increase the pressures.

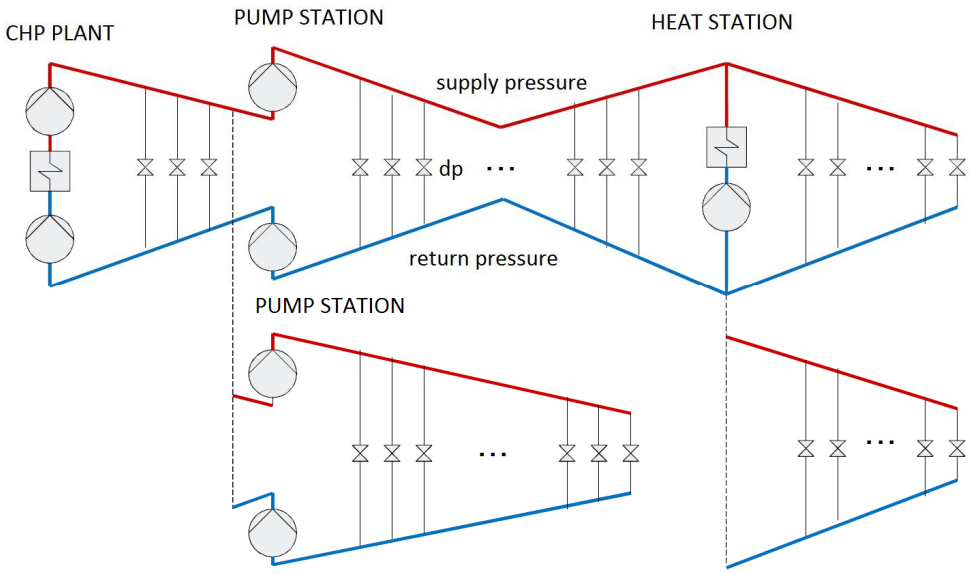

Figure 13. *Pressure levels and flow distribution* (Kaivosoja 2016)

Pumping work depends on the magnitude of the differential pressure and mass flow. (Frederiksen & Werner 2013)

$$P_{p,el} = \frac{\Delta p_p}{\eta_p \rho} \dot{m}, \qquad (2\text{-}23)$$

where Δp_p is pressure difference over pump, η_p pump efficiency and $P_{p,el}$ pump electrical power. Equation (2-23) shows that both mass flow rate and differential pressure are proportional to power. To reduce pumping costs, the income of mass flow rate and differential pressure needs to be minimized. According to (2-21) the pressure loss decreases as mass flow decreases that would mean the pumping energy drops significantly if mass flow can be decreased.

Increasing supply temperature would decrease flow rate, reducing pumping costs, but also raising the heat losses. As most of the energy used for pumping will transform into heat, raising the water temperature, the pumping energy remains in the process. Part of the pumping energy transfers into heat during pumping process and part of it converts into heat as pressure drops in the pipe flow. Temperature increment caused by pump can be derived from Equation (2-9), into form

$$\Delta T = \frac{P_{p,el}\eta_h}{c_p \dot{m}}, \qquad (2\text{-}24)$$

where η_h is the coefficient of pump input power converted into heat of water.

2.3.2 Pipe heat loss

The negative effect of higher supply temperature is higher heat loss. Heat loss results from temperature difference between DH water and surroundings of the pipe. There is

forced convection that transfers the heat from flowing water into inner surface of the pipe. From inner surface it conducts into surroundings and also from hot supply pipe into cold return pipe according to cross-section cut of supply and return pipes in Figure 14.

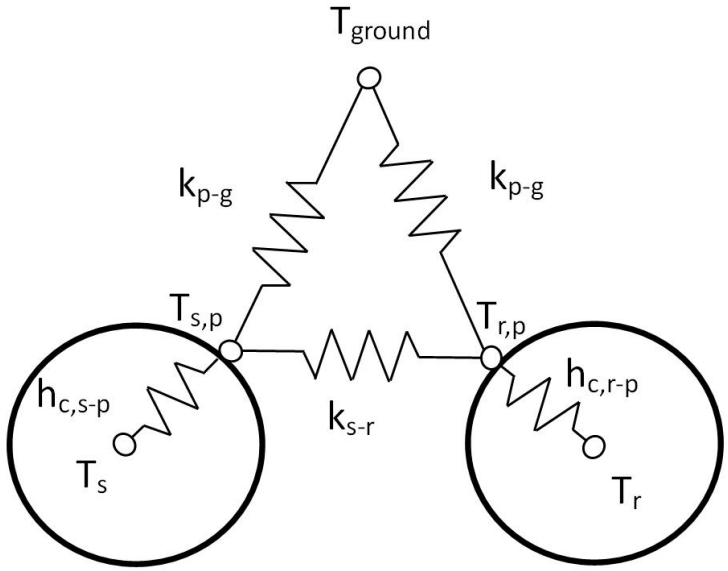

Figure 14. *Heat transfer and thermal resistances.T_s and T_r are the supply and return water temperatures, $T_{s,p}$ and $T_{r,p}$ are pipe surface temperatures, k_{p-g} heat conductivity between pipe and ground, k_{s-r} is heat conductivity between supply and return pipe, $h_{c,s-p}$ and $h_{c,s-r}$ between flowing water and pipe surface.*

The overall heat resistance consists of heat convection between flow and pipe surface and convection in solid materials as pipe metal shell, pipe insulation and soil. The resistance R between water and ground is calculated as (Mills 1999)

$$\frac{1}{R} = \frac{1}{h_{c,s-p}r} + \frac{1}{k_{p-g}+\frac{k_{s-r}k_{p-g}}{k_{s-r}+k_{p-g}}}, \qquad (2\text{-}25)$$

where pipe radius r, conductivities k_{p-g} and $\mathrm{k_{s-r}}$ are constant and heat transfer coefficient $h_{\mathrm{c,s-p}}$ is dependent on water characteristics and velocity. The convective heat transfer coefficient is calculated as (Mills 1999)

$$h_{c,s-p} = \frac{k}{d}\overline{Nu}_d, \qquad (2\text{-}26)$$

where k is heat transfer coefficient of pipe and $\overline{Nu}_d$ Nusselt number. Nusselt number determines the heat transfer of convective flow and it is dependent on velocity of fluid. Figure 15 demonstrates the dependency of heat transfer coefficient and flow velocity in average pipe of Kuopio DHN when the flow is assumed to be turbulent.

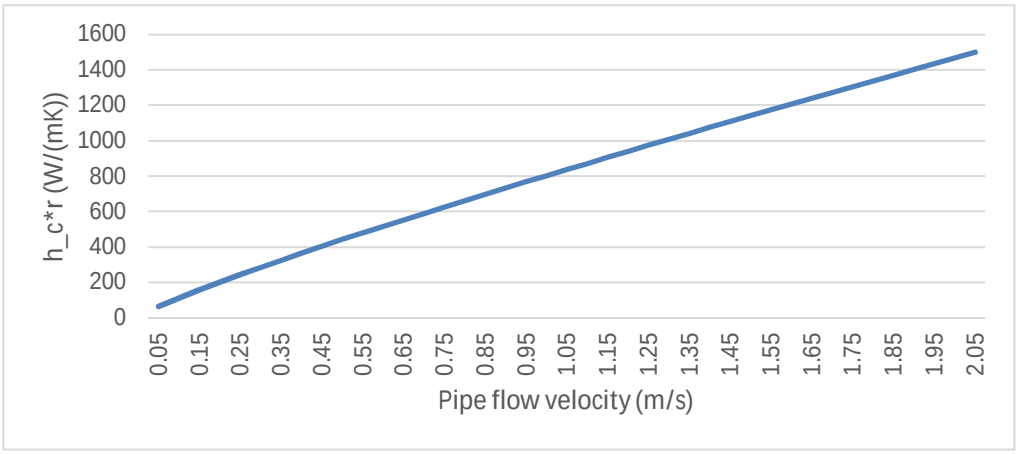

Figure 15. *Heat transfer coefficient of convection in turbulent pipe flow. Calculations made using example values from case study of Kuopio DHN and equations by (Mills 1999)*

As the DH pipe overall heat loss coefficient normally is $R = 0.7 \dots 3\, W/(mK)$ depending on insulations (Ljubenko et al. 2011), the convective heat transfer coefficient is nearly inconsequential when the flow is at normal level of DH. The convective heat transfer from flow to pipe surface is hereby ignored and pipe surface is assumed to be at same temperature than the flowing water. The heat loss of supply pipe is a balance between conduction from supply pipe to ground and to return pipe. The balance is dependent on temperatures and conductivities.

Pipes are insulated to minimize heat conduction, but the insulation thickness is a compromise of manufacturing costs and heat loss costs. Heat transfer between pipe and surroundings comes from (Frederiksen & Werner 2013)

$$\phi_{loss,s} = R_{s-g}\pi L\left(T_s - T_{ground}\right) + R_{s-r}\pi L(T_s - T_r), \qquad (2\text{-}27)$$

$$\phi_{loss,r} = R_{r-g}\pi L\left(T_r - T_{ground}\right) + R_{s-r}\pi L(T_r - T_s), \qquad (2\text{-}28)$$

where heat losses ϕ_{loss} are determined by resistances R $[\frac{W}{mK}]$, based on conductivities in series in Figure 14.

Temperature drop along the pipe is derived from (2-27) into form (Frederiksen & Werner 2013)

$$T_{s,c} = T_{s,s} - \frac{R_{s-g}\pi L\left(T_s - T_{ground}\right) + R_{s-r}\pi L(T_s - T_r)}{\dot{m}c_p}, \qquad (2\text{-}29)$$

where T_s is the average supply water and T_r average return water temperature in the network. Return temperature can be calculated similarly by replacing (2-27) by (2-28) in (2-29). The return temperature may rise if heat transfer from supply pipe to return pipe is greater than heat transfer from return pipe to surroundings. However, for CHP the heat loss in return pipe may be desirable, whereas in supply pipe it is always undesirable.

2.4 Other components

Other components in DHS are heat pumps, accumulators, coolers and connection loops.

2.4.1 Heat pumps

Heat pumps heat the DH water by transferring heat from another, colder substance such as air or water. Heat is transferred by evaporating refrigerant in low pressure and condensing it in high pressure. This way heat can be transferred from low to high temperature. Efficiency of heat pump is determined by coefficient of performance (COP), which is the factor of transferred heat per pumping power. Averfalk et al. (2014) states that the usage of heat pumps is a good way to increase flexibility and usage of renewable energy in DHSs. Power-to-heat technology means that heat is produced using electricity. It is general in Norway and Sweden, where occasionally very low-priced electricity can be produced by hydroelectric power and also by nuclear power in Sweden. There are also heat pumps in Finland, for example in Helsinki and Espoo (Kaivosoja 2016).

Heat pumps are used when the heat source cannot produce high enough temperature to heat supply water with heat exchanger, as geothermal heat or waste heat of industry. The COP of heat pump depends on temperature of DH Supply water. E.g. there are few heat pumps in Lund DHN in southern Sweden, which are dependent on supply temperature. They cannot transfer heat into DH water that is warmer than $76°C$ or $80°C$ depending on pump. Also the COP increases significantly when the DH water temperature is decreased with only few degrees lower. (Falkvall & Nilsson 2013)

2.4.2 Accumulators

Accumulator is a DH water storage that is used for balancing daily variations of DH consumption and production. Accumulator is a large water tank, which is connected to both supply and return DH pipes. Hot supply water floats on top of the accumulator and colder return water is sunken on bottom. Because there is no mixing in the accumulator, hot water with lower density floats on top of the cold water (Persson & Larsson 2014). Accumulators are not usually pressurized in Finland, because pressured tanks are significantly more expensive. That limits the accumulator supply temperature at $100\ °C$, which is the boiling temperature of water at normal pressure. Accumulators are often situated next to CHP plant to provide consistent condensing conditions for CHP, so that heat and electricity production are not that much dependent on DH consumption. Respectively, in Jyväskylä, Finland, the accumulator is situated at the city centre to be close to the consumption (Kaivosoja 2016).

Accumulators are used for levelling the variations of production and consumption, but they are also a good backup if problems emerge in production. The financial advantage is gained when the accumulator is charged at time of low heat demand using low cost fuel

and uncharged at high heat demand preventing usage of expensive fuels at heat-only stations. In Lund DHS the accumulator capasity is 1200 MWh, which could cover the heat demand of the whole network for hours. (Persson & Larsson 2014)

2.4.3 Coolers

Cooler (aka. Auxiliary condenser) is a unit that supports electric production in CHP plant. It cools down hot district heating water returning it back to plant at very cold temperature. The heat is transferred for example to lake or sea through heat exchangers. Cooler is used when electric production is feasible, but DH demand is not high enough to cool down the condenser of CHP plant. Cooler wastes the heat, which makes it poor way to artificially increase the DH consumption for short periods of time. Cooler is practical in case of disruptions in DHN, so that the power plant and its electricity production will not be disturbed, as the heat can be transferred into lake until DHN is in operation again.

2.4.4 Connection loops

Connection loops are thin pipe loops that circulate hot DH water into return water pipe. They are located in the end of connecting pipes which are installed in the DHN such that new DH customers are easily connected into network. Hot supply water flows from supply pipe into return pipe through circulation loop at the flow rate determined by pressure difference over the loop according to (2-21). Heat loss in the loop is minimal but the biggest disadvantages are the increased mass flow and the exergy loss when hot supply water increases the return temperature. The disturbance is most significant when the heat consumption is low at the summer. Connection loops are meant to be temporary, but they may become permanent elements of DHN.

The action of a by-pass loop is similar to connection loop, but it is used to control the flow rate in the end of the network to reduce the cool down during low heat load in summer. Hereby, connection loops may be beneficial during summer if there are no by-pass valves in the DHN.

2.5 Temperature controls

This chapter considers the regulations that set the limitations for controls and what are the possibilities of control systems to manage the process.

2.5.1 Regulations and instructions

Energiateollisuus ry (ET) is the Finnish energy association that sets the regulations and instruction for district heating systems in Finland. Energiateollisuus has set the requirements for substation devices such that heat supplier has certain margins both in supply

temperature and pressure. Table 1 shows the regulations that concern the heat suppliers. There are also regulations for substation control valve actuation that limit the fluctuation and error. However, they are ignored as they have no effect in supply temperature optimization. (Energiateollisuus 2014)

Table 1. *Supply temperature and pressure limitations by Energiateollisuus*

	$\mathbf{T_{s,c}(°C)}$	$\boldsymbol{p_{s,c}(bar)}$	$\boldsymbol{\Delta p(bar)}$
max	120	16	-
design	70	-	-
min	70	-	0.6

According to Table 1, the substations are designed for supply temperature of 70 ℃, which is the minimum allowed supply temperature at customer. Hereby the minimum supply temperature at supplier $T_{s,s}$ has to be higher, such that even the furthest customers receive at least the minimum temperature. In Figure 2 is the instructional control curve of supply temperature. It is dependent on outdoor temperature and is a good guideline for most of the DHSs. However, it is a general guideline and it does not consider the total costs of pumping and heat loss of a real DHS.

2.5.2 Temperature control possibilities

When production mix optimization is excluded, the controls in DHN can be divided into temperature and pressure controls. Temperature controls is based on measured and estimated variables expressed in Figure 3. The total heat load of consumers ϕ_{del} depends on the behaviour of consumers. The mean consumer return temperature $T_{r,c}$ depends on consumer behaviour and substation characteristics. The consumer mass flow $\dot{m}$ is determined by the consumer dependent values ϕ_{del} and $T_{r,c}$ and the customer supply temperature $T_{s,c}$. Customer supply water temperature $T_{s,c}$ is the only variable that can be controlled by supply temperature at supplier $T_{s,s}$. The main objective in supply temperature controls is to find the right balance between mass flow and supply temperature, both of them have their advantages. The challenge is that nowadays only $T_{s,s}$, $T_{r,s}$, ϕ_{prod} and $\dot{m}$ are measurable online, such that they can be used for control purposes.

There are few strategies that are used to control the supply temperature in Finnish DHSs (Kaivosoja 2016)

- Relatively high temperature all the time in accordance with season
- Supply temperature by control curve based on current outdoor temperature, similar to Figure 2
- Network accumulation by manual supply temperature control by experienced operator

- Supply temperature optimization to minimize total costs

Two first methods do not require prediction of future loads. They are simple, but the supplier must have reserve production capacity to respond to the changes of heat consumption. There has to be some buffer in supply temperature so that pumping capacity is high enough during unexpected consumption peaks. The temperature buffer leads to unnecessarily high temperatures in steady conditions. The third method can be executed manually by operators, but they have to predict the peak load and transport delay based on their experiences, weather forecast and history data. This prediction process demands concentration from operators and is inclined to human errors. Fourth method requires computational prediction of heat load and delays that are used in optimization and modelling of the DHN dynamics. Accuracy of prediction and performance of optimization algorithms determine the exploitability of optimized supply temperature curve.

2.5.3 Factors for low temperatures

Low temperature levels lead to smaller heat losses in accordance with (2-27) and (2-28). Lower temperature levels are the current trend in development of the 4th generation DH systems. To be able to apply considerably lower supply temperature, also return temperatures have to be decreased to avoid raise in flow rate levels (Gadd & Werner 2014). It would require updates in substation regulations and substations themselves. For CHP plant, lower temperature level means better electricity production coefficient as condensing temperature decreases according to (2-8). According to Saarinen (2008), lowering the supply temperature increases the power-to-heat ratio α more than lowering as much the return temperature. In 170MW CHP plant in Örebro, decreasing supply temperature by 5 °C would increase electricity production by 4.2 GWh/a and respectively 1.1 GWh/a, if return temperature had been decreased by 5 °C. Low return temperature is also targeted as it increases the efficiency of flue gas condenser, that is e.g. acknowledged in Kuopio CHP plant (Seppälä 2016).

As heat losses reduce along with reduced supply temperatures, the pumping costs will rise. However, pumping costs are usually lower compared to heat losses at high supply temperatures (Saarinen 2010). This is partly consequence of the relatively inexpensive electricity in Nordic countries. Also, the heat losses of pumping are not totally wasted energy as most of the heat is transferred into DH water (Falkvall & Nilsson 2013). Low supply temperature also increases the COP of heat pumps, which was found to be the most important advantage in lowering supply temperature in Lund DH network (Falkvall & Nilsson 2013). Additionally, good results of lowering supply temperature has received also from Nyköping (Saarinen 2010) and Uppsala DHSs (Saarinen & Boman 2012). Based on these results, the low supply temperature is an aim while designing a new control system.

3. METHODS

This chapter examines the methods used in supply water temperature optimization of district heating networks. Methods are explained and reasons for choosing them are presented.

Chapter 3.1 presents a delay distribution model that models the supply water temperature delays from the heat supplier to consumers in the network. In many other studies the delay was regarded as a scalar variable. Saarinen & Boman (2012) applied similar load distribution method in controls, which was based on TERMIS simulation. Delay distribution model in this study is based on calculations of network dimensions, and production and consumption data.

Neural network model presented in Chapter 3.2 predicts the customer heat load and return water temperature. Stochastic model was chosen, because deterministic mathematical model for human behaviour would be too complex task and no such implementation exists. Even though there is a strong correlation between outdoor temperature and return temperature. Saarinen & Boman (2012) implemented a simple temperature curve based on outdoor temperature to estimate return temperature. Stochastic models as ARX (Saarinen 2008), SARIMA (Grosswindhager et al. 2011), soft computing (Protić et al. 2015) and neural network (Eriksson 2012) have been applied for load prediction. As the heat load and return temperature predictors are not the main focus in this research, no further analysis between the methods was done. Neural network was chosen for its satisfactory accuracy, versatile opportunities to compare dependencies and a proper Matlab tool.

Brute force optimizer presented in Chapter 3.3 optimizes the supply temperature to minimize pumping and heat loss costs. Standard linear and nonlinear optimization algorithms were considered but varying transport delay turned out to be problematic. Linear parameter varying model (LPV) with transport delay as varying parameter proved to be plausible solution in marine cooling system (Hansen et al. 2011), but formulation and implementation were challenging at DH (Jochumsen 2010). Hereby simple brute force optimization was chosen for its robust operation and satisfactory performance.

3.1 Delay distribution model

The delay distribution model determines the water and heat transfer dynamics of the network. It is a model that calculates the average customer supply temperature based on a linear combination. It weighs the history supply temperature values by distribution function of delay. The delay distribution function is based on real pipe network layout, which

is used to determine the range and attainability of each customer at certain production plan.

The model is constructed as follows. Firstly, it is assumed that network is well designed, such that water flow can proceed along the shortest route in network from supplier to consumer. As an example, there are two parts of Kuopio DHN in Figure 16, where black dots are individual customers, black lines are the medium to large DH pipelines and red lines are the generalized connections to the nearest nodes of the pipeline. Summing the reference consumption of each consumer and the distance to supplier, histogram in Figure 17 is received.

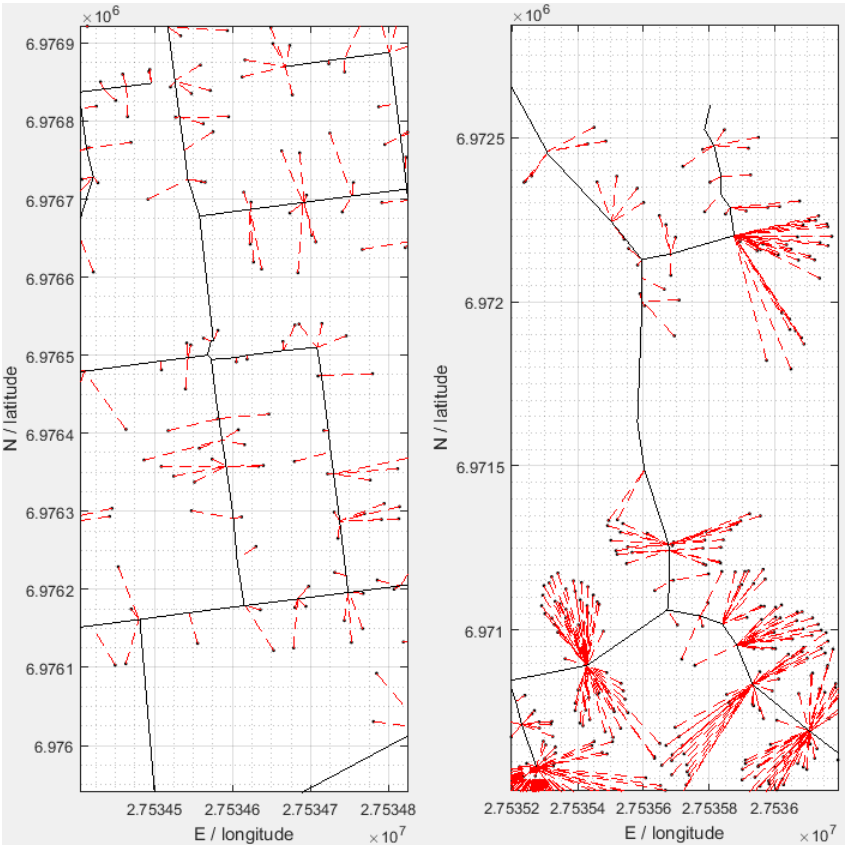

Figure 16. *Parts of Kuopio DHN layout. Distance between customer and supplier is calculated through shortest route along the network through the closest node of the customer. The coordinates are on ETRS-TM35FIN projection.*

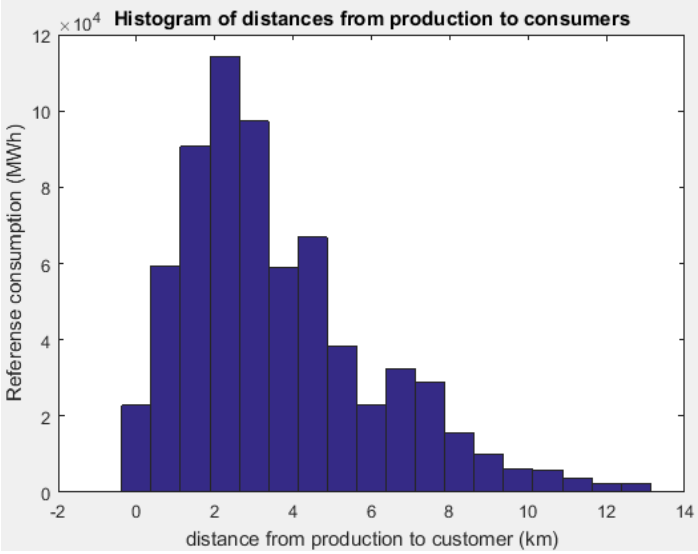

Figure 17. *Histogram of customer consumption in function of distance to supplier*

Assuming that water is incompressible, it can be stated that delay is dependent on distance L and pipe diameter d and inversely proportional to mass flow $\dot{m}$

$$\tau = \frac{\rho L d^2}{\dot{m}}. \qquad (3\text{-}1)$$

According to Figure 18, there are $d \in \mathbb{N}$ consumers. Each consumer is a group of real DH customers that have even delays. Each consumer is fixed such that the 1st consumer has delay of 1 time step, the 2nd consumer has a delay of 2 time steps etc. The shape of distribution function is determined by distance histogram of reference heat loads. In optimization the histogram must be as a function of discrete time delay rather than kilometres.

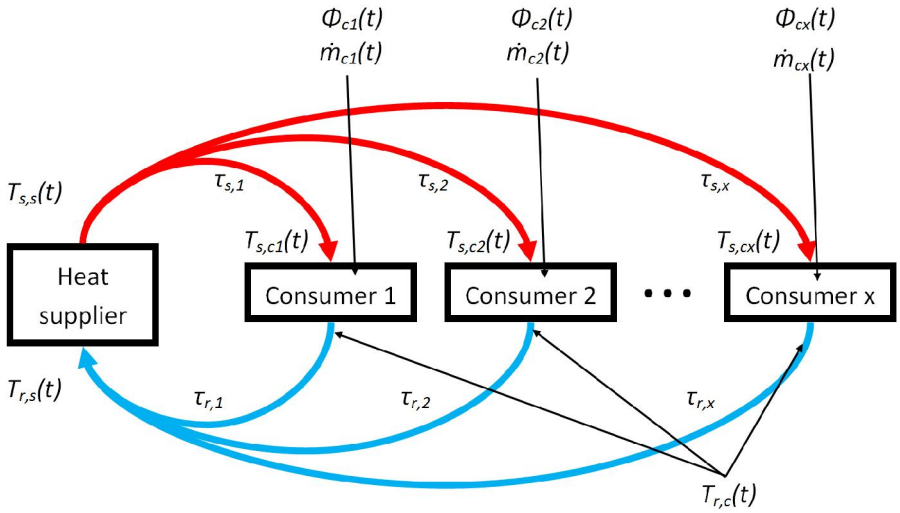

Figure 18. *There are x consumers that are formed by their time delay that is based on their distance to the heat supplier.*

All the real individual customers have reference consumptions $\phi_{c,y}$ and certain distance from presumed production plant that is dependent on current production plan. With the

exact network data, it is possible to calculate how much consumption exists within certain range from suppliers.

$$\phi_p = \sum_{y\in(y_{p-1},y_p)} \phi_{c,y}, \tag{3-2}$$

where $p \in \mathbb{N}$ is the range interval between suppliers and customers, y is the distance of customer to presumed supplier, ϕ_p is the total heat load within certain range where y_p is the maximum range. Histogram of heat load is formed using (3-2) and placed into

$$\boldsymbol{f_{range}} = \frac{1}{\sum_{p=1}^{x} \phi_p} \begin{bmatrix} \phi_1 \\ \phi_2 \\ \vdots \\ \phi_x \end{bmatrix}, \tag{3-3}$$

where unscaled probability vector $\boldsymbol{f_{range}}$ is based on predetermined heat load distribution on range axis. The distribution is scaled according to reference mass flow of the network $\dot{m}_j$ to fit into time scale j time steps. The probability function is scaled into time axis by scaling function f with following inputs. The discrete moment of time $k \in \mathbb{Z}$ and the discrete time step of optimization Δt is a constant, such that $\Delta t \in \mathbb{R}, \Delta t > 0$.

$$\boldsymbol{f_{time}}(k\Delta t) = f\left(\boldsymbol{f_{range}}, \dot{m}_j(k\Delta t)\right). \tag{3-4}$$

Function f scales the $\boldsymbol{f_{range}}$ according to scaling parameter $\dot{m}_j$ such that low value spreads the function in time scale. Finally f fits the scaled probability function into vector of j time steps. Matlab script of f can be found in Appendix A, script 1. The example in Figure 19 describes the function f.

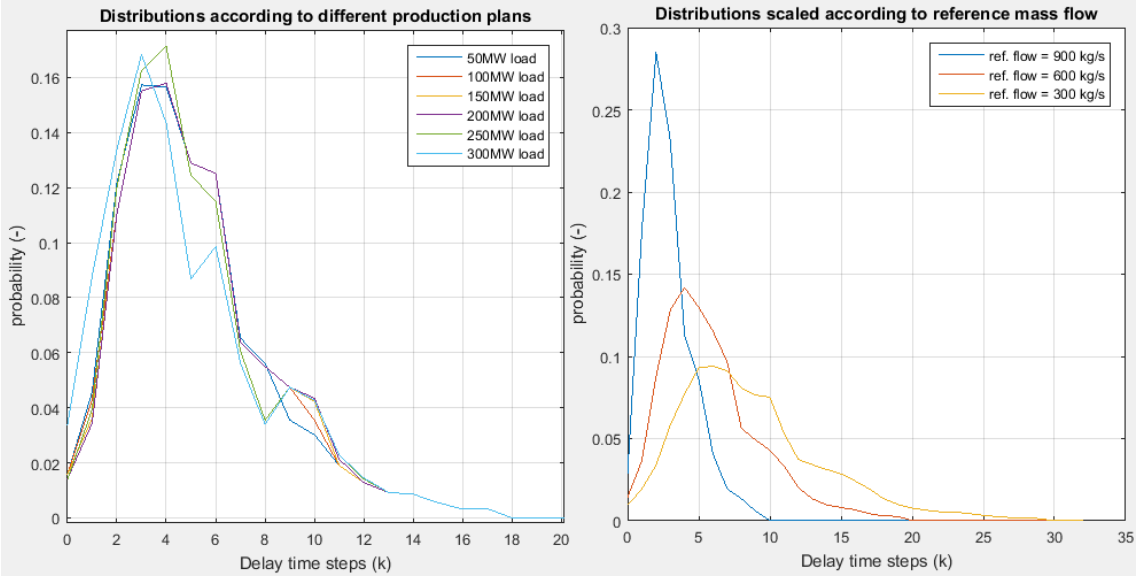

Figure 19. *Function f calculates the* $\boldsymbol{f_{range}}$ *vector into time scale. On the left graph there is variation between* $\boldsymbol{f_{range}}$ *because production is more distributed into different plants as heat load is high. The mass flow is constant to demonstrate the different shapes on different loads. On the right graph the reference mass flow scales the function while* $\boldsymbol{f_{range}}$ *is constant.*

Theoretical customer temperature $T_{s,c,th}$ without disturbances is

$$T_{s,c,th}(k\Delta t) = \left[T_{s,s}(k\Delta t)\, T_{s,s}\big((k-1)\Delta t\big) \cdots T_{s,s}((k-j)\Delta t)\right] \boldsymbol{f_{time}}(k\Delta t). \quad (3\text{-}5)$$

Delay distribution model also considers heat losses and pumping energy, which are considered with network-specific parameters in equation

$$T_{s,c}(k\Delta t) = T_{s,c,th}(k\Delta t) - K_1\hat{\tau}(k\Delta t)\left(T_{s,c,th}(k\Delta t) - T_g(k\Delta t)\right) - K_2\hat{\tau}(k\Delta t)\big(T_{s,c,th}(k\Delta t) - T_{r,c}(k\Delta t)\big) + K_3\dot{m}_c(k\Delta t)^x, \quad (3\text{-}6)$$

where K_1 is heat loss factor to surroundings, K_2 is heat loss factor to return pipe, $\hat{\tau}$ the average delay, K_3 pumping energy factor, T_g temperature of ground surrounding the pipes and *x* the parameter to determine the relation between pressure difference and mass flow. The return temperature at supplier is calculated similarly, except the heat transfer from supply pipe increases the temperature of return water

$$T_{r,s}(k\Delta t) = T_{r,s,th}(k\Delta t) - K_1\hat{\tau}(k\Delta t)\left(T_{r,s,th}(k\Delta t) - T_g(k\Delta t)\right) + K_2\hat{\tau}(k\Delta t)\big(T_{s,c,th}(k\Delta t) - T_{r,c}(k\Delta t)\big) + K_3\dot{m}_c(k\Delta t)^x. \quad (3\text{-}7)$$

3.2 Neural network predictor

Artificial neural networks (ANN)s were used to predict both customer heat load and customer return water temperature. Both of them are weather dependent, and they have cyclic patterns, affected by human behaviour. Return temperature fluctuation patterns are more predictable, but the overall variations are much less significant than with heat load. Hereby, creating a reliable heat load model is more important and challenging task compared to customer return temperature.

Heat load prediction is highly dependent on outdoor temperature and daily cycles. Correlation to outside temperature is significant, because heating demand increases as temperature decreases. Another factor for total heat load is a social load, which means an increase or decrease in heat load because of human behaviour. Some consumption habits depend on day of the week and some ones on time of the day, as hot water usage. Heat load model should thus model both heating demand and the influence of human behaviour.

There are several stochastic methods to predict heat load according to measurement data. Autoregressive-moving-average model ARMAX, was used to predict the load by Saarinen (2008). Soft computing approach to heat load prediction was examined by Protić et al. (2015). ANN modelling of heat load was applied by Eriksson (2012). ANN approach was chosen based on those results and also for positive experience and tutorials with Matlab neural network -tool. The main difference between this study and (Eriksson 2012) is that the target is not to predict the supply heat load, but the consumed heat load.

ANN is a stochastic model where the neurons in hidden layer are trained to produce demanded output with given inputs. Each neuron has inputs $q_1 \dots q_n$, that are weighed by factors $w_1 \dots w_n$, n being the number of inputs. Multilayer perceptron (MLP) is an ANN model that is used in this work. Figure 20 shows the MLP construction.

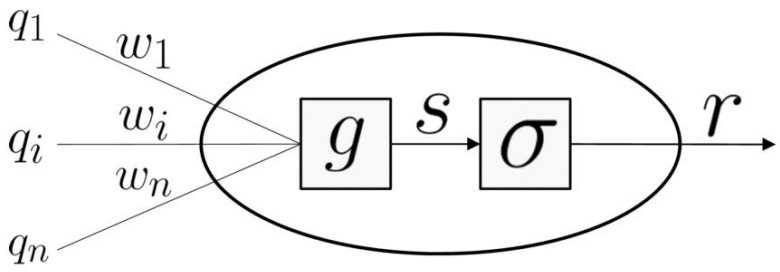

Figure 20. *Hidden neuron of MLP (Eriksson 2012).*

Using Figure 20 notations, the value of neuron is *s* that comes from function

$$s = \sum_{i=1}^{n} w_i q_i. \qquad (3\text{-}8)$$

The sigma σ in Figure 20 is an activation function, which for example may be a sigmoid or a hyperbolic tangent function. It activates and determines the direction of neuron output according to magnitude of function s. (Eriksson 2012)

There are several training algorithms to train the hidden layer neurons. Training is an optimization problem, where mean square error is the cost function and weights are the optimized variables. The optimization algorithm used in this work is Levenberg–Marquardt backpropagation that is used to train the network. The ANN models used in this study consist of 7 inputs and 10 neurons in hidden layer. The layout and inputs of heat load predictor can be seen in Figure 21.

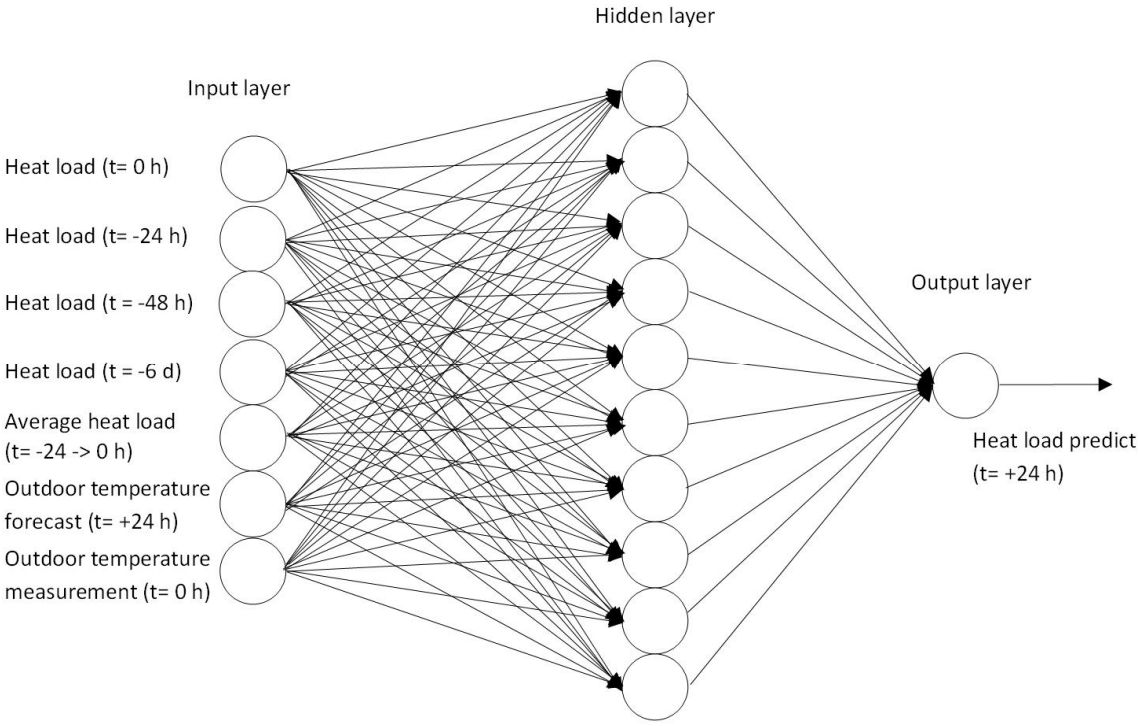

Figure 21. *Neural network model of heat load predictor set up. Return temperature predictor is similar, but heat load measurements are replaced by Return temperature measurements*

Also customer return water temperature was predicted using ANN. Inputs were same than in heat load predictor in Figure 21 set up, but heat loads are replaced by customer return water temperature measurement history.

3.3 Brute force optimizer

The brute force optimizer is based on brute force search that simply calculates the costs for all of the given alternatives to find the lowest cost. The supply temperature trajectories are made for 24 hours in the future with discrete time step of 0.5 hour. The heat loss and pumping work are modelled, costs are calculated and lowest of them is chosen.

The optimizer determines the best plan for supply temperature for next 24 hours to gain minimum total running costs. Optimization algorithm uses predicted heat load and return temperature to predict the behaviour of the system. The variables used in optimization are:

- Customer heat load prediction
- Customer return temperature prediction
- Supply temperature history data
- Fuel price estimation tables
- Electricity price tables

Delay distribution model is embedded into optimization algorithm to model the dynamic response of supply temperature. Delays are calculated for each time step, but all of the trajectories use the same delays. However, they are recalculated after optimization is completed and optimization is iterated as long as delays settle. Delays are calculated by integral

$$\int_{z-del}^{z} \dot{m}(k\Delta t)dk\Delta t = cm, \qquad (3\text{-}9)$$

where reference delay del is calculated by integrating mass flows to the history as long as network mass m multiplied by network coverage parameter $c \in (0:1)$ is reached. There is a chart of data flow in Figure 22 that describes the data flow of optimizer.

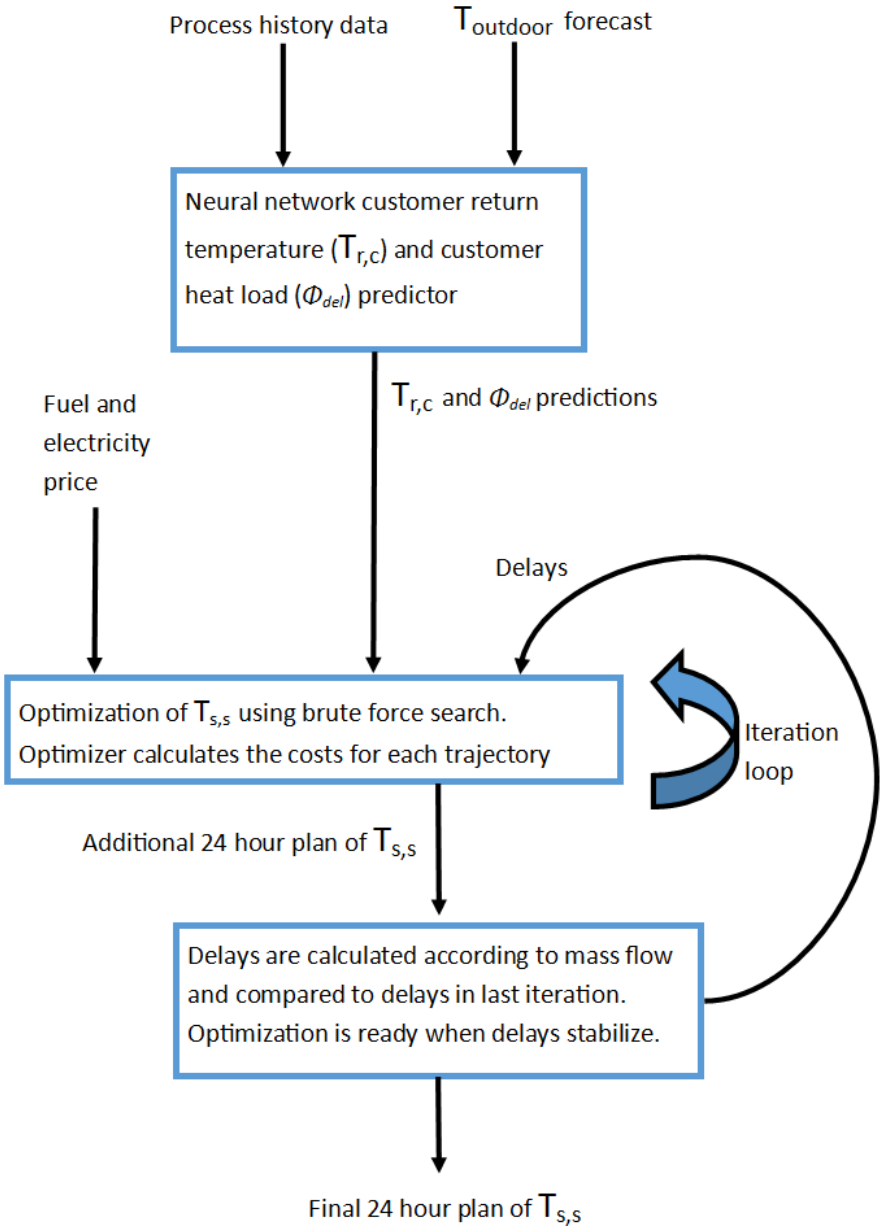

Figure 22. *Block diagram of optimization.*

3.3.1 Trajectory creation

Optimizer creates all the possible supply temperature trajectories 6 steps ahead and continues another 18 steps with fixed values to ensure that the final state of DHN accumulation in all of the trajectories is same. Without that, the optimizer would naturally minimize the accumulated energy in the network in the end of each optimization. The time step is $\Delta t = 0.5$ hours which is short enough compared to the transport delays. To restrict the number of trajectories, there are only seven possible gradients: 0 °C/Δt, ±1 °C/Δt for minor changes, ±2 °C/Δt for moderate changes and ±5 °C/Δt for extreme changes. Within these limitations together with minimum and maximum temperature limitations, the trajectories are created. Trajectories form a diamond-shaped figure that can be seen in Figure 23.

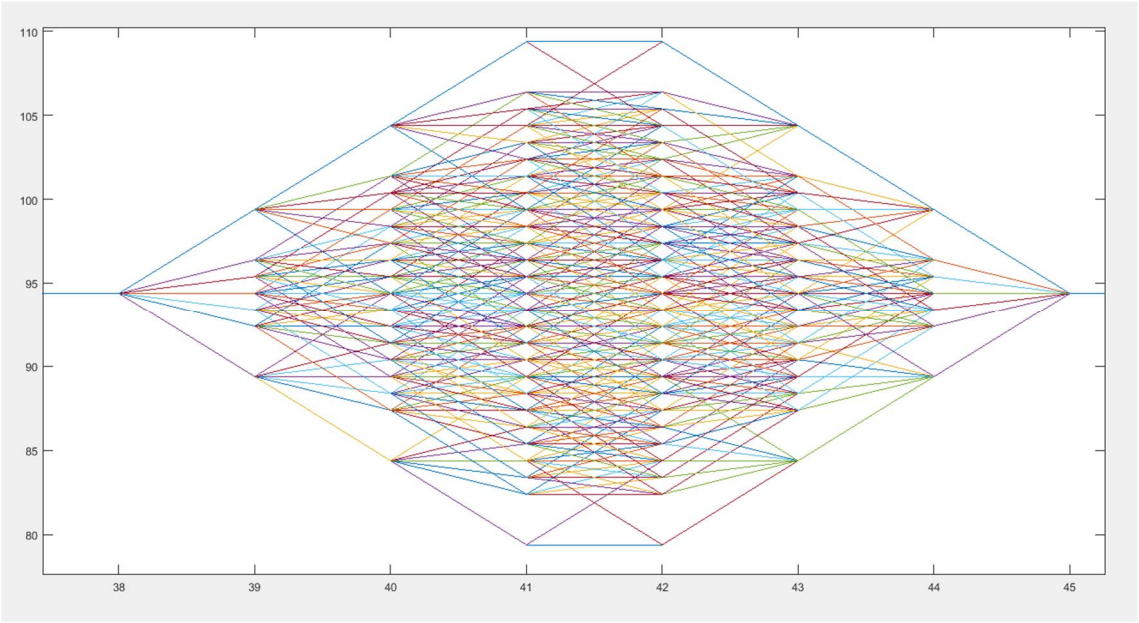

Figure 23. *Supply temperature trajectories. Note that 6 steps are optimized such that 7th step is fixed. All of the trajectories has steps 7-24 fixed such that the final customer temperature in all of the trajectories would be same.*

Even though the system is optimized 6 time steps forward, only the first step value is acknowledged and the same routine is repeated 48 times to optimize whole 24 hours.

3.3.2 Cost calculation

After trajectories are created, the customer supply temperature is calculated through delay distribution model (3-6) and mass flow from energy equation to all of the time steps for all trajectories. Functions used in optimization are presented below. They are formed to take into account all of the main cost factors. Cost function (3-10) does only consider usage of DHN, not electricity production.

$$J(k\Delta t) = C_{pump}(k\Delta t) + C_{heatloss}(k\Delta t) + C_{penalty}(k\Delta t), \quad (3\text{-}10)$$

which consists of simplified cost functions

$$C_{pump}(k\Delta t) = a_1 E_{el}(k\Delta t)\Delta p(k\Delta t)\dot{m}_c(k\Delta t), \quad (3\text{-}11)$$

$$C_{heatloss}(k\Delta t) = a_2 E_{fuel}(k\Delta t)\frac{\left[K_1\left(T_{s,s}(k\Delta t) - T_g(k\Delta t)\right) + K_2\left(T_{s,s}(k\Delta t) - T_{r,c}(k\Delta t)\right)\right]}{\dot{m}(k\Delta t)}, \quad (3\text{-}12)$$

$$C_{penalty}(k\Delta t) = a_3\left[T_{s,s}(k\Delta t) - T_{s,s}((k-1)\Delta t)\right]^2, \quad (3\text{-}13)$$

where a_1 and a_2 and are constant parameters depending on system dimensions, a_3 is a tuning parameter, Δp is the reference pressure difference over the pumps, T_g the ground temperature around the DH pipes. E_{fuel} is the average price of fuels used hourly and E_{el} the total price of electricity based on hourly spot price.

The result of optimization is a supply temperature curve for next 24 hours with discrete time step of 0.5 hours. The result is a local optimum but not a global one because of discreteness and restricted gradients. Optimization restrictions stated earlier in paragraph 3.3.1 are compromises of optimization accuracy and calculation performance. To loosen the restrictions, the result might get closer to global optima but respectively optimization time would be extended.

4. CASE STUDY

This chapter firstly introduces the case of Kuopion Energia. The Kuopio DHN was modelled, parameters were chosen and models were verified by measurement data. No test runs were conducted by real DHS of Kuopio, the results are based on simulations with verified models. The second part of this chapter analyzes the network based on production and consumption data.

4.1 Case Kuopion Energia Oy

Kuopio is a town of 112 201 inhabitants (Väestörekisterikeskus 2016) in Eastern Finland. Climate in Kuopio is rather cold compared to towns in southern Finland, average temperature of January and February being $-9\ °C$ and the extreme around $-37\ °C$ (Weatherbase 2016). The possibility of very cold winter temperatures affect the design temperatures of the DHS. Therefore the system has to be designed for high demand of heat. The Figure 24 describes the monthly average and record temperatures of Kuopio.

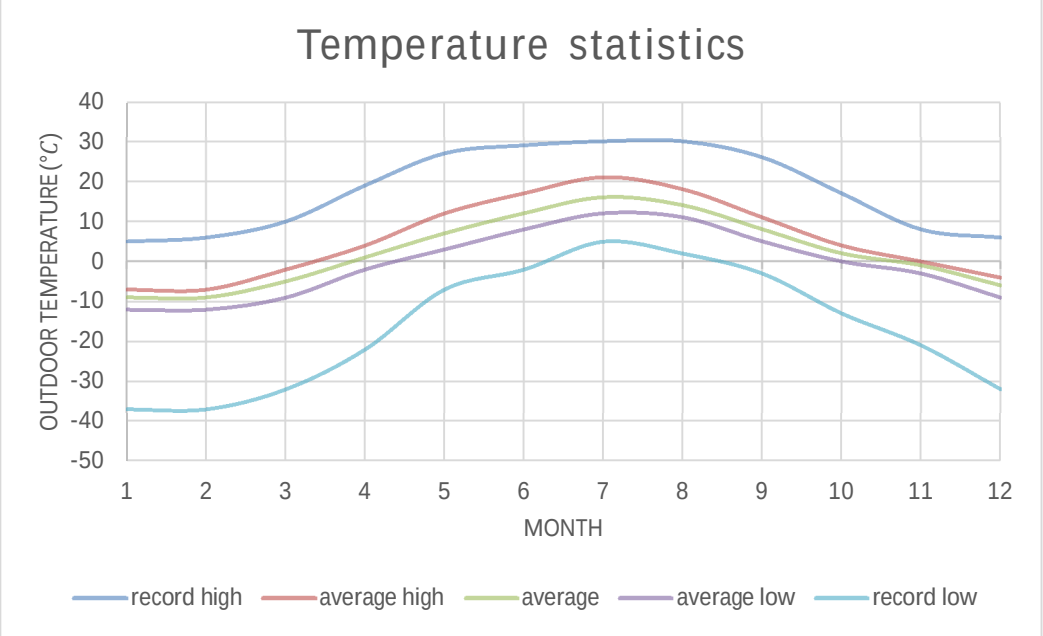

Figure 24. *Kuopio average outdoor temperatures (Weatherbase 2016)*

The main statistics concerning the DHS of Kuopio are collected into Table 2.

Table 2. *Network statistics are based on latest data of DHN construction. Data with *(2014) are based on year 2014 statistics collected by Energiateollisuus (2015)*

Network statistics		
Total length (SUPPLY/RETURN)	470	km
Volume (SUPPLY+RETURN)	17 280	m3
Total DH water mass	$1.676*10^7$	kg
Average pipe diameter	153	mm
Number of customers *(2014)	5778	
Annual DH production *(2014)	971	GWh
Annual DH consumption *(2014)	865	GWh
Consumed energy/length *(2014)	1.84	GWh/km

The DHN consists of different sized pipes and customers. The largest transfer pipes and all of the customers are drawn in Figure 25. Only the locations of consumers are presented, not their consumption. Biggest consumption is in the city central, where most of the apartment houses are located. The locations of CHPs and heat stations (HS) are also presented in Figure 25. More information about production units is listed in Table 3.

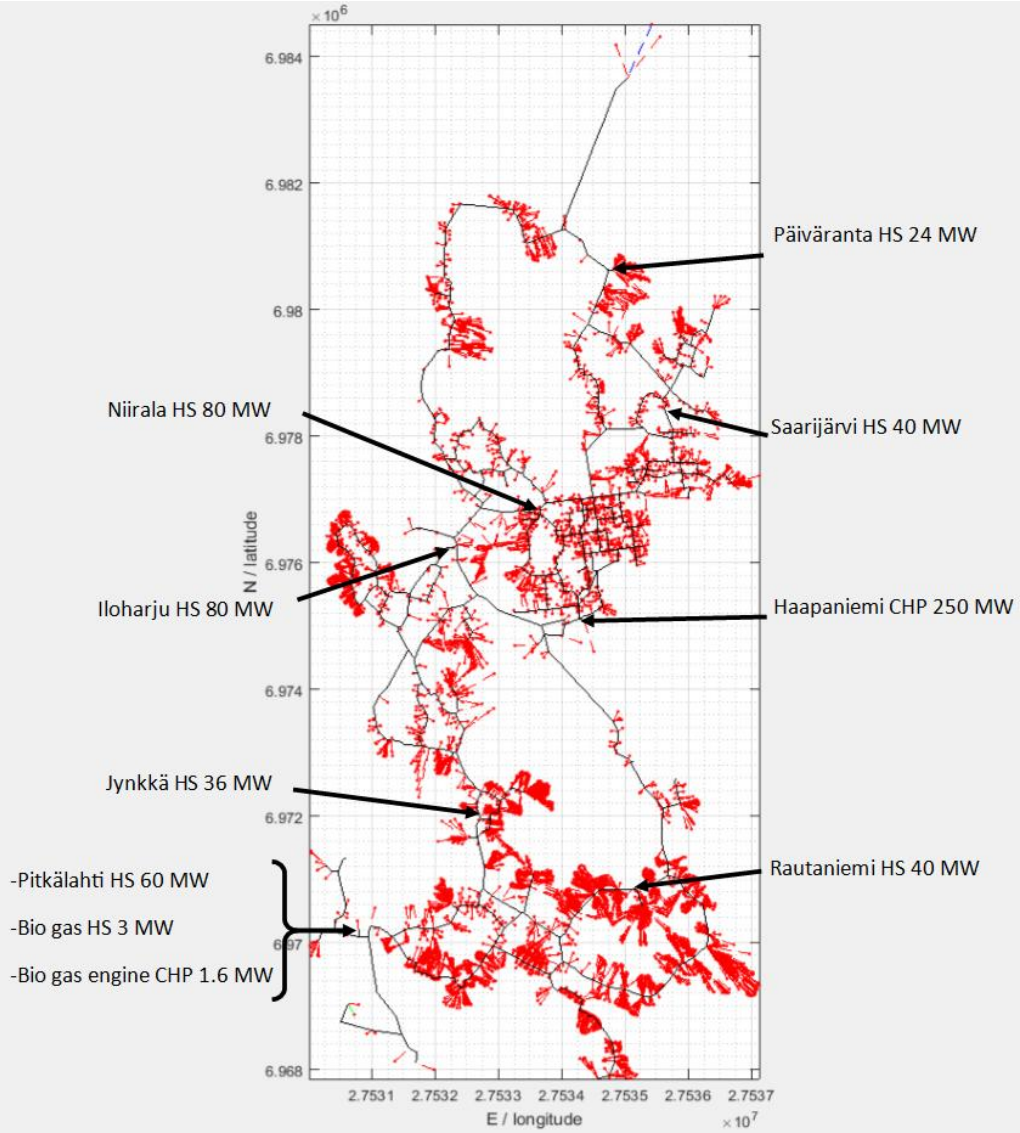

Figure 25. *Kuopio DHN, main transfer pipes are marked as black lines, customers as red dots and production plants are marked and named with arrows. Nominal heat production of HS and CHP have also been marked.*

The total heat consumption of DH customers in 2015 is presented in Figure 26. Demand is low during summer, when building heating is minimal. Most of the heat is used for heating the domestic water. In winter the heat consumption is much higher, especially during the three peaks in January caused by cold outdoor temperatures. However, the winter 2015 was warmer than the average, which decreased the number of high heat load days and the maximum peak loads.

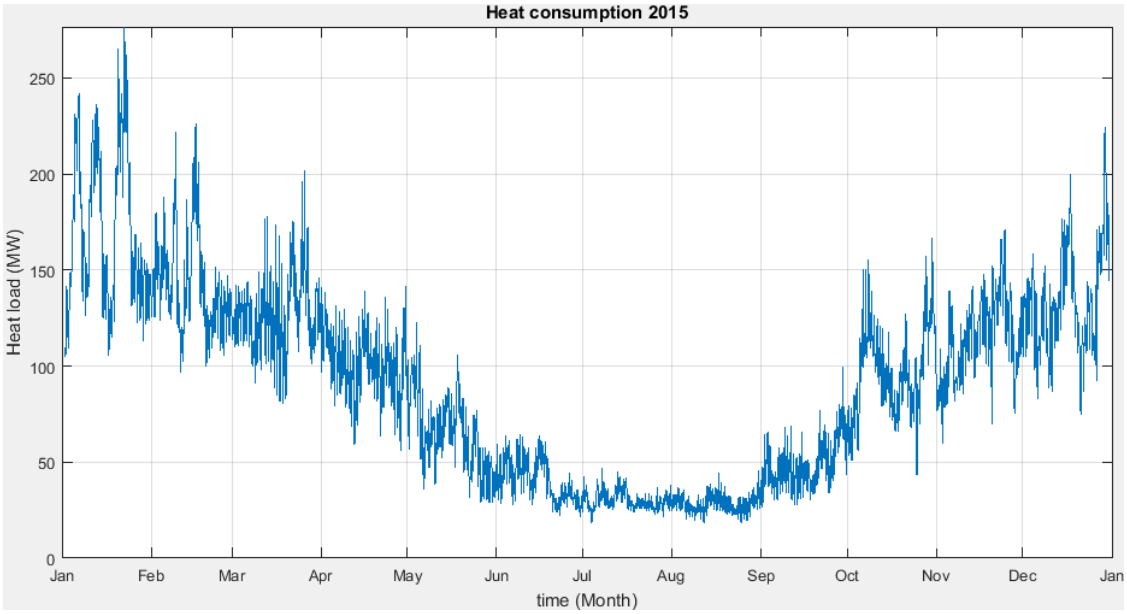

Figure 26. *Heat consumption of Kuopio DHN in 2015*

The information of heat production stations is shown in Table 3. The production fleet consists of two CHP sites, Haapaniemi and Pitkälahti bio gas engine plant, that produce most of the demanded heat. The site in Pitkälahti consists of 2 x 30 MW fuel oil heat-only boilers, one 3 MW bio gas heat-only boiler and a bio gas CHP engine with 1.6 MW DH production capacity. There are also six heat stations in the network that use heavy or light fuel oil and they are used only when the heat production of CHP and bio gas plants is insufficient. Also two transferable 7.4 MW heat stations exist in reserve that are not marked in Figure 25 as they were not used at all in 2015. The peak load time with full production capacity is 64 days and 9 hours (1545 hours).

Table 3. *CHP plants and heat stations statistics*

Plant	**Heat production capacity (MW)**	**Fuels**	**Production (MWh) (2015)**
Haapaniemi 2 & 3	250 (300*)	Wood chip and peat, coal as reserve, oil for start and stop	902596
Pitkälahti bio gas engine CHP and bio gas HS	1.6 (CHP) + 3 (HS)	bio gas	12767
Saarijärvi	40	heavy fuel oil	4095
Jynkkä	36	heavy fuel oil	3182
Niirala	80	fuel oil	2940
Päiväranta	24	fuel oil	733
Iloharju	80	fuel oil	454
Rautaniemi	40	heavy fuel oil	157
Pitkälahti	60	fuel oil	55
Kelloniemi (movable)	7.4	fuel oil	0
Neulamäki (movable)	7.4	fuel oil	0
Total	628.4		926980

*From autumn 2015

Heat is produced mainly in Haapaniemi CHP plant site which consist of two units. Haapaniemi I was put into service in 1972, Haapaniemi II in 1982 and Haapaniemi III replaced Haapaniemi I in 2013. They all are situated in the same site and therefore in perspective of district heating network they can be seen as one heat source.

Kuopion Energia has an interest on maximizing bio fuels and peat usage, and minimize oil usage, especially heavy fuel oil. With construction of Haapaniemi III and modernization of Haapaniemi II in 2010s, the production capacity by CHP has increased to 300 MW. Hereby Haapaniemi can cover most of the demand with its two units. The oil fired heat-only stations are used to fulfil the deficiency of heat only during highest winter peaks. Heat stations were more important before the construction of Haapaniemi III, also DHS should be able to deliver the heat even if the largest unit is out of order. Kuopion Energia is aiming to terminate the usage of heavy fuel oil at latest 2018. Based on Table 3 and Figure 27, which shows the annual total fuel usage of CHP in Haapaniemi, the total heat production by fossil oil is 1.3 %.

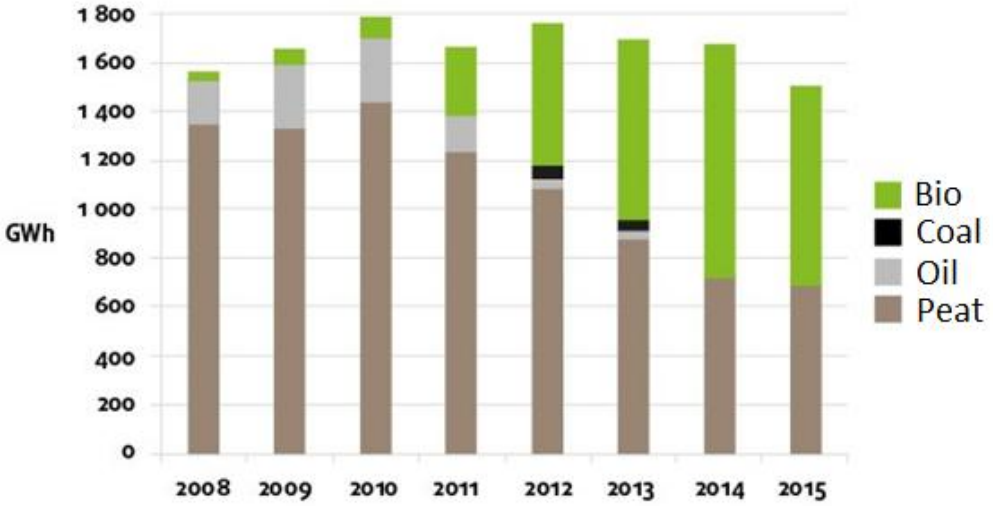

Figure 27. *Heat sources of Haapaniemi CHP plants. Bio (wood chips, bio gas and industrial waste wood), peat (grinded peat) and oil (fuel oil and heavy fuel oil). (Kuopion Energia 2016)*

4.2 Data analysis in Kuopio DHN

Kuopio DHN is reviewed on basis of data from year 2015. Production data is based on history database of Valmet DNA automation system, consumption data is based on average numbers of customer substation measurements from customer billing system and network dimensions are based on pipe network data.

Supply temperature controls in Kuopio are based on current outdoor temperature and supply temperature curve by Energiateollisuus. They also do manual accumulation to load the network before heat load peaks. It is rather good baseline and also implemented quite

successfully based on Figure 28. There are no values over 110 ℃, because of underpowered condensing pump in Haapaniemi. Therefore maximum supply temperature during 2015 was 110 ℃. The pump was planned to be upgraded during 2016, which allows supply temperatures up to 120 ℃ (Seppälä 2016). This limitation is taken into account in optimizer restrictions.

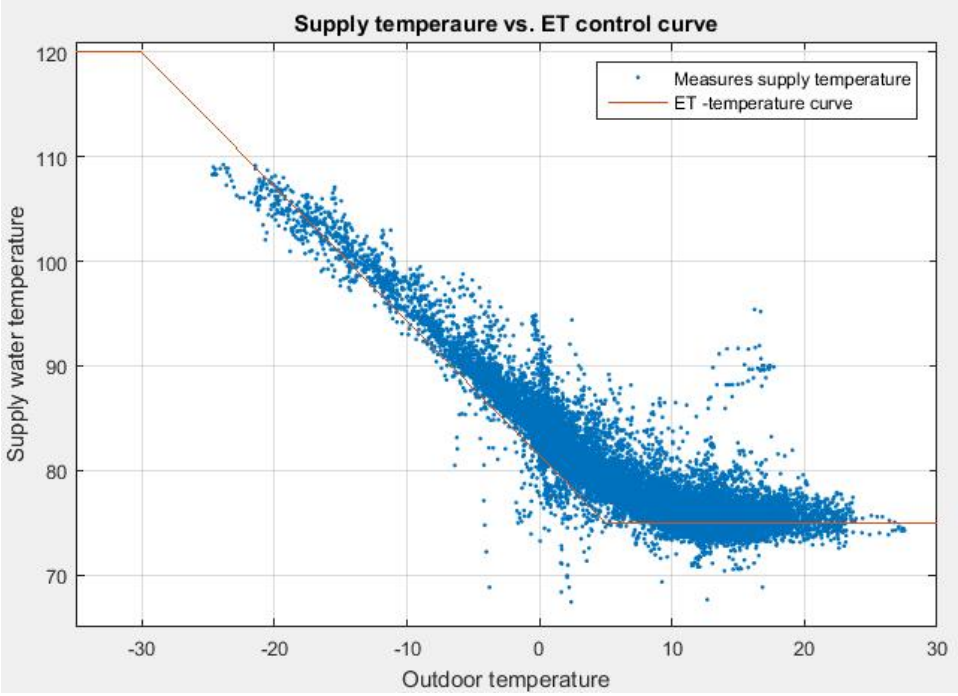

Figure 28. *Measured supply temperature and control curve by Energiateollisuus as a function of outdoor temperature.*

The comparison between supplied and consumed mass flows appoint that there is an difference between 80 – 130 kg/s. The difference could be a by-pass flow, caused by the connection loops mentioned in paragraph 2.4.4. However, further calculations on return water temperature and total heat loss proved that the flow cannot be that significant. Based on these calculations, it is assumed that consumption flow should be 35 kg/s higher round the year, reducing the by-pass flow. The corrected by-pass flow is presented in Figure 29 together with produced mass flow.

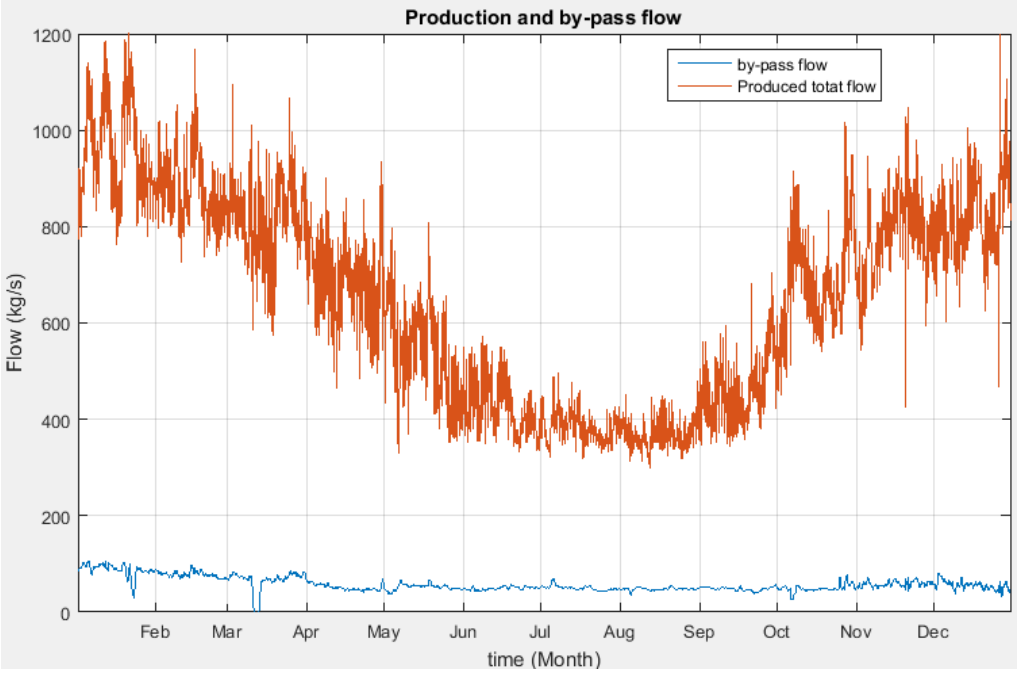

Figure 29. *Mass flow rates of production and corrected by-pass flow caused by connection loops. The by-pass flow is a 24 h moving average, to reduce the noise caused by transport delay.*

The percentage of heat loss to heat production is calculated in Figure 30. The heat loss is quite constantly between 5 – 9 % from autumn to spring. At summer the heat loss rises up to around 16 – 20 %. Reduced flow rate increases the temperature drop, while heat loss is dependent on temperature difference between flowing water and ground. Consequently, heat consumption decreases more radically than heat losses during summer.

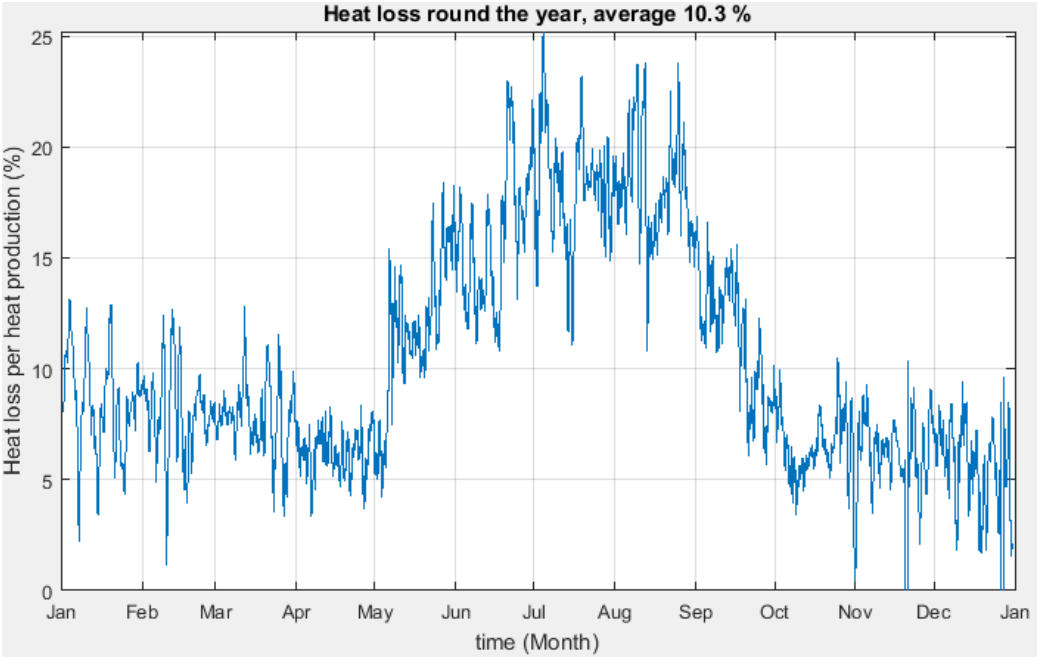

Figure 30. *Heat loss in percentage to heat production. Moving average of 24 hours reduce the noise, caused by the heat transport delay.*

The by-pass flow through connection loops is also seen as increased return temperature as hot supply water mix with return water from customers. Return water temperature should not cool or heat much on the way back from consumer substations to production plant as heat transfer from supply pipe is roughly at the same level than the heat loss to the ground. However, because of the connection loops and pumping energy, the return water temperature increases according to Figure 31. The temperature increase is around 2 - 3.5 ℃ whole year.

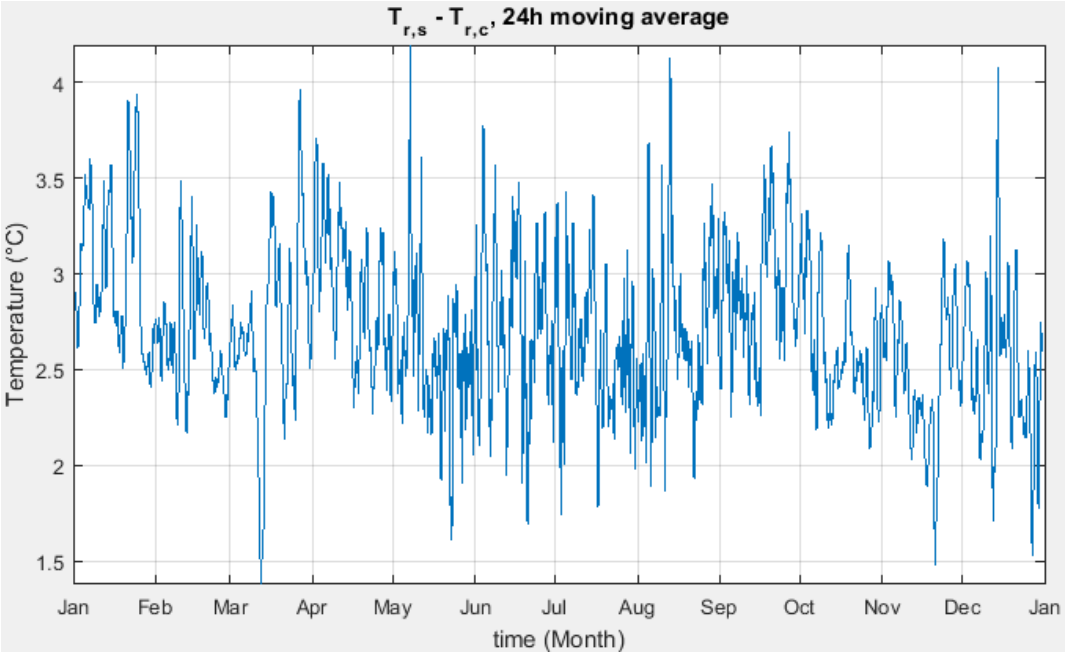

Figure 31. *Temperature rise of return temperature from customer to supplier.*

The customer return temperature behaviour can be seen in Figure 32. The shape is distinctive and verifies the conclusions made in chapter 2.2. Domestic water heating is detached from outdoor temperature, but dependent on time of the day. At day time the return temperature is lower than at night time as return water from domestic water heater is considerably lower than from estate heating heat exchanger. When the outdoor temperature is < 6℃ the water temperature in radiator circulation sets the return temperature. The radiator circulation temperature increases as heat load rises. When outdoor temperature is over 15 ℃, the domestic water heating is dominant, but because of the HWC the return temperature rises if not hot water is used. Highest return temperatures (52 ℃) are most likely received during summer nights when HWC has formed a relatively high share of the heat consumption.

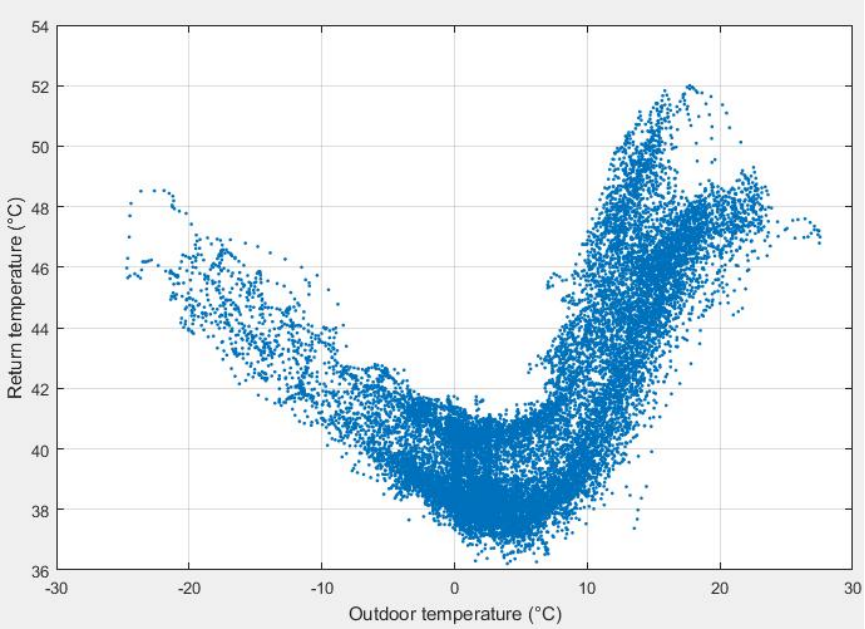

Figure 32. *Customer return temperature as a function of outdoor temperature*

5. MODEL CALIBRATION

This chapter covers the calibration of the models presented in the Chapter 3 with data of Kuopio DHS. The performance of heat load model and delay distribution model are considered and set-up for optimization is introduced.

5.1 Heat load and return temperature modelling

Customer heat load and return temperature predictions of Kuopio DHN are modelled by ANN. The ANNs were calculated by Matlab's nftool. The prediction window used in this work is always 24h. Inputs are as stated in Figure 21, but there are two ways to define them, measurements on consumption data and estimations from production data.

Training of ANN needs enough data to find out the connections between input and output data reliably. To train an ANN, 70 % of the data is used for training to find the connections, 15 % is used for validation and 15 % for testing. The mean squared error and regression between output and target are used to measure the performance of trained ANN. The network is assumed to create a similar output with case data as it does with the training data, but change of the season and network overfitting are two main reasons why the ANN output may differ from target. If the ANN is overfitted, it cannot create anything sensible output with other than training data. This is avoided by separately training 10 parallel networks and using an average of the six median values as an output. To guarantee that the 10 parallel ANNs are up to date, one of them is retrained every 25 hours with the measurement data from last 3500 hours. 3500 hours was chosen as the accuracy of prediction increased considerably as the period was prolonged until 3500 hours.

There were data available from 1.1.-31.12.2015 in this study. As this method updates the ANN predictors continuously, the same data can be first used as a target data and later as a training data. Hereby the same data can be used for validation and training. Challenge was to get the training data for first months, as 2014 data was not available. It was solved by assuming that the end of the year 2014 was similar to 2015, and hereby 2015 data was used for training as 2014 data.

5.1.1 Return water temperature modelling

Return water temperature prediction is simpler than heat load prediction, as it is directly measured both at customer substations and at suppliers. The return temperature that needs to be modelled is the average customer return temperature. It is measured in every customer substation, but the data is not usually available online for automation system. If substation data is not available online, the reference return temperature for customer can be estimated from delayed supplier return temperature. The delay is calculated by Eq. (3-

9). The neural network is trained with both data input methods, but the target data is the measured consumer return temperature. The resulting curves can be seen in Figure 33. Predictions are very accurate during winter because of relatively high usage of house heating heat exchangers and respectively quite inaccurate during summer because of relatively low usage of predictable house heating heat exchangers.

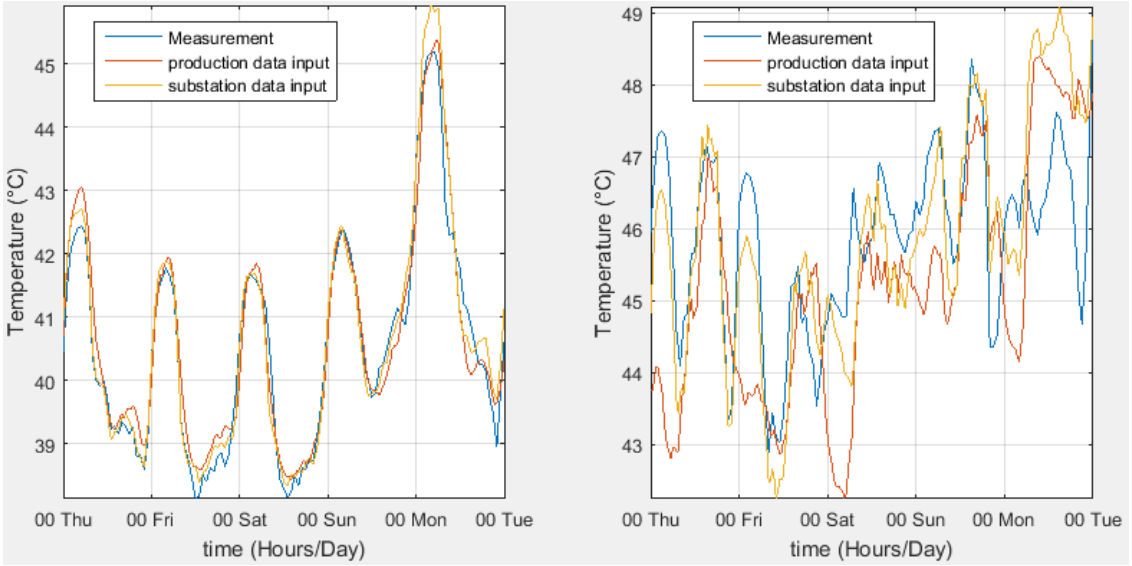

Figure 33. *Return temperature predictions vs. measurement. Graph on the left is from winter and on the right from summer.*

Figure 34 shows the histogram of prediction accuracy on both methods.

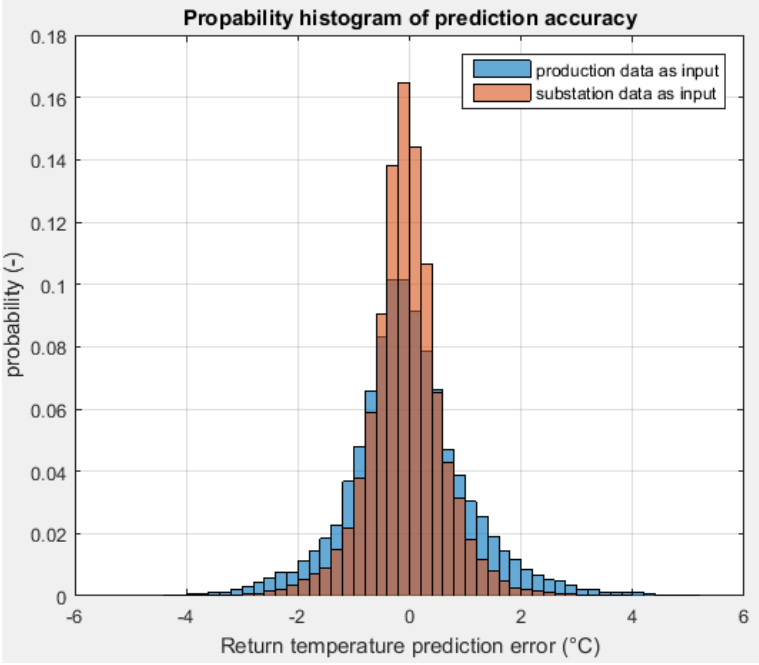

Figure 34. *Return temperature prediction accuracy. The standard deviation is 0.78* ℃ *for production data input and 0.49* ℃ *for substation data input.*

5.1.2 Heat load modelling

Heat load model predicts the total heat consumption of the customers in the DHN. Heat load can be accurately calculated by energy equation using customer substation data, but the data may be impossible to get online in most DHSs. The heat load can also be estimated from measured production data by Eq. (2-18) such that supply delay is calculated by Eq. (3-9). Network was trained with production and substation data as inputs and measured heat consumption as a target.

There is a comparison of heat load prediction methods and measured heat load in Figure 35. Predictions correlate quite accurately with the measurements when the daily patterns of the curves are clear. In these examples the challenge of irregular peaks can be seen.

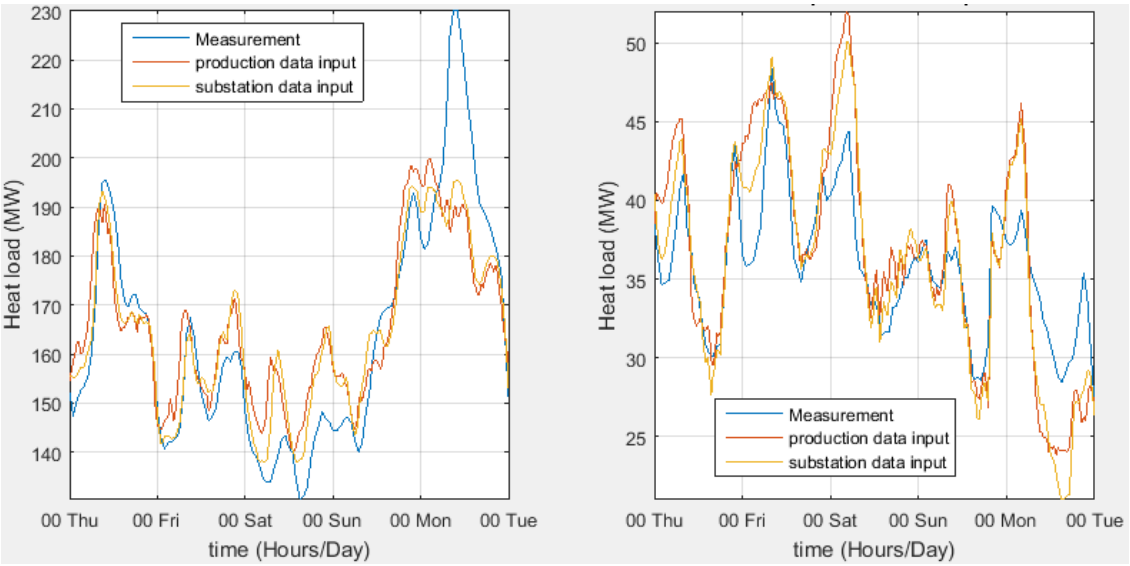

Figure 35. *Heat load predictions vs. measurement. Graph on the left is from winter and on the right from summer.*

Histogram of prediction accuracy is shown in Figure 36.

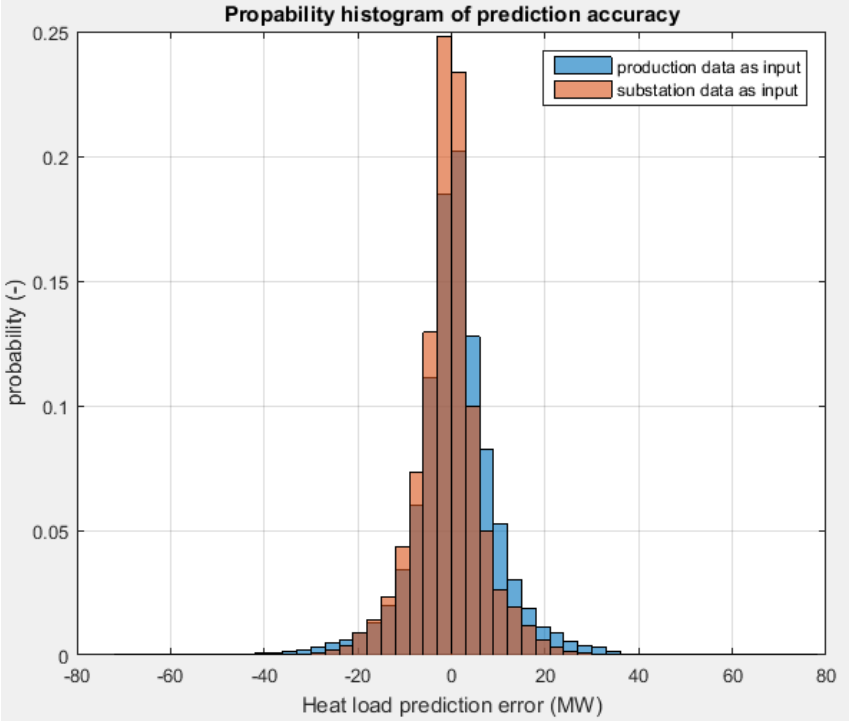

Figure 36. *Heat load prediction accuracy. The standard deviation is 6.30 MW for production data input and 4.90 MW for substation data input.*

5.1.3 Conclusions of neural network modelling

According to figures above, all of the models are quite accurate and applicable for optimization. The ones where substation data was used as measurement data are clearly more accurate than predictions. Doubtless the prediction of future values of certain measurement are more precise if history values of the same measurement can be utilized as a training material. However, production data method is chosen for ANN input data because it is more realistic in current situation, even though the accuracy is weaker. Possibly the DHN monitoring progresses in the future, providing more useful data to import for predictions.

One problem on training ANNs with data from last 3500 hours (~4.8 months) for prediction of the next 250 hours (~10 days), is that the training data is mostly from different season. The greatest error occurs during first cold temperatures in autumn demonstrated in Figure 37. When temperature drops, the predictions drag predicting too low heat loads. After the predictions have caught the target value, the predictions drag again predicting too high heat loads.

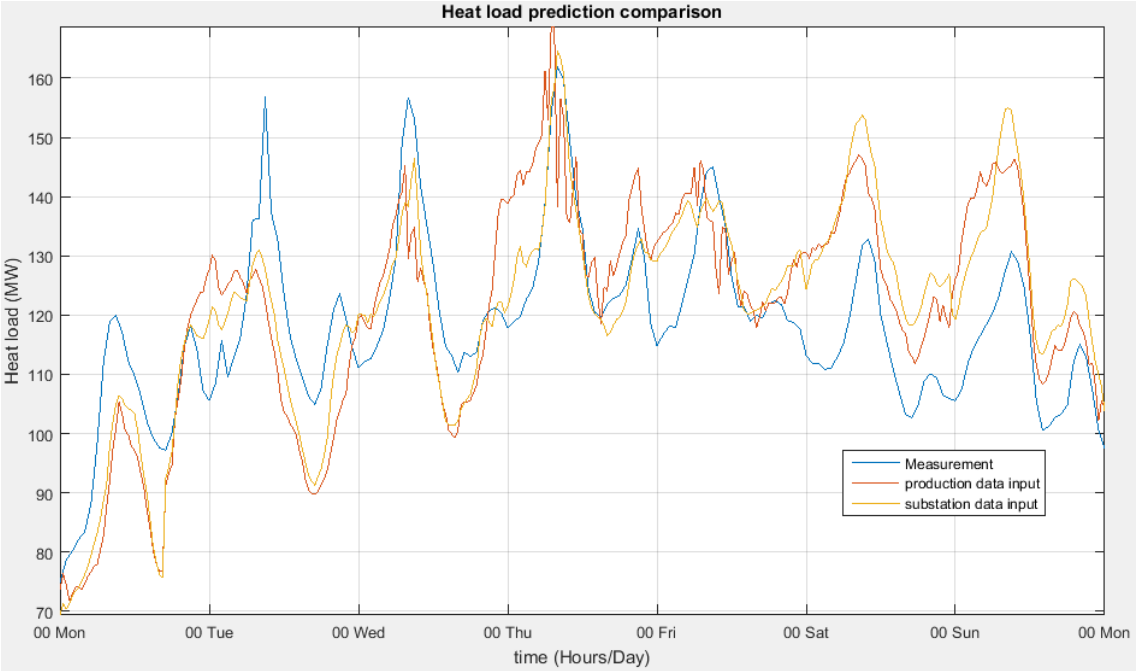

Figure 37. *Prediction error is most significant during first cold outdoor temperatures in autumn*

The error in Figure 37 that occurs during change of season, could be compensated by training some of the 10 parallel ANNs with data from year last year at the same season.

5.2 Pumping energy estimation

Pumping energy cannot be measured precisely as not all of the pressures and mass flow are measured. To determine the total pumping energy, some estimations have to be made to define all the cost parameters. Also for optimization, the pressure has to be a function of mass flow.

Pressure difference in the system is important, because it has a significant effect on pumping costs, and it increases together with mass flow rate. Hereby, the correlation between pressure difference and flow rate needs to be defined. According to measurements in Figure 38, the pressure difference correlate quite linearly to mass flow rate with $\Delta p \approx k_1 \dot{m}_c$, where k_1 is a constant parameter. Total pressure difference is formed from pressure difference over customer control valves and pressure loss from pipe transports (2-21). When the heat demand increases, customers open their control valves to increase the mass flow similarly decreasing the pressure difference over the valve. Hereby the share of pressure loss of water flow and the pressure difference over the control valve varies according to mass flow. The linear trend line and correlation of pressure difference over Haapaniemi CHP plant can be seen in Figure 38.

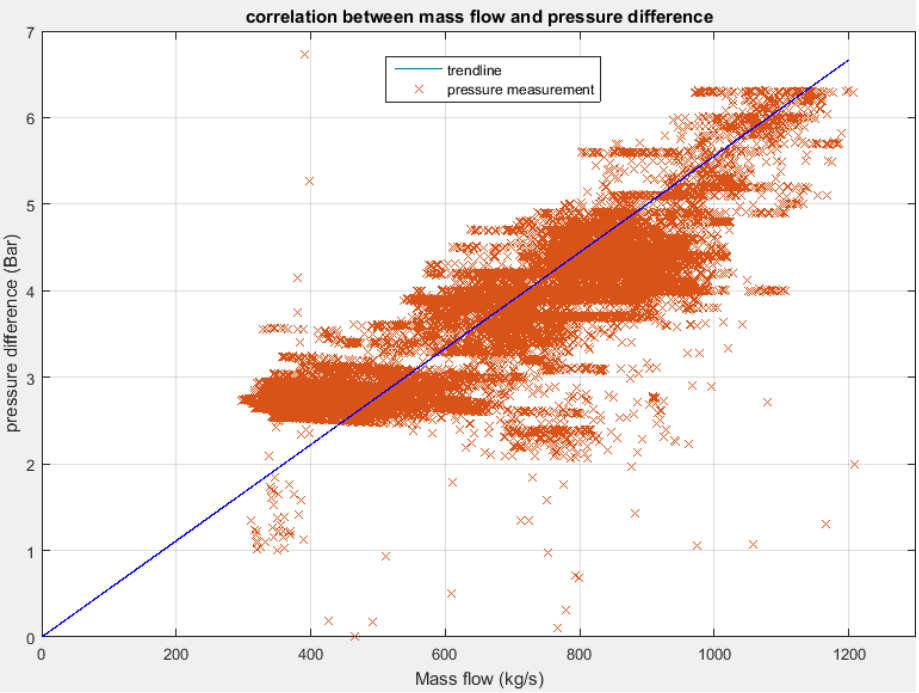

Figure 38. *Correlation between mass flow and pressure difference*

The trend line was fitted into Figure 38 to assume the relation between mass flow and pressure difference. Slope appointed to be $k_1 \approx \frac{dp}{\dot{m}} = \frac{1}{180}\left[\frac{bar}{(\frac{kg}{s})}\right]$, starting from $500\ \frac{kg}{s}$. The correlation is not perfect because of the disturbance caused by other pumping stations and production interferences in Haapaniemi. Data from all pump stations was not available so that Haapaniemi distribution pumps as a predominant pumping unit was used to determine the pressure loss of the network.

Total pumping energy of the network behaves according to (2-23), but there has to be a scaling parameter. According Hakuinen (2009) the pumping work in Kuopio is 0.9 % of heat production, then it can be assumed to be $P_{p,el} \approx 0.009\phi_{prod}$. Pumping electricity for the whole network is Eq. (2-23) multiplied by scaling parameter k_2.

$$P_{p,el} = k_2 \frac{dp}{\eta_p \rho} \dot{m} \qquad (5\text{-}1)$$

By the constants $\rho = 980\ \frac{kg}{m^3}$, $\eta_p = 0.9$ and and calibration data it was determined that $k_2 \approx 0.338$. Combining (2-24) and (5-1) the pumping effect on water temperature can be calculated when correlation k_1 is used

$$\Delta T_p = \frac{k_2 \dot{m} \eta_h}{k_1 c_p \rho \eta_p} \qquad (5\text{-}2)$$

5.3 Delay distribution

To create the distribution function of delay, the whole pipe network was analysed. The network consists of more than 70 000 pipe parts that form a network with length of 470 km and an average diameter of 153 mm. The real network connects over 5 500 customers to 10 suppliers. Even though there are 10 suppliers, most of the time only two of them are used. Hereby only three suppliers are included in the model. Including all of the sites into the model would need further improvements in production distribution algorithm. The pipe network is generalized by connecting the pipes together and removing the smallest ones based on diameter. The final number of pipe parts was 1 500, leaving out the smallest pipes that are used to connect individual customers to the network. Those pipes are generalized by straight line connection in the model. In Figure 39 the black lines are real DH pipes and the red and blue lines are the generalized connection pipes between customer and nearest node.

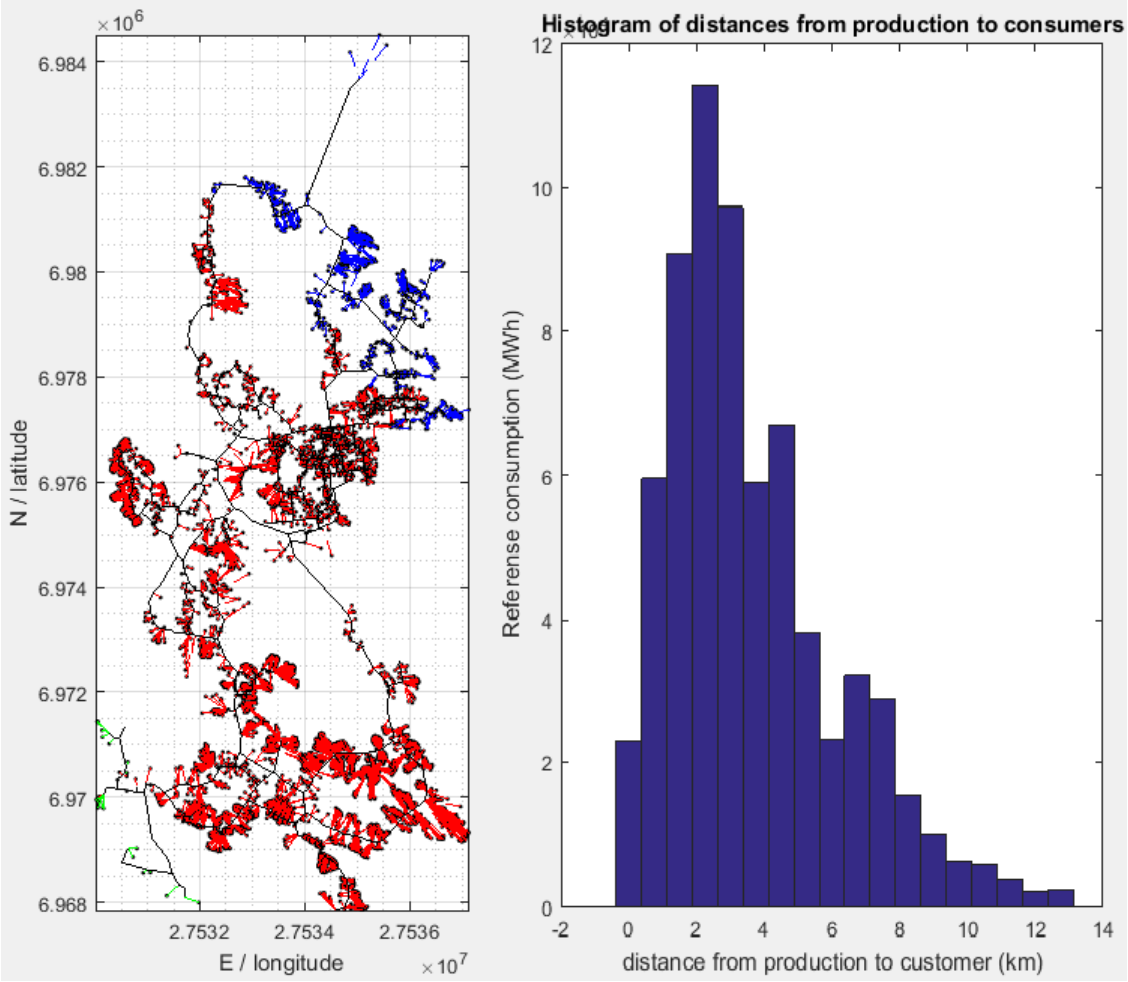

Figure 39. *Case example of supply areas at specific heat load and combined delay distribution from distances along the distribution lines. Exact location of suppliers can be seen in Figure 25*

Algorithm optimizes the routes and distances such that all of the customers are connected to the most likely supplier such that production and consumption heat loads match. There is an example case in Figure 39 where total heat production is *300 MW*, such that Haapaniemi (*248 MW*) produces heat to areas marked with red colour, Saarijärvi (*50 MW*) produces heat for blue area and Pitkäniemi bio (*2 MW*) produces for the green area. Histogram forms the shape of the delay distribution function, and it is transformed from distance scale to time scale according to relative delay that is based on total mass flow in the network.

To determine the supply temperature at the average customer, the model weights the recent temperatures supplied to the network. Figure 40 shows the modelled customer temperature.

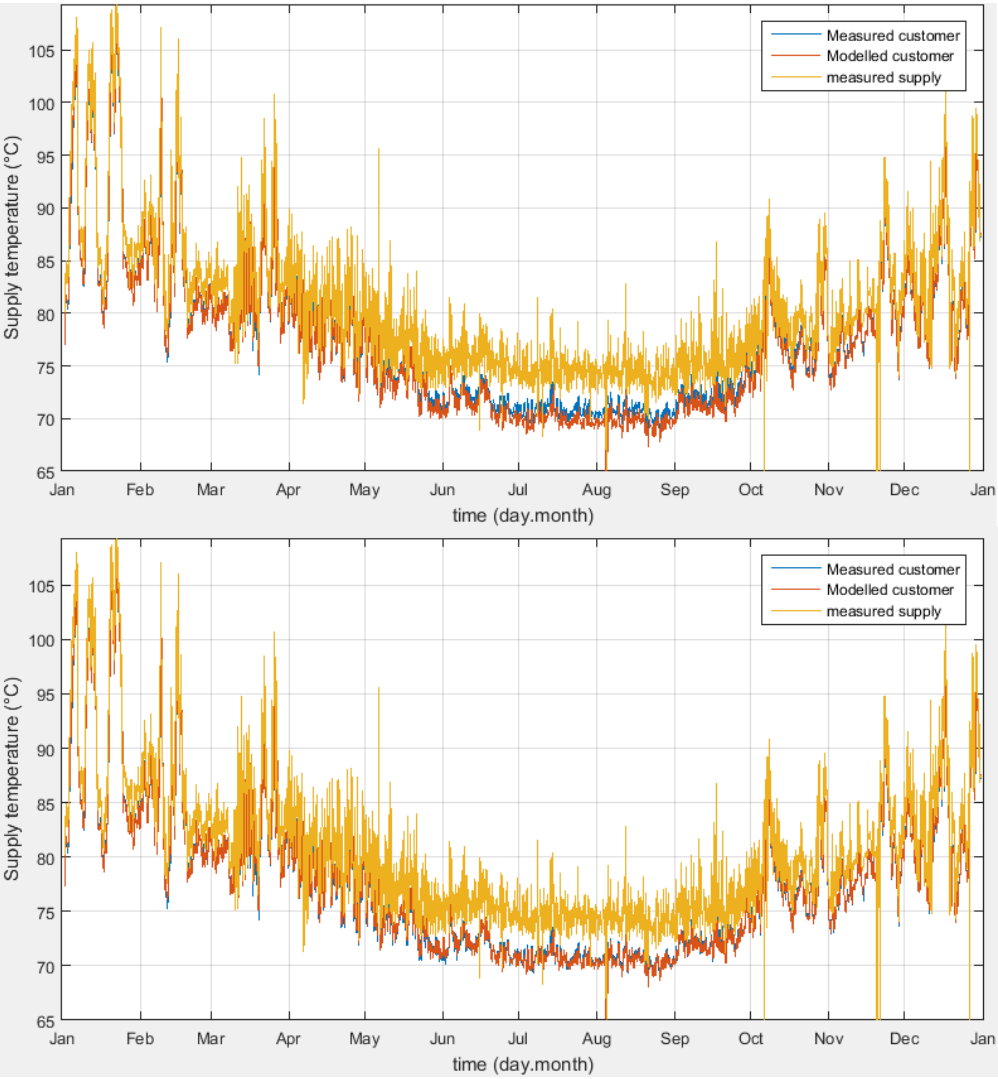

Figure 40. *The first graph shows the customer supply temperature based on theoretical model introduced in (3-6). Second graph is fitted to match measurements by correction factor that weighs temperature difference. The function for corrected model is presented in (5-3). Uncorrelated performance values are* $ME = 0.38\ ℃$, $SD = 0.52\ ℃$ *and* $VAR = 0.53\ ℃^2$ *and for corrected model* $ME = 0.067\ ℃$, $SD = 0.30\ ℃$ *and* $VAR = 0.27\ ℃^2$.

According to Figure 40, the temperature drop is lower in summer than modelled. Weighting more the temperature gradient, the model responds more accurately also during warm season. Equation (3-12) is rewritten with heat loss correction and pressure difference dependency correlation into

$$T_{s,c}(k\Delta t) = T_{s,c,th}(k\Delta t) - \left(\frac{K_1\hat{\tau}(k\Delta t)\left(T_{s,c,th}(k\Delta t)-T_g(k\Delta t)\right)-K_2\hat{\tau}(k\Delta t)\left(T_{s,c,th}(k\Delta t)-T_{r,c}(k\Delta t)\right)}{4.55}\right)^{1.37} + K_3\dot{m}_c(k\Delta t), \qquad (5\text{-}3)$$

Figure 41 shows the corrected model response more closely during high heat load season and low heat load season. It can be seen that the model is more accurate during winter when delays are short reducing the environmental disturbances.

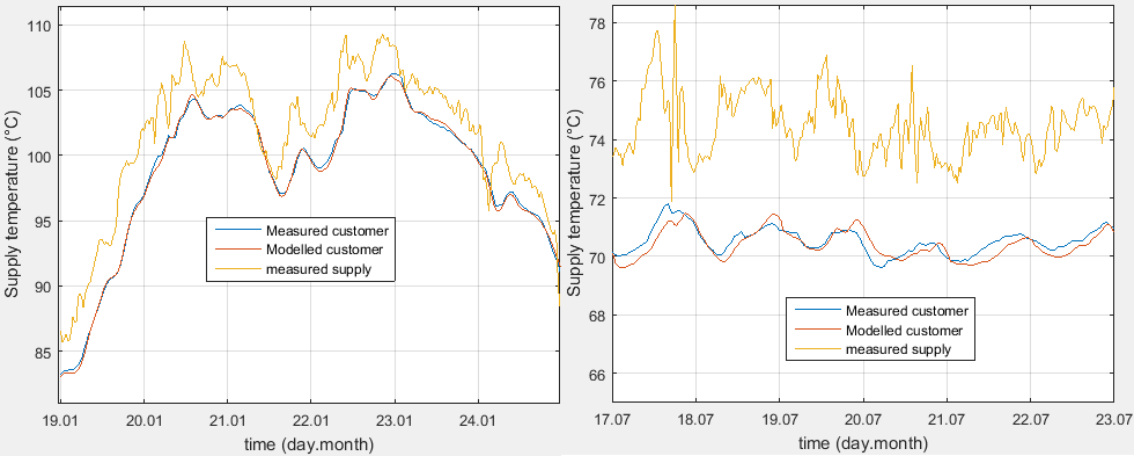

Figure 41. *The modelled average customer temperature by (5-3) compared to measured supply temperature and average customer temperature. There is season of high heat load on the left and season of low heat load on the right. Yellow is the measured supply temperature, blue is the measured average customer temperature and red is the modelled average customer temperature.*

5.4 Optimization

Supply temperature optimization was carried out using heat load and return temperature prediction and delay distribution models. Optimizer balances between heat loss cost and pumping cost to find the optimal supply temperature. Determination of prices of heat and mass flow production determine the utility of optimization result. Figure 42 demonstrates the optimization problem. It shows the steady state correlation between supply temperature and heat loss costs and pumping costs. Heat loss cost is always quite linear to supply temperature, whereas pumping cost increase exponentially while supply temperature reduces. However, there are plenty of factors that have an impact on the gradient or mean value of the costs that are explained later in this chapter. Optimizer uses delay distribution model to calculate costs of dynamic response.

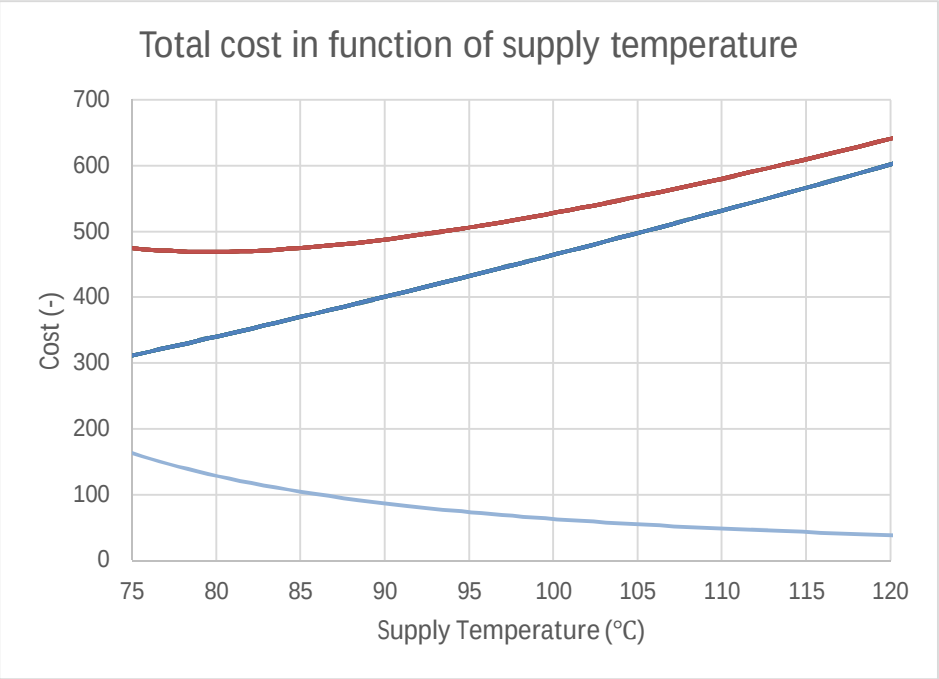

Figure 42. *Costs are presented as a function of supply temperature. In static analysis the heat load is constant and costs on y-axis are dependent on supply temperatures on x-axis. Light blue presents pumping cost, dark blue is heat loss cost and red is the total cost.*

5.4.1 Heat loss cost

The cost of heat loss depends on actual heat loss by (2-27) and the price of the heat. The price depends on fuel price, fuel mix, production efficiency and taxes. The rough running order of the CHP production boilers and heat stations depends on heat demand and the cost of the production shown in Table 4.

Table 4. *Rough production plan based on outdoor temperature. (HP) Haapaniemi.*

Outdoor temperature (℃)	Plants running	Production (MW)
> +5	HP 3	100
+5 ... -10	HP 2	200+
-10 ... -20	HP 2 & HP 3	300+
-20 >	HP 2 & HP 3 & Heat-only stations	>300+

The heat price is mostly dependent on the price and taxes of used fuel, which depend on production plants. In the optimization, tax free peat and biomass prices are regarded as constant and for light fuel oil monthly average prices are used. Total cost of heat production is the price of the fuels used to heat the water.

5.4.2 Pumping costs

Pumping costs are caused by the energy consumed by distribution pumps. The energy can be integrated from pump input power (2-23). Unlike fuel price, the electricity price has massive variations during a day and a year. There is an example of electricity price variations in Figure 43.

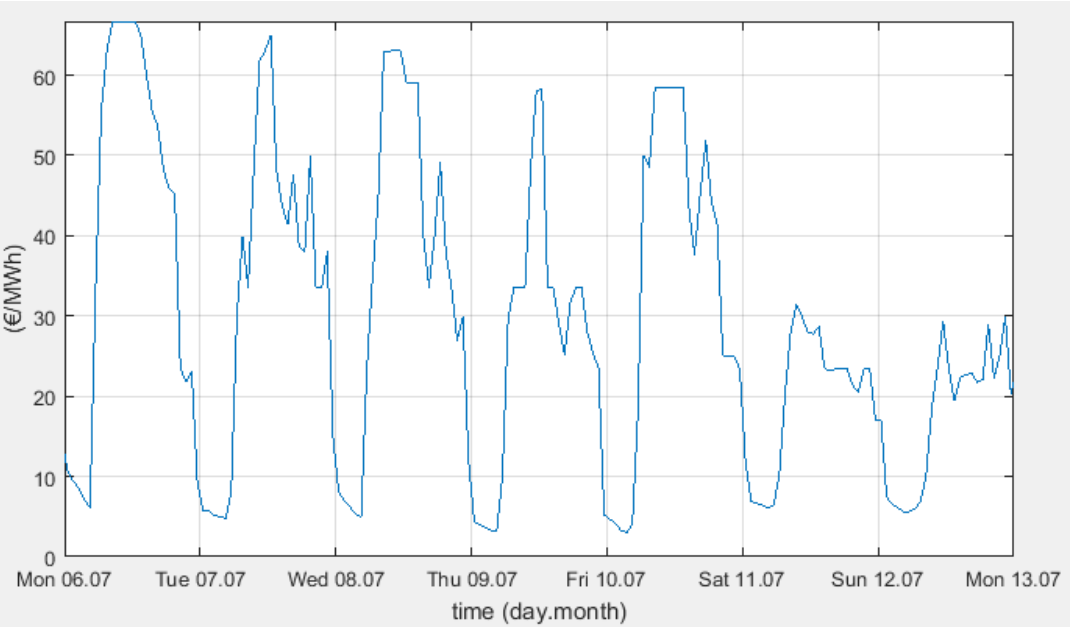

Figure 43. *Tax free electricity market price in Finland. An example from a week from July 2015.*

Even though fixed electricity taxes and transmission fees level the relative variation during a day, there are still significant fluctuations. Haapaniemi is a CHP plant why it can use produced electricity for pumping without taxes or transmission fees. Heat-only and pumping stations have to pay full taxes and transmission fees.

Also the pumping energy heats the water, therefore pumping may be feasible way to produce heat when the electricity price is low.

6. RESULTS

In this chapter the results of optimization are calculated and compared to other methods. The first part describes the behaviour and features of optimization with graphs and the second part with numbers. The results presented here diverge from the paper (Laakkonen et al. 2016) as the results were recalculated after the minor corrections were made in the models and cost functions.

The optimized supply temperature plan is compared with the measured supply temperature during observation period. The optimization results are compared to two baselines. The first baseline is the real measured supply temperatures (Meas). The another baseline is based on outdoor temperature control curve shown in Figure 2 (ET). Time period 2.1. – 30.12.2015 was optimized using predicted heat load and return water temperature. Delay distribution was used to model supply temperature at customer $T_{s,c}$ and return temperature at the production plant $T_{r,s}$.

The actual electricity consumption of DH pumps was not available in the measurement data. There is a parameter that scales pumping cost such that higher value of tuning parameter lead to high supply temperature and low mass flow. Respectively low parameter value leads to high mass flow and low supply temperature. As the actual value for the balancing parameter could not be determined, three cases with different parameter values were created and optimized. Optimizations were tuned according to the total costs of ET and Meas, in assumption that ET would provide some savings compared to Meas i.e. the cost parameter was tuned such that the total yearly costs of ET would be lower than the costs of Meas. The three cases are Opt1, Opt2 and Opt3 with different pumping cost parameters. Opt1 is the case of economical pumping, where the ET would give savings of 1.13 % compared to Meas. For Opt2 the pumping is a bit more expensive giving savings of 0.55 %. Opt3 is the case where pumping is so expensive that the ET is 0.08 % more expensive than Meas. Total costs are based on the values of cost function from whole optimization period. The mean supply temperatures are listed in Table 5.

Table 5. *Mean supply temperatures of five methods of year 2015*

Method	Mean supply temperature (°C)
Meas	80.64
ET	78.88
Opt1	77.87
Opt2	79.66
Opt3	81.81

Most likely the real pumping parameter value is somewhere between cases Opt1 and Opt3. All of the three optimizations act similarly, but at different temperature level.

6.1.1 Comparison of the three optimizations

There is a comparison of the optimization results of three cases in Figure 44. The supply temperatures of optimizations are gradually higher such that Opt1 is the lowest and Opt3 is the highest. Only difference between the cases is the cost parameter that defines the price of pumping. Hereby the main difference in optimization is the average supply temperature level, otherwise the behaviour is similar as long as they are above the minimum limit of 75 °C.

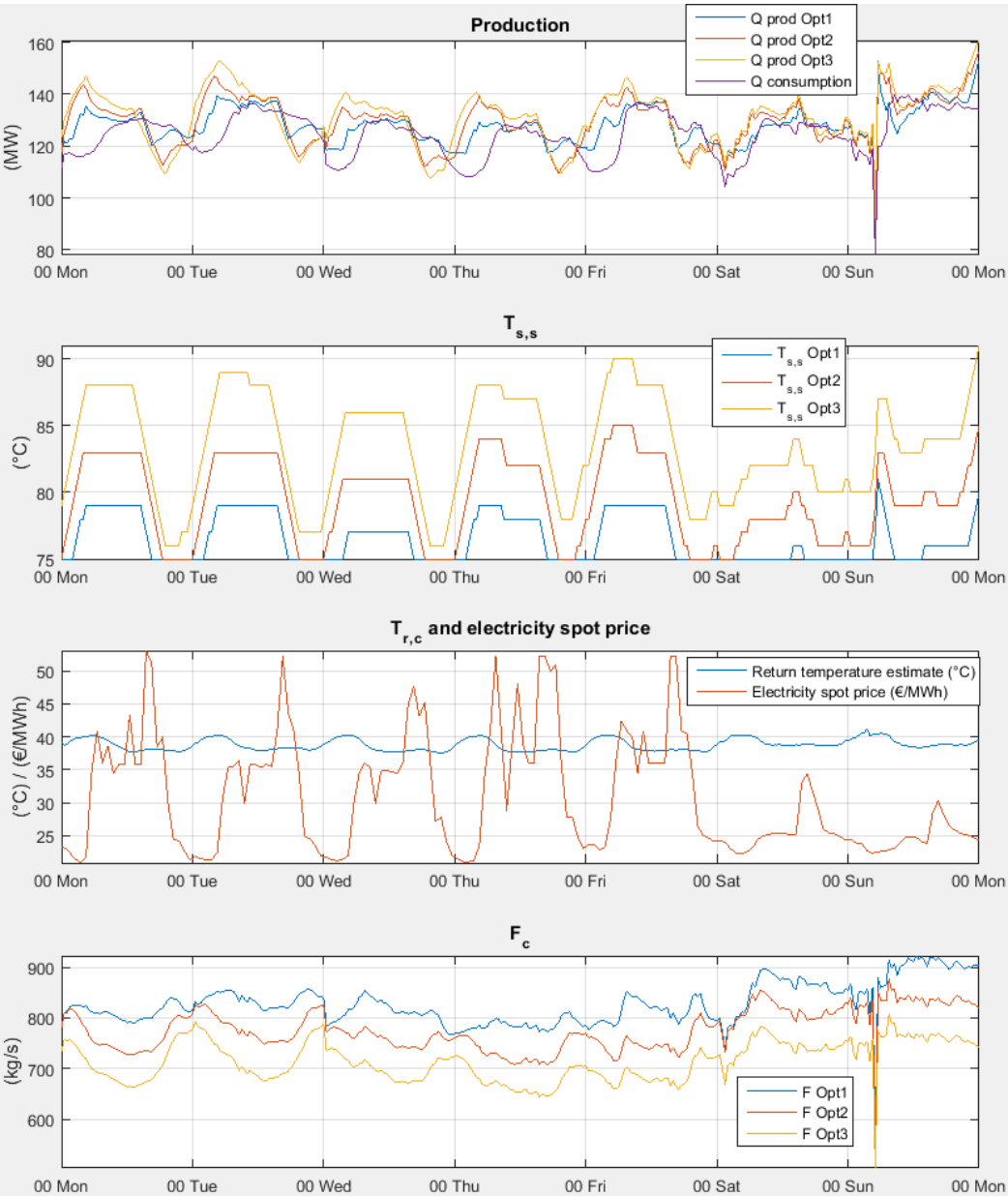

Figure 44. *Comparison of the three optimizations during medium heat load at late autumn (16-23.11.2015.). The average reference delay is 2.6 hours.*

The Opt2 is chosen for comparison as it is the medium between the two extreme optimizations. The following figures are based on Opt2, but Opt1 and Opt3 are also concerned in the final results.

6.2 Behaviour of optimization

When comparing optimized supply temperature Opt2 and ET, in function of outdoor temperature in Figure 45, a lot of variation can be seen. On warm outdoor temperatures the supply temperature is always 75 ℃. When $T_{out} < 12$℃, there is significant fluctuations on both sides of the ET curve. Firstly, the optimized temperature takes into account the temperature transport delay from heat supplier to heat consumer. Secondly, the electricity price is a significant term in pumping costs, which is why hotter water is supplied when electricity price is known to be rising and vice versa. Thirdly, even though the correlation between outdoor temperature and heat load is considerable in ET, the neural network estimator in Opt2 is more accurate in heat load prediction than linear temperature dependency in ET. Meas is much more dependent on outdoor temperature at cold temperatures than Opt2, as it is not dependent on electricity price nor there is not delay advancement. As the Meas is a measurement it may differ from set point which causes most of the fluctuations on high outdoor temperatures.

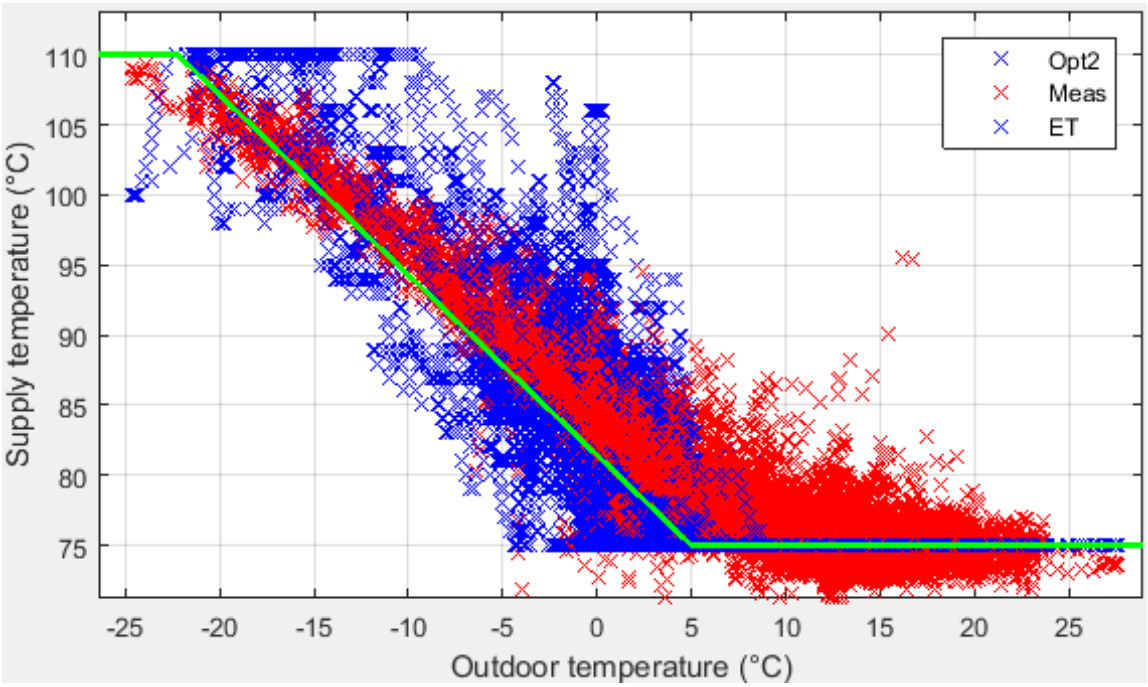

Figure 45. *Optimized and measured supply temperatures as a function of outdoor temperature. ET curve is the green line. All of the methods are limited into maximum of* 110 ℃ *as the condensing pump could not allow higher temperatures.*

There is a comparison of three supply temperature control methods from high heat load in January in Figure 46.

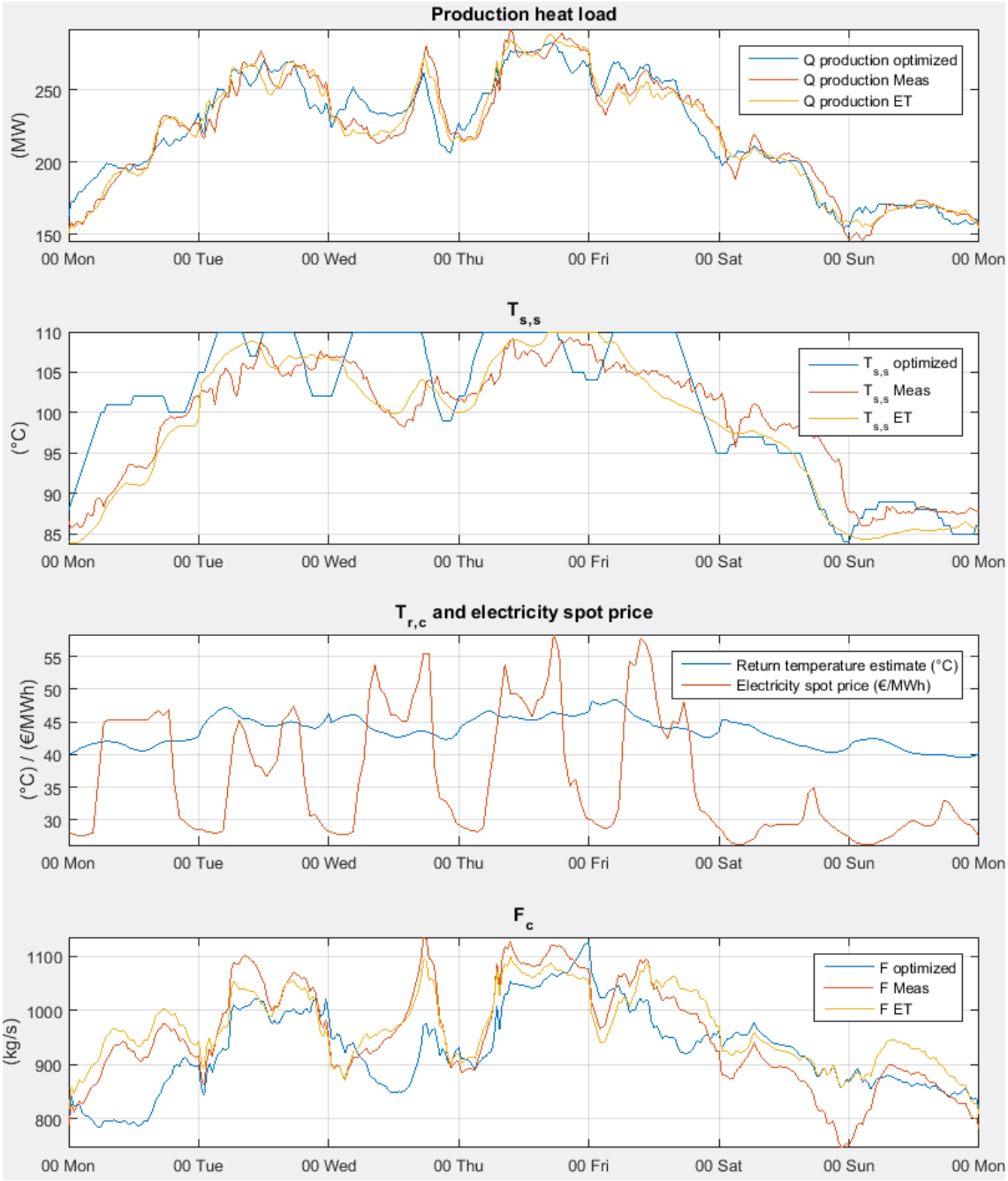

Figure 46. *Three methods (Opt2, Meas & ET) compared during one week on high heat load in winter (19-25.1.2015). Average reference delay is 2.0 hours.*

Figure 46 shows the three different strategies and their impact on flow rate and heat production. Measured supply temperature 'Meas' is quite noisy, whereas outdoor temperature based instruction curve 'ET' is smooth because of the smooth behaviour of the outdoor temperature measurement. The optimized supply temperature curve is quite conservative because of the penalty for unnecessary fluctuations and steep gradients. The advantage of optimization is the delay consideration, which levels the flow peaks especially when the pumping costs are high.

Optimization Opt2 is compared to Meas from one week in autumn in Figure 47. Speciality in this case are the extremely high electricity price peaks that increase the pumping price significantly. As a result there are considerable supply temperature peaks in Wednesday, Thursday and Friday mornings to reduce the costs of pumping.

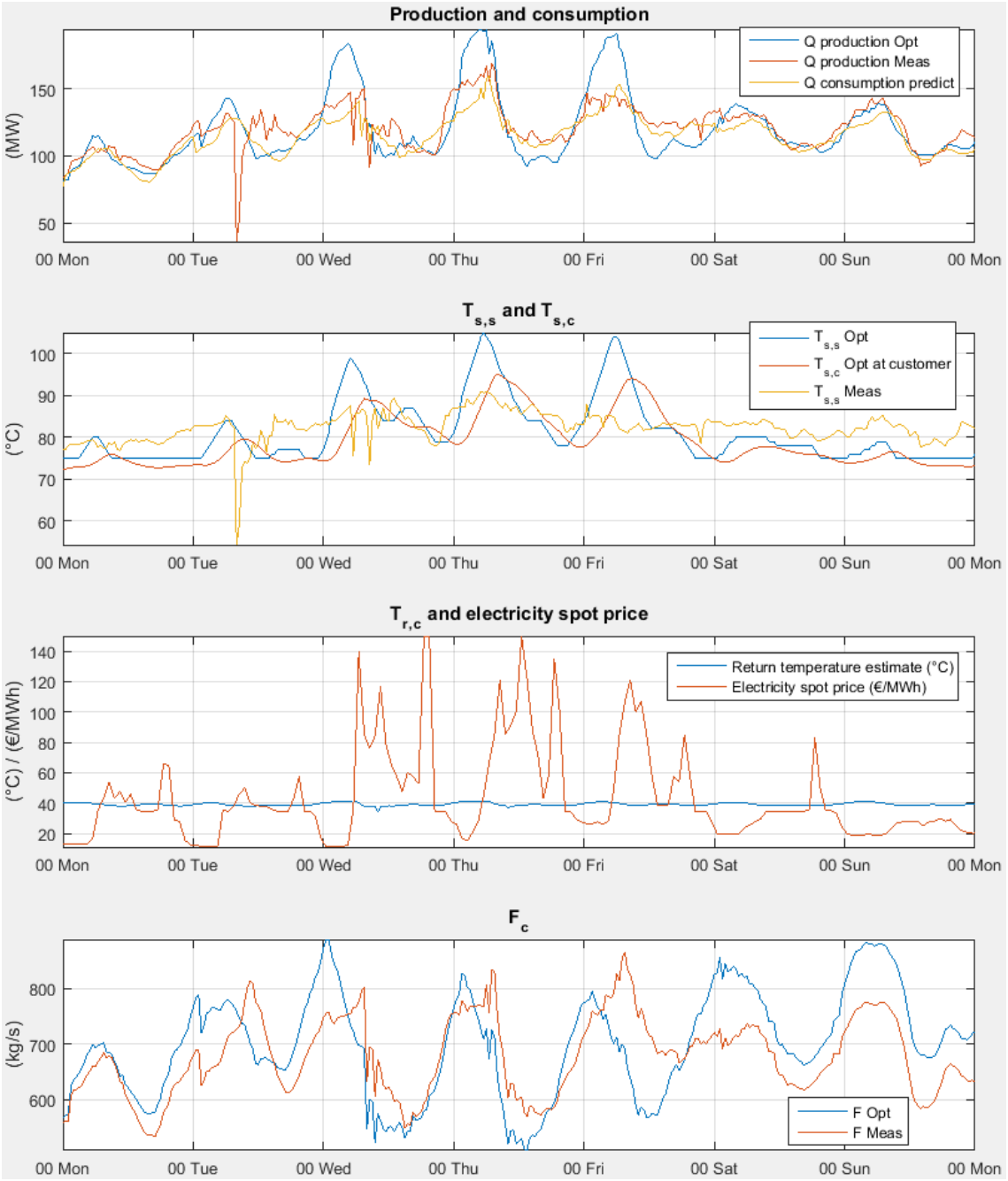

Figure 47. *Results are compared with measured supply temperature during one week on medium heat load in autumn (5.-11.10.2015.) to demonstrate the effect of high electricity price in optimization. Average reference delay is 2.7 hours.*

6.2.1 Optimization during summer

At summer, the significance on optimization decreases as most of the time supply temperature is saturated at minimum limit. There is a comparison of Opt2, Meas and ET in Figure 48 in July. It can be seen that the outdoor temperature is more than +5 ℃ whole week as $T_{s,ET}$ is saturated at 75 ℃ whole week. The optimization is also at 75 ℃, even the electricity price peaks are not high enough to lift the supply temperature as the heat load is so low.

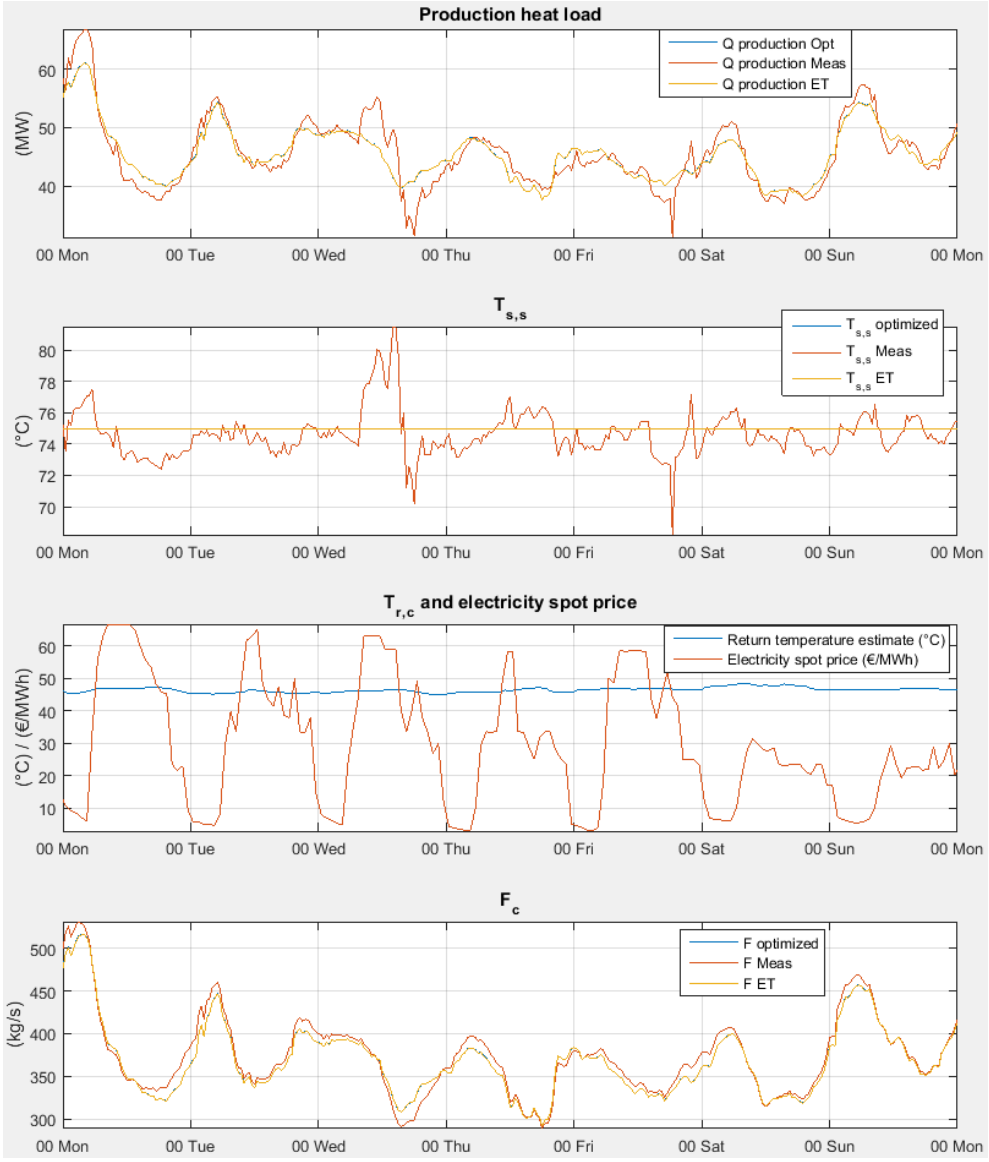

Figure 48. *Comparison of three methods during low heat demand in summer (6-12.7.2015.). Average reference delay is 4.7 hours.*

6.2.2 Delay dynamics of supply temperature

Even though the supply temperature by the ET –curve would be appropriate in static analysis, it does not consider the transport delay dynamics. The transport delay dynamics of

Opt2 and ET are observed in Figure 49. Easter was chosen, because electricity price is stable and daily heat load variations are noticeable. There are supply temperatures at supplier (blue & yellow) and at customer (red & violet) on second screen of Figure 49. The optimized supply temperature at customer correlate well with the heat consumption (yellow on first screen) and also quite well with ET supply temperature $T_{S,S,ET}$. It can be seen that the supply temperature by ET –curve reaches the customer too late compared to heat consumption. As a result the production according to ET –curve fluctuates more than optimization between nights and days with bigger gradients.

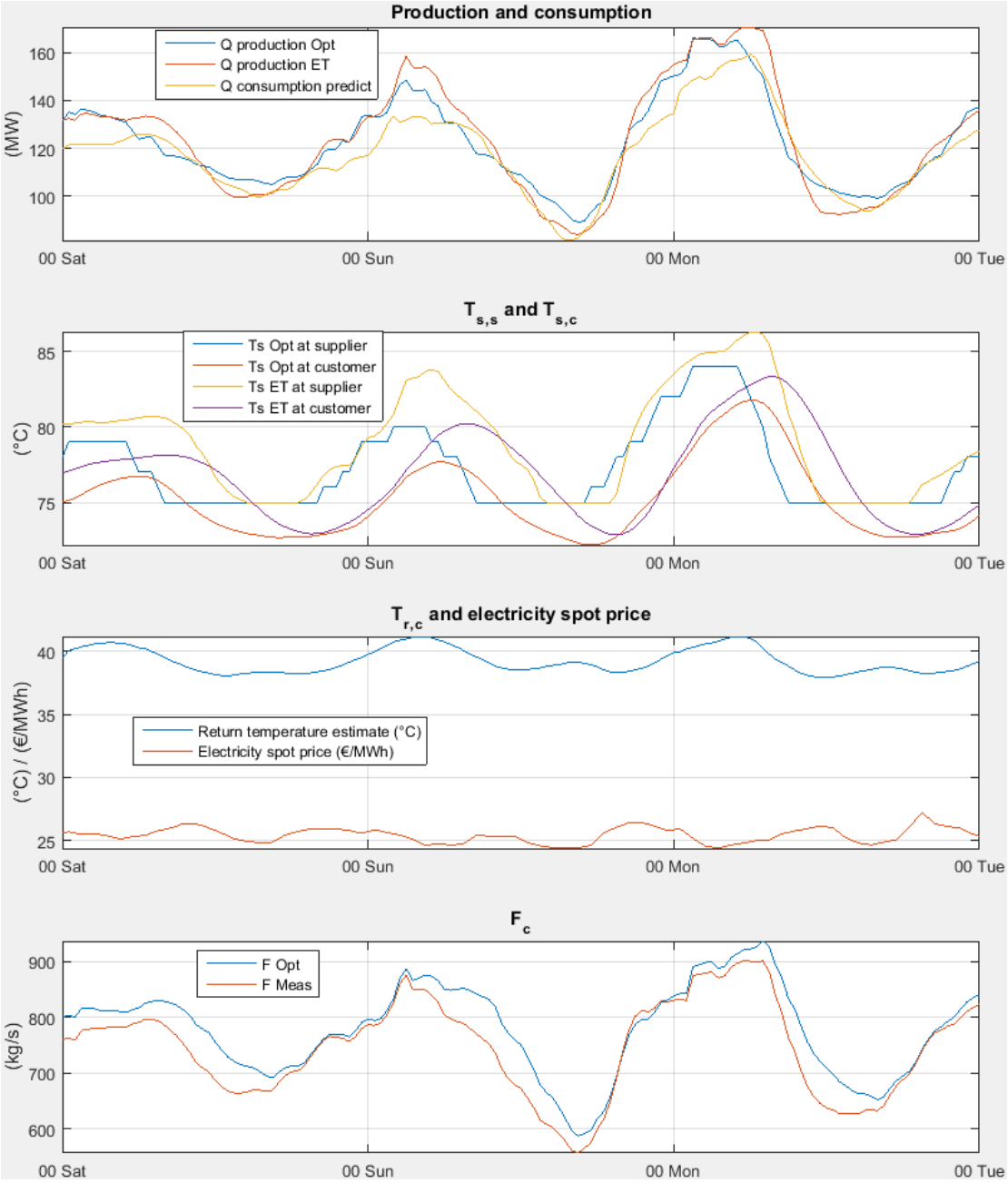

Figure 49. *Heat transfer dynamics from Easter 2015 (4-6.4.2015.). Average reference delay is 2.4 hours.*

6.3 Result calculations

To compare the benefits of the three optimizations, they are compared to the two baselines: measured (Meas) and ET –curve (ET). Optimization period is 2.1. – 30.12.2015. Results are presented in Table 6 and Table 7, such that (-) is decrease and (+) increase comparing optimization to the baseline.

Table 6. *Optimizations compared with measured supply temperature. Values are differences between optimization and baseline (Opt - Meas).*

	Opt1	**Opt2**	**Opt3**
Total delivery cost (%)	-1.70 %	-1.18 %	-1.36 %
Heat production (GWh)	-9.97	-3.88	+2.36
Heat production (%)	-1.12 %	-0.43 %	+0.26 %
Mean return temperature (℃)	-0.26	-0.11	+0.11
Mean supply temperature (℃)	-2.77	-0.98	+1.17
Pumping energy (%)	+17.01 %	+4.99 %	-6.36 %
Pumping cost (%)	+14.11 %	+1.53 %	-9.79 %

Table 7. *Optimizations compared to instructional ET –curve (Opt - ET).*

	Opt1	**Opt2**	**Opt3**
Total delivery cost (%)	-0.66 %	-0.72 %	-1.54 %
Heat production (GWh)	-4.00	+2.09	+8.33
Heat production (%)	-0.45 %	+0.24 %	+0.94 %
Mean return temperature (℃)	-0.08	+0.08	+0.30
Mean supply temperature (℃)	-1.01	+0.78	+2.93
Pumping energy (%)	+7.17 %	-3.84 %	-14.23 %
Pumping cost (%)	+4.24 %	-7.26 %	-17.59 %

The optimization analyses are based on Table 6 and Table 7. Opt1 has the lowest mean supply temperature of all. It has the smallest heat loss and the highest pumping costs of all. It is considerably more cost efficient than Meas and only moderately more compared to ET, as in that case the pumping costs are relatively low. Opt2 situates between ET and Meas in consideration of mean supply temperature, but still closer to ET. As Opt1, also Opt2 is a significant improvement compared to Meas and moderate improvement compared to ET. Opt3 has the highest mean supply temperature of all. The pumping cost parameter is so high that Meas is more feasible strategy than ET.

Heat production is clearly proportional to supply temperature as heat losses increase along with increased supply temperature. Respectively flow rate and pumping energy reduce along with increased supply temperature. However, the optimizer strives to pump when electricity price is low. For this reason, the savings of pumping energy are not as good as savings on pumping costs. The most suitable optimization depends on the sum of real pumping costs, otherwise the optimal pumping cost parameter could not be determined.

The optimization generally lowers the supply temperature significantly, which also lowers the return temperature slightly. According to Eq. (2-1), the power production increases along with lower temperature levels. Also the mean flow rate increases when the supply temperature decreases enabling faster heat load changes according to Eq. (2-12) that increases the flexibility of CHP supplier.

6.4 Impact of prediction error on flow rate and heat production

Prediction errors in heat load and return water temperature possibly lead to false optimizations. Falsely optimized supply temperature will result as an error in flow rate if the real consumption and return temperature do not match with the prediction. Error in flow rate is directly reflected into current heat production. Table 8 presents error mean (EM) and standard deviation (SD) of error caused by neural network prediction error. Measured heat load and customer return temperature are the corresponding benchmarks.

Table 8. *Prediction errors' reflection to flow rate and heat production.* $(Error = Prediction - Real)$

	Measured	**ET -curve**	**Opt1**	**Opt2**	**Opt3**
Heat prod ME (MW)	0.909	0.928	0.770	0.816	0.871
Heat prod ME (%)	1.77 %	1.82 %	1.52 %	1.60 %	1.70 %
Heat prod SD (MW)	5.68	5.67	5.57	5.62	5.67
Heat prod SD (%)	11.08 %	11.15 %	10.99 %	11.01 %	11.03 %
Flow ME (kg/s)	10.84	11.66	10.87	10.54	10.24
Flow ME (%)	1.83 %	1.85 %	1.68 %	1.71 %	1.75 %
Flow error SD (kg/s)	32.92	34.58	35.43	33.52	31.64
Flow error SD (%)	5.57 %	5.60 %	5.55 %	5.52 %	5.50 %

According to Table 8, the mean error in heat production and flow rate is generally less than two per cent. The SD of mass flow rate is at the same level than the SD of heat load predictor. The heat production SD is almost double to the SD of mass flow, because the errors of mass flow, supplier return temperature and delay reflect to heat production.

The results are based on predictions, where all inputs can be measured with automation system nowadays. That was agreed to provide worse results than prediction that is based on customer substation measurements in Chapter 5.1. Customer substation data would give better results when they can be connected into automation system.

7. DISCUSSION

The results of these work proves that the DHN could be modelled and optimized without exact simulators to provide savings. The aim is to predict the cost effect of the current supply temperature decision and that can be calculated with the application developed in this project. Possible savings in this case are not that high, as supply temperature controls in Kuopio DHS are relatively good compared with many other Finnish DHSs. This application could be tuned into other DHSs giving possibly more savings. As heat production is becoming more important product of CHP for providers, the efficiency in DHN will be seen as more significant factor. That will rise the demand for efficiency improvements by supply temperature controls.

The neural network predictors act as they are trained. They are tools that process the input data providing some result. It is good tool for this application, if the data has some repetitive cyclic behaviour and strong connections to target data. The success of prediction is dependent on choosing and processing the input data and choosing the time scale such that the DHS functions similarly whole time period. The predictors performed rather reliable when there were 10 parallel networks and only 6 median values were chosen. Weakness was the ability to respond to season changes, which could be improved by using training data from last year.

The delay distribution model is a deterministic model to calculate the average supply temperature of the customer. The model was developed to model more exactly the heat transportation delay and what is the weight of supplied temperature at the certain moment of time. Also the disturbances were adjusted to give accurate results. The model does not take into account the maximum nor minimum temperatures in the network that might be an issue in some cases. The delays are based on the distances between suppliers and consumers that may be a poor assumption in some cases where water moves significantly faster in wide transfer pipes than in thin distribution pipes. As the delay distribution model in this work is just a concept, it has much improvement potential, but it already has proved to be useful and accurate.

As neural network predictor, also the optimizer is a tool that provides a solution according to defined cost functions and delay distribution model. The performance of brute force search may become an issue if time step is wanted to be reduced, number of gradients is wanted to be increased or optimization window is wanted to be increased. Optimization of 24 hours takes some 60 seconds that is enough for this work. The optimizer is very simple and robust, but the performance could be enhanced by advanced optimization methods.

In this study, the cost functions were created to serve DHS, such that power production was excluded. Optimization minimizes the flow rate during high electricity price to avoid expensive pumping and vice versa. However, to maximize the production of CHP the condensing heat load of steam turbine should be as high as possible to enhance the power output of turbine and boiler. Thus the flow rate should be high to provide a maximum cooling load. Pumping costs and condensing load are partly in contradiction. Therefore, condensing load should be in cost function to provide an optimization that fully satisfies the requirements of CHP suppliers. The challenge would be the determination of the balance between revenues of produced electricity and costs of used electricity for pumping, as the balance between pumping and heat production also proved to be challenging itself.

The resulting supply temperatures or the temperature gradients may be too extreme for operating real DHS. In this work there are no more limitations than Energiateollisuus ry. demands. To implement the optimization in real DHS there would be limiting controls for extreme values of supply temperature and mass flow that would prevent operating with unsuitable supply temperatures. Hereby the savings of the results would not that high in real DHS as stated in the results, as gradients and extreme values were limited.

8. CONCLUSIONS

This research was carried out because of the low level of supply water temperature controls in district heating systems (DHS). The aim was to find a solution to control the supply temperature such that there would be more flexibility and predictability in perspective of heat and power co-generation. Also, improved cost and energy efficiencies were objectives. Heat load demand and return water temperature of district heating (DH) customers were predicted by neural network predictors. The dynamic response of supply temperature was modelled through delay distribution model. The supply water temperature was optimized by brute force optimizer that minimizes the total costs of heat loss and pumping. The research was carried out by modelling the DHN of Kuopio by scaling and validating the models with the system data and measurements.

The optimization was performed for period of one year with three different values of pumping cost tuning parameters. Optimizations were compared with measured supply temperature and instructional supply temperature curve. Compared with measured values, total operating costs would be reduced in three cases by 1.2 – 1.7 % depending on pumping cost parameter. Savings could be achieved by mean supply temperature alterations of +1.2 – -2.8 ℃ between the three cases compared to measured values. Hereby the optimal temperature is dependent on total costs and thus it could be higher than the measured one if pumping costs are high. Cumulative error caused by prediction error was rather small as the standard deviation of heat production was only 11 %.

The results of optimization are good and in accordance with the definitions. The most remarkable factor determining the supply water temperature, was the rapidly fluctuating electricity price that sets the pumping costs. The results did not give remarkably high savings in total operating costs as the supply temperature could not be lowered that much. The most important result is, that there is a cost function that defines the desirable result and the system can deliver it well.

The aim of this work was to create an application that solves the problem of predictive determination of supply water temperature. The solution consists of three methods that can also be regarded separately. Neural network was a ready tool that was utilized to predict heat load and return temperature. Delay distribution model was created as no decent model was found to determine the heat transport delay and network heat balance. The model is really useful and can be applied in other purposes apart from optimizer. The third method is the optimizer, which determines the supply water temperature utilizing the mentioned models. The optimization result depends on the defined cost function.

9. FUTURE WORK

The most significant aspect in development of this optimization is an addition of power output of steam turbine into cost function. That would extend the optimization into CHP-production, such that optimal usage of DHN could support electricity production by supply temperature control. This demands the modelling of steam turbine costs, revenues, efficiency and dynamics.

Study to measure real pumping costs and their relation to pumping mass flows would enable to choose the correct cost parameters.

To improve the optimization algorithm, linear parameter varying (LPV) state-space model would enhance the speed and accuracy of the optimization. The varying delay is challenging for basic state-space model. Formulation of LPV model of DHS would be similar to marine cooling systems, which is modelled by Hansen et al. (2011). LPV model is also formulated for DHS, but was failed to implement due to numerical difficulties (Nielsen et al. 2002). Brute force optimizer is very robust which is important in process automation. Advanced models should reach the same level of robustness.

REFERENCES

Averfalk, H., Ingvarsson, P., Persson, U. & Werner, S. (2014) On the use of surplus electricity in district heating systems, The 14th International Symposium on District Heating and Cooling.

Benonysson, A., Bøhm, B. & Ravn, H.F. (1995) Operational optimization in a district heating system, Energy Conversion and Management, Vol. 36(5), pp. 297–314.

Boysen, H. (2004) Selection of district heating house stations, Euroheat and Power (English Edition), Vol. (3), pp. 46–51.

Energiateollisuus ry. (2015) District heating statistics 2014 excel -file. Available: http://energia.fi/tilastot/kaukolammitys.

Energiateollisuus ry. (2014) Rakennusten kaukolämmitys, Määräykset ja ohjeet, Available: http://energia.fi/sites/default/files/julkaisuk1_2013_20140509_0.pdf.

Eriksson, N. (2012) Predicting demand in district heating systems - A neural network approach, Uppsala University, Available: http://www.diva-portal.org/smash/get/diva2:530099/FULLTEXT01.pdf.

Falkvall, M. & Nilsson, V. (2013) Optimerad framledningstemperatur i Lunds fjärrvärmenät, Lund University, Available: http://www.ees.energy.lth.se/fileadmin/ees/Publikationer/Ex5299-OptimeradFramtempLundsFjaerrvaerme-Falkvall-Nilsson.pdf.

Frederiksen, S. & Werner, S. (2013) District Heating and Cooling 1st ed., Lund.

Gadd, H. & Werner, S. (2014) Achieving low return temperatures from district heating substations, Applied Energy, Vol. 136, pp. 59–67, Available: http://www.sciencedirect.com/science/article/pii/S0306261914009696.

Gadd, H. & Werner, S. (2013) Heat load patterns in district heating substations, Applied Energy, Vol. 108, pp. 176–183, Available: http://dx.doi.org/10.1016/j.apenergy.2013.02.062.

Grosswindhager, S., Voigt, A. & Kozek, M. (2011) Online short-term forecast of system heat load in district heating networks, Available: http://www.forecasters.org/submissions/GROSSWINDHAGERSTEFANISF2011.pdf.

Haikarainen, C., Pettersson, F. & Saxén, H. (2014) A model for structural and operational optimization of distributed energy systems, Applied Thermal Engineering, Vol. 70(1), pp. 211–218, Available: http://linkinghub.elsevier.com/retrieve/pii/S1359431114003135.

Hakuinen, A. (2009) Energiatehokkuusselvitys kaukolämmityksen pumppausjärjestelyistä, Pöyry Energy Oy, Espoo.

Hansen, M., Stoustrup, J. & Bendtsen, J.D. (2011) An LPV Model for a Marine Cooling System with Transport Delays, Proceedings of the 14th International Conference on Harbor, Maritime & Multimodal Logistics Modelling and Simulation, pp. 119–124. Available: http://www.control.aau.dk/~jakob/selPubl/papers2011/hms_2011.pdf.

Jochumsen, A. (2010) Modeling and control of a District Heating System, Aalborg University, Available: http://projekter.aau.dk/projekter/files/32311803/report.pdf.

Kaivosoja, J. (2016) Valmet internal material.

Koskelainen, L., Saarela, R. & Sipilä, K. (2006) Kaukolämmön Käsikirja, Energiateollisuus ry, Helsinki.

Kuopion Energia (2016) Kuopion Energia Web Page, [Accessed March 14, 2016], Available: https://www.kuopionenergia.fi.

Laakkonen, L., Korpela, T., Kaivosoja, J., Vilkko, M., Majanne, Y. & Nurmoranta, M. (2016) Predictive supply temperature optimization of district heating networks using delay distributions, The 15th International Symposium on District Heating and Cooling.

Ljubenko, A., Poredoš, A. & Zager, M. (2011) Effects of hot-water-pipeline renovation in a district heating system, Strojniski Vestnik/Journal of Mechanical Engineering, Vol. 57(11), pp. 834–842.

Mills, A.F. (1999) Basic Heat & Mass Transfer Second Edi., Los Angeles, Prentice Hall.

Nielsen, T.S. Madsen, H., Holst, J. & Sogaard, H.T. (2002) Predictive control of supply temperature in district heating systems, Informatics and Mathematical Modelling, Technical University of Denmark.

Nord Pool Spot (2016) Nord Pool Spot –Database, [Accessed August 8, 2016], Available: http://www.nordpoolspot.com/historical-market-data/.

Persson, J. & Larsson, M. (2014) Innovations in District Heating, p. 42.

Protić, M., Shamshirband, S., Anisi, M.H., Petković, D., Mitić D., Raos, M., Arif, M. & Alam, K.A. (2015) Appraisal of soft computing methods for short term consumers' heat load prediction in district heating systems, Energy, Vol. 82(0), pp. 697–704. Available: http://www.sciencedirect.com/science/article/pii/S0360544215001036.

Raiko, R. & Saarenpää, I. (2014) Thermal power plants 1 (Höyrytekniikka), TUT Course lecture book, Tampere university of technology, Power plant & Combustion technology.

Saarinen, L. (2010) Model-based control of district heating supply temperature, Stockholm. Available: http://www.varmeforsk.se/rapporter?action=show&id=2483.

Saarinen, L. (2008) Modelling and control of a district heating system, Uppsala University, Available: http://www.diva-portal.org/smash/get/diva2:461661/FULLTEXT01.pdf.

Saarinen, L. & Boman, K. (2012) Optimized district heating supply temperature for large networks, Stockholm, Available: http://www.varmeforsk.se/rapporter?action=show&id=2729.

Seppälä, P. (2016) Phone interview with Peter Seppälä (Kuopion Energia Oy) 14.4.2016.

Statistics Finland (2016) Statistics Finland -Web database, [Accessed August 9, 2016], Available: http://tilastokeskus.fi/.

Swamee, P. & Jain, A. (1976) Explicit equations for pipe-flow problems, Journal of the Hydraulics Division (ASCE).

The Engineering ToolBox (2015) Water - Speed of Sound, The Engineering ToolBox web page, [Accessed December 10, 2015], Available: http://www.engineeringtoolbox.com/sound-speed-water-d_598.html.

Weatherbase (2016) Kuopio weather, Weatherbase web page, [Accessed March 14, 2016], Available: http://www.weatherbase.com/weather/weatherall.php3?s=71920&refer=&units=metric.

Velut, S. Larsson, P., Windahl, J., Boman, K. & Saarinen L. (2013) Non-linear and Dynamic Optimization for Short-term Production Planning, Stockholm, Available: http://www.varmeforsk.se/rapporter?action=show&id=4454.

Vesterlund, M. & Dahl, J. (2014) A method for the simulation and optimization of district heating systems with meshed networks, Energy Conversion and Management, Vol. 89, pp. 555–567, Available: http://linkinghub.elsevier.com/retrieve/pii/S0196890414008838.

Viander, T. (2014) Optimization of district heating network usage, Lappeenranta University of Technology, Available: https://www.doria.fi/bitstream/handle/10024/102299/Diplomityo_Tero_Viander_08122014.pdf?sequence=2.

Väestörekisterikeskus (2016) Asukasluku kunnittain. Väestörekisterikeskus Web page. Available: http://vrk.fi/default.aspx?docid=8908&site=3&id=0.

APPENDIX A: MATLAB SCRIPT

Script 1. Script of function *f* Eq. (3-4)

```
function y=distribution(distribution_fun,delmeas)
% This function scales the distribution according to flow rate

x1=distribution_fun(:,1);                          % x -coordinates of
distribution histogram
y1=distribution_fun(:,2);                          % y -coordinates of
distribution histogram
for q=1:size(delmeas,2)

    del_ref=1.8;                                     % Reference scaling
factor
    fx=delmeas(q)/del_ref;                         % fx factor
    fy=1/fx;                                       % fy = is inverse to
fx
    x2=[];
    y2=[];
    x2=x1*fx;                                      % vectors x2 and y2
    y2=y1*fy;

    if fx<=1                                       % when delay is
shorter than reference
        x2=[x2;(x1(end)+1)];                       % one step is added
with value 0 for calculation algorith
        y2=[y2;0];                                 % because x2(end) must
be greater than x1(end) for next 'for' -loop
    end

    for j=1:length(x1)                             % this loop scale the
function y2 to y3 according
        i=1;
        while x2(i)<=x1(j)
            i=i+1;
        end
        i=i-1;
        deltay=(y2(i+1)-y2(i))/(x2(i+1)-x2(i)); % slope delta-y/delta-
x
        y3(j)=(x1(j)-x2(i))*deltay+y2(i);          % y3 = y2 + lineariza-
tion
    end

    y(:,q)=y3/sum(y3);                             % sum of function set
to 1
end

end
```